OPTIMIZATION PROBLEMS IN ATTITUDE CONTROL AND ORBIT TRANSFER OF SPACE VEHICLES(Dissertation_全文)

AUTHOR(S):

Sannomiya, Nobuo

OPTIMIZATION PROBLEMS IN ATTITUDE CONTROL AND ORBIT TRANSFER OF SPACE VEHICLES

NOBUO SANNOMIYA

DEPARTMENT OF ELECTRICAL ENGINEERING
KYOTO UNIVERSITY

SEPTEMBER, 1968

OPTIMIZATION PROBLEMS
IN ATTITUDE CONTROL AND ORBIT TRANSFER OF SPACE VEHICLES

NOBUO SANNOMIYA

SEPTEMBER, 1968

INTRODUCTION

This paper deals with some problems in attitude control and trajectory optimization for space vehicles. Optimization theory has played an important role in space flight from the very beginning. In 1925 W. Hohmann first studied the minimum-fuel transfer between coplanar circular orbits [7, 15].* Minimization of fuel consumption and maximization of payload are still key problems in vehicle design and mission planning. For many types of mission, it is furthermore necessary to control the attitude orientation of space vehicles.

There is no fundamental difference in principle between the problems associated with the attitude control of a space vehicle and those that arise in connection with the stabilization of a body free to rotate about any axis. The purpose of an attitude control system is to maintain coincidence between a set of axes fixed in the vehicle and a reference frame. There have been a number of papers on single-axis attitude control systems [8, 9, 19, 34]. The problems discussed here are concerned with three-axis control systems. The attitude motion of the vehicle rotating in the three dimensional space is described by three second-order differential equations in terms of attitude deviation angles. These equations contain nonlinear and time-varying terms. The equations may be linearized in the case of small attitude deviations from the reference frame.

In the design of attitude control systems, there are many criteria to be considered. Minimization of fuel requirement and achievement of time-

---

* Numbers in brackets indicate references on pages 147 to 150.

optimal response are of major considerations. The technique applied for obtaining the optimal controls is due to Pontryagin's maximum principle [30].

The problem of space trajectory optimization considered in this paper is the minimum-fuel transfer between neighboring elliptic orbits. Simplifying assumptions are made in the mathematical model of this problem. If the motion of the vehicle in the transfer does not deviate significantly from the terminal orbits, linearization of the equation of motion is permissible. In the case of circular terminal orbits, the symmetry of the orbits about their common center allows arbitrary choice of the optimal point of departure from the initial orbit. The orbital velocity of the vehicle revolving along an elliptic orbit varies periodically in time. This variation produces terms with periodic coefficients in the equation of motion; furthermore, it results in the variation of fuel consumption depending upon the point of departure from the initial orbit.

The propulsion system that effects the orbital changes is assumed to be power-limited; i.e., it operates at a constant exhaust power with a thrust magnitude inversely proportional to the exhaust velocity. The direction and the magnitude of the thrust are to be determined as functions of time so as to minimize the fuel consumption. The optimization technique applied is also due to the maximum principle.

The text consists of three chapters. The first two chapters are concerned with the optimal attitude control of a satellite which is in a steady orbit around the earth. The orbit is either circular or elliptic with a small eccentricity. The satellite is assumed to be a rigid body. Since the attitude control with respect to the earth is considered, the earth-centered triad

is taken as a reference frame of the attitude. In the case of a circular orbit, the gyrodynamical equations of the satellite consist of terms with constant coefficients; while in the case of an elliptic orbit, terms with time-varying coefficients appear in the equations owing to periodical change of the angular velocity of the orbital motion.

The torque-producing elements considered in Chapter 1 are reaction gas jets. Most of modern gas-jet systems are characterized by on-off type behavior. In this case the actuator torque is considered as a control function. The time-optimal control and the minimum-fuel control are discussed in this system. The optimal switching policy of the control functions is investigated, and the shortest settling time and the minimum fuel consumption are determined for various initial states of angular deviation. Influence of a transition time on the amount of fuel consumption is also discussed. Control of the original nonlinear system is briefly mentioned by illustrating particular numerical examples.

Chapter 2 deals with the control system using reaction wheels. The driving torque is provided by armature-controlled, permanent-magnet d-c motors. The input voltage to the motor is taken as a control function. The optimization criteria considered in this chapter are to minimize the settling time and the amount of input energy to the motors. The optimal switching policy of the control functions is investigated for any initial state of angular deviation. The energy consumption under the action of the optimal controls is also determined.

Chapter 3 is concerned with the minimum-fuel transfer between neighboring elliptic orbits for a low-thrust power-limited propulsion system. The problem

of optimal low-thrust trajectories in the inverse-square force field has been studied by several investigators [5, 6, 10, 11, 18, 20, 33]. Among them, F. W. Gobetz [10] has treated the variable-thrust transfer between close circular orbits and obtained an exact solution analytically. This chapter extends his work and obtains the optimal thrust program for transfer between close elliptic orbits.

The analysis is carried out in two different sets of state variables. First, the equation of motion of a vehicle is expressed in terms of the coordinates of a rotating rectangular system with the origin moving along an initial orbit about the earth. In this analysis it is assumed that only small deviations of the vehicle from the initial orbit are allowed. Therefore the gravitational terms in the equation of motion may be linearized; however, terms with time-varying coefficients appear in the equation. When the eccentricity of the orbits is small, the time-varying terms in the equation of motion are also small. The small parameter method is applied for obtaining an approximate solution of the differential equation with periodic coefficients.

Secondly, we introduce another set of state variables, i.e., the elements of an orbit. The orbital elements are constant if there is no force other than the inverse-square central gravitational force. The values of elements, however, change under the effect of the thrust force. If the thrust force is small compared with the central force, the instantaneous values of the elements change slowly with time. Consequently, another form of the linearized equation of motion is obtained.

These two methods of analysis are used for the study of the optimal thrust program. The motion of the vehicle and the fuel consumption under the action

of the optimal thrust are calculated. The dependence of the fuel consumption on the transfer time and on the position of departure from the initial orbit is also studied. Due to the difference of the assumptions for linearization, the two methods give slight disagreement in the results.

The results obtained by the linear analysis are compared with the numerical solutions which were previously obtained by W. G. Melbourne [20] and C. Saltzer [33]. Comparisons are made for the heliocentric transfer between the orbits of the earth and Mars.

The text is supplemented by four appendixes. In Appendix I are calculated the time intervals between switchings of the control in the reaction-jet attitude control system. Appendix II gives supplementary remarks concerning the time-optimal control in the reaction-wheel attitude control system. Appendix III describes the solutions of the equation associated with the motion of a vehicle in the transfer. Appendix IV derives the boundary condition of the transfer orbit.

ACKNOWLEDGMENTS

The author owes a lasting debt of gratitude to Professor Dr. C. Hayashi, who has suggested the field of research of the present thesis and has given him constant and generous guidance and encouragement in promoting this work.

In the preparation of the present paper the author has been given many aids and useful advices by Assistant Professor Dr. Y. Nishikawa.

The author is also grateful to the staffs and the graduate students of Dr. Hayashi's Laboratory for their excellent cooperation.

The KDC Digital Computer Laboratory of Kyoto University has made time available to the author. The author wishes to acknowledge the kind considerations of the staffs of these organizations.

CONTENTS

Introduction ii

Chapter 1. Optimal Attitude Control of an Orbiting Satellite Using Reaction Gas Jets

1.1 Introduction 1

1.2 Structure of an Attitude Control System 3

1.3 Gyrodynamical Equations of an Orbiting Satellite 3

1.4 Reaction Gas-Jet System 6

1.5 Time-Optimal Control 7

(a) Control of the Pitch Motion (System of Two Variables) 8

(b) Control of the Roll and Yaw Motion (System of Four Variables) 10

1.6 Minimum-Fuel Control 13

(a) Control of the Pitch Motion (System of Two Variables) 15

(b) Control of the Roll and Yaw Motion (System of Four Variables) 16

1.7 Attitude Oscillation of a Satellite in an Elliptic Orbit (Effect of Parametric Excitation) 19

1.8 Concluding Remarks 20

Chapter 2. Optimal Attitude Control of an Orbiting Satellite Using Reaction Wheels

2.1 Introduction 36

2.2 Reaction Wheel System 37

2.3 Time-Optimal Control 40

(a) Control of the Pitch Motion (System of Two Variables) 40

(b) Control of the Roll and Yaw Motion (System of Four Variables) 42

2.4 Minimum-Energy Control 43

(a) Control of the Pitch Motion (System of Two Variables) 44

(b) Control of the Roll and Yaw Motion (System of Four Variables) 50

2.5 Concluding Remarks 53

Chapter 3. Optimal Variable-Thrust Transfer between Neighboring Elliptic Orbits

3.1 Introduction 66

3.2 System Description 68

(a) Coordinate System 68

(b) Equations of Motion of the Vehicle 69

(c) Power-Limited Propulsion System 71

3.3 Optimal Control Functions 73

3.4 Boundary Conditions 78

3.5 Numerical Examples 81

(a) Transfer between Coplanar Ellipses of a Same Eccentricity Whose Axes Are Aligned and Oriented in the Same Sense 81

(b) Transfer between Coplanar Ellipses of a Same Eccentricity Whose Axes Are Aligned and Oriented in the Opposite Senses 84

(c) Transfer between Non-Coplanar Ellipses 86

3.6 Method of Analysis by Using Orbital Elements of a Space Vehicle 87

3.7 Orbital Elements and Their Perturbation 88

3.8 Equations of Motion of the Vehicle 90

3.9 Optimal Control Functions in Terms of Orbital Elements 93

3.10 Numerical Examples 97

(a) Transfer between Coplanar and Coaxial Ellipses of a Same Eccentricity 97

(b) Transfer between Non-Coplanar Ellipses 99

(c) Transfer from Earth to Mars 99

3.11 Concluding Remarks 103

Appendix I. Calculations of the Time Intervals between Switchings of the Controls (Reaction-Jet Attitude Control System) 128

Appendix II. Supplements Concerning Optimal Switching Policy of the Controls (Reaction-Wheel Attitude Control System) 132

Appendix III. Solutions of the Equation of Motion 139

Appendix IV. Derivation of the Boundary Condition 144

References 147

CHAPTER 1

OPTIMAL ATTITUDE CONTROL OF AN ORBITING SATELLITE USING REACTION GAS JETS

1.1 Introduction

Many satellites usually require some kind of attitude control system. The type of attitude control system depends upon the mission of orbiting satellites. For example, astronomical satellites must keep an inertial-fixed orientation, while satellites for communications and geophysical purposes require control to an earth-oriented reference.

There are essentially three different ways in which attitude control can be attained [16, 31, 32, 37]. Spin-stabilization techniques may be used when only one space-craft axis must be oriented in some inertial direction. Passive control techniques make use of the enviromental fields to generate control torques. The most common of these is gravity-gradient stabilization. The utilization of solar radiation pressure and earth's magnetic field may also provide passive stabilization. Active control techniques provide the greatest design flexibility for the controlled orientation of a satellite in the presence of disturbing torques. Optimization problems in active attitude control systems are, therefore, of great interest. There have been a number of papers on single-axis attitude control systems [8, 9, 19, 34]. The problems discussed here are concerned with three-axis control systems.

The first two chapters deal with the optimal attitude control of a

satellite which is in a steady orbit around the earth [21 - 24]. The orbit is either circular or elliptic with a small eccentricity. The satellite is assumed to be a single rigid body. Since attitude control with respect to the earth is considered, the earth-centered triad is taken as a reference frame of the attitude. The angular deviation of a satellite body relative to the reference frame is defined by the so-called modified Euler angle. The gyrodynamical equations of a satellite rotating in the three dimensional space consist of six first-order differential equations with three deviation angles and their time derivatives as dependent variables. These equations contain nonlinear terms, i.e., trigonometric functions of the angles. The equations are reduced to linear if one assumes that the angular deviations and their time derivatives are sufficiently small. In the case of a circular orbit, the gyrodynamical equations consist of terms with constant coefficients; while in the case of an elliptic orbit, terms with time-varying coefficients appear in the equations owing to periodical change of the angular velocity of the orbital motion.

Most modern attitude control systems employ either reaction gas jets or motor-driven reaction wheels to develop control torque [4, 12, 29, 39]. The former act as a means of transferring momentum away from the vehicle, and the latter as a momentum storage device. The torque-producing elements considered in this chapter are reaction gas jets. The time-optimal control and the minimum-fuel control are discussed in this system. The maximum principle is used for obtaining optimal control functions. The optimal switching policy of the control functions is investigated. The minimum settling time and the minimum fuel consumption are also determined for various initial states of the angular deviation.

1.2 Structure of an Attitude Control System

Figure 1.1 shows the schematic diagram of an active attitude control system [31]. The controlled element dynamics is characterized by a set of differential equations relating torques to the angular response of a satellite. Sensors detect deviation angles and rates of deviations of the satellite relative to a specified attitude reference frame. Control computer generates signals for the desired control torque components in response to sensed attitude errors. Function of control actuators is to apply desired torques to the satellite on the basis of control signals.

1.3 Gyrodynamical Equations of an Orbiting Satellite

Since equations for motion of the mass center of a satellite and equations for the attitude are independent each other, only the attitude equations are derived in what follows. Figure 1.2 shows earth-centered reference axes I, J, K. The I, J, K frame moves with its origin O at the gravity center of the satellite, where axis J is directed outward along the local vertical, and axis I lies in the opposite direction of motion. Axis K is normal to the orbit plane and directed so as to make I, J, K a right-handed triad. In Fig. 1.3 the attitude of the body is defined by modified Euler angles ϕ, θ, ψ, which determine the orientation of body-fixed axes i, j, k with respect to reference axes I, J, K. The right-handed triad i, j, k is fixed along the principal axes of inertia of the body. The angles ϕ, θ, and ψ are defined as follows:

1. Rotation through the angle ϕ about axis K brings I, J, K to $\bar{I}$, $\bar{J}$, K frame (pitching).

2. Rotation through the angle θ about axis $\bar{J}$ brings $\bar{I}$, $\bar{J}$, K to i, $\bar{J}$, $\bar{K}$ frame (yawing).

3. Rotation through the angle ψ about axis i brings i, $\bar{J}$, $\bar{K}$ to i, j, k frame (rolling).

The following symbols are introduced to describe the motion of the satellite.

A, B, C: principal moments of inertia about axes i, j, k, respectively.

$\mathbb{M}$: external torque applied to the satellite*; M_1, M_2, M_3 are its i, j, k components, respectively.

$\mathbb{h}$: angular momentum of the satellite.

Ω : angular velocity of the reference axes I, J, K relative to the inertial space.

ω : angular velocity of the satellite and the body axes i, j, k relative to the inertial space; ω_1, ω_2, ω_3 are its i, j, k components, respectively.

ω_r : angular velocity of the satellite relative to the reference axes.

The angular velocity of the reference frame is

$$\begin{aligned}\Omega &= 0\mathbb{I} + 0\mathbb{J} + \Omega\mathbb{K} \\ &= -\Omega \sin\theta\, \mathbb{i} + \Omega \sin\psi \cos\theta\, \mathbb{j} + \Omega \cos\psi \cos\theta\, \mathbb{k} \end{aligned} \qquad (1.1)$$

where Ω is the angular velocity of the radial line from the gravity center of the earth to the satellite. $\mathbb{I}$, $\mathbb{i}$, $\cdots$ denote the unit vectors along axes I, i, $\cdots$, respectively. The relative angular velocity ω_r is resolved into i, j, k components as†

---

* Here and throughout the text, gothic letters denote vector quantities.

$$\omega_r = (-\phi' \sin\theta + \psi')\,\mathring{i} + (\phi' \sin\psi \cos\theta + \theta' \cos\psi)\,\mathring{j} + (\phi' \cos\psi \cos\theta - \theta' \sin\psi)\,\mathring{k} \tag{1.2}$$

The angular velocity ω of the satellite is given by

$$\omega = \Omega + \omega_r \tag{1.3}$$

which is rewritten in terms of i, j, k components as

$$\left.\begin{aligned} \omega_1 &= -(\Omega + \phi')\sin\theta + \psi' \\ \omega_2 &= (\Omega + \phi')\sin\psi \cos\theta + \theta' \cos\psi \\ \omega_3 &= (\Omega + \phi')\cos\psi \cos\theta - \theta' \sin\psi \end{aligned}\right\} \tag{1.4}$$

The Euler equation of the rotational motion is [38, pp. 111-113]

$$M = h' + \omega \times h \tag{1.5}$$

where the prime denotes time derivative in the rotating body-fixed frame. In component forms Eq. (1.5) becomes

$$\left.\begin{aligned} M_1 &= A\omega_1' - (B - C)\omega_2\omega_3 \\ M_2 &= B\omega_2' - (C - A)\omega_3\omega_1 \\ M_3 &= C\omega_3' - (A - B)\omega_1\omega_2 \end{aligned}\right\} \tag{1.6}$$

Substitution of Eqs. (1.4) into (1.6) yields a set of the second-order differential equations where angles ϕ, θ, and ψ are dependent variables. Equations (1.6) contain nonlinear terms in angles ϕ, θ, and ψ. However, the nonlinear terms may be disregarded under the assumption that the deviation angles and their time rates are sufficiently small. Furthermore, we

---

† Here and throughout the text, primes denote differentiations with respect to time t.

assume the satellite to be a spherical body. Then, retaining terms linear in ϕ, θ, ψ and letting A = B = C yields

$$\left.\begin{aligned} \psi'' - \Omega\theta' - \Omega'\theta &= M_1/A \\ \theta'' + \Omega\psi' + \Omega'\psi &= M_2/A \\ \phi'' + \Omega' &= M_3/A \end{aligned}\right\} \tag{1.7}$$

The first and second equations are mutually related; while the third equation is independent of the first two. In other words, the roll and yaw motions described by ψ and θ are coupled each other; while the pitch motion described by ϕ is decoupled from the other motions.

When an orbit is circular, the angular velocity Ω of the orbital motion is constant. Sections 1.4, 1.5, and 1.6 are concerned with an investigation of the optimal control of the linear system described by Eqs. (1.7) with Ω constant. Control of the original nonlinear system (1.6) is briefly mentioned by showing particular numerical examples. A problem related to an elliptic orbit is studied in Sec. 1.7.

1.4 Reaction Gas-Jet System

The torque-producing elements considered in this chapter are reaction gas jets. The gas jets are assumed to expend negligible mass as compared with the total mass of the satellite. Most of modern gas-jet systems are characterized by the on-off type behavior [29, 39]. In this case the actuator torque is considered as a manipulated variable, or a control. For convenience, we introduce nondimensional quantities defined by

$$\left.\begin{aligned} &x_1 = \psi \quad x_2 = \dot{\psi} \quad x_3 = \theta \quad x_4 = \dot{\theta} \quad x_5 = \phi \quad x_6 = \dot{\phi} \\ &c = t_m\Omega \quad u_i = M_i/M_0 \ \ (i = 1,2,3) \quad \tau = t/t_m \quad t_m = \sqrt{A/M_0} \end{aligned}\right\} \tag{1.8}$$

where M_0 stands for the maximum value of the torque. A dot over a quantity denotes differentiation with respect to the normalized time τ.

By use of the quantities in Eqs. (1.8), Eqs. (1.7) are rewritten as

$$\left.\begin{aligned} \dot{x}_1 &= x_2 & \dot{x}_2 &= cx_4 + u_1 \\ \dot{x}_3 &= x_4 & \dot{x}_4 &= -cx_2 + u_2 \end{aligned}\right\} \tag{1.9}$$

and

$$\dot{x}_5 = x_6 \qquad \dot{x}_6 = u_3 \tag{1.10}$$

1.5 Time-Optimal Control

In the absence of disturbing torques, the satellite is rotating about axis K with angular velocity Ω, and the body-fixed axes of the satellite are coincident with the reference axes, i.e., $x_i = 0$ (i = 1 to 6). Now suppose that through the action of a disturbance the system at time $\tau = 0$ is not in the desired state, but in some other state x_i^0 (i = 1 to 6). Then we consider the problem of determining the control function in such a way that the system state is transferred from x_i^0 to the desired state $x_i = 0$ in the shortest possible time.

Time-optimal controls for the system described by Eqs. (1.9) and (1.10) can be obtained by use of Pontryagin's maximum principle. A Hamiltonian function for this system is given by [30, pp. 9-21]

$$H = p_1x_2 + p_2(cx_4 + u_1) + p_3x_4 + p_4(-cx_2 + u_2) + p_5x_6 + p_6u_3 \tag{1.11}$$

where the auxiliary variables p's satisfy the set of differential equations

$$\left.\begin{aligned} \dot{p}_1 &= 0 & \dot{p}_2 &= -p_1 + cp_4 \\ \dot{p}_3 &= 0 & \dot{p}_4 &= -p_3 - cp_2 \end{aligned}\right\} \tag{1.12}$$

and

$$\dot{p}_5 = 0 \qquad \dot{p}_6 = - p_5 \tag{1.13}$$

Maximum principle demands that, at every instant of time τ, the H-function must be maximum with respect to all admissible controls u_i ($i = 1,2,3$) [30, pp. 9-21]. This condition is satisfied by choosing the optimal controls $\bar{u}_i$ as

$$\left.\begin{aligned} \bar{u}_1(\tau) &= \operatorname{sgn} p_2(\tau) \\ \bar{u}_2(\tau) &= \operatorname{sgn} p_4(\tau) \end{aligned}\right\} \tag{1.14}$$

$$\bar{u}_3(\tau) = \operatorname{sgn} p_6(\tau) \tag{1.15}$$

Therefore the optimal controls must be of a bang-bang type.

Solving Eqs. (1.12) and (1.13) yields

$$\left.\begin{aligned} p_2(\tau) &= R \sin (c\tau + \theta) + P_2 \\ p_4(\tau) &= R \cos (c\tau + \theta) + P_4 \end{aligned}\right\} \tag{1.16}$$

$$p_6(\tau) = - P_5 \tau + P_6 \tag{1.17}$$

where R, θ, P_2, P_4, P_5, and P_6 are constants to be determined by the initial conditions.

(a) Control of the Pitch Motion (System of Two Variables)

First, we discuss the control of the pitch motion described by Eqs. (1.10) [8; 30, pp. 23-27]. As we see in Eq. (1.17), p_6 is linear in time τ. Hence, by virtue of Eq. (1.15), the optimal control $\bar{u}_3$ is piecewise constant and can switch, at most, once. Two modes of switching listed in Table 1.1 are the only candidates for the time-optimal control of this system. We can solve Eqs. (1.10) using the value of $\bar{u}_3$ in Table 1.1 with

the initial conditions $x_5 = x_5^0$ and $x_6 = x_6^0$. A phase trajectory of the solution thus obtained is shown in Fig. 1.4. The optimal trajectory consists of generally two adjoining parabolic segments. A switching curve is shown dotted in the figure.

The time intervals τ_1 and τ_2 of Mode I are related to initial values x_5^0 and x_6^0 by

$$\left.\begin{aligned} x_5^0 &= (\tau_2^2 - \tau_1^2)/2 + \tau_1 \tau_2 \\ x_6^0 &= \tau_1 - \tau_2 \end{aligned}\right\} \tag{1.18}$$

The signs of x_5^0 and x_6^0 should be reversed for Mode II. Equations (1.18) give

$$\left.\begin{aligned} \tau_1 &= [(x_6^0)^2/2 \pm x_5^0]^{1/2} \pm x_6^0 \\ \tau_2 &= [(x_6^0)^2/2 \pm x_5^0]^{1/2} \end{aligned}\right\} \tag{1.19}$$

where the plus signs correspond to Mode I, and the minus signs are for Mode II. The shortest settling time τ is given by

$$\tau = \tau_1 + \tau_2 = [2(x_6^0)^2 \pm 4x_5^0]^{1/2} \pm x_6^0 \tag{1.20}$$

Table 1.1. Mode of switching of $\bar{u}_3(\tau)$ for the time-optimal control

Mode	Time interval τ_1	τ_2
I	- 1	1
II	1	- 1

(b) Control of the Roll and Yaw Motion (System of Four Variables)

Secondly, we are concerned with the control of the roll and yaw motion described by Eqs. (1.9) [21, 22]. From Eqs. (1.16), a representative point on the p_2p_4 plane moves along a circle at the uniform rate c, as shown in Fig. 1.5. In the figure the arrows indicate the direction of motion of the representative point with increasing time τ. The sign of $\bar{u}_1$ is reversed at the instant in which the representative point traverses axis p_4; while $\bar{u}_2$ is reversed when the point passes through axis p_2. Considering that the normalized angular velocity of the orbital motion c is small and that the settling time is also small because of slight angular deviations, we may conclude that the reversal of the signs of $\bar{u}_1$ and $\bar{u}_2$ occurs three times at most.

Equations (1.9) may be rewritten in a vector form as

$$\dot{\mathcal{X}} = A\mathcal{X} + \mathcal{U} \tag{1.21}$$

where

$$\mathcal{X} = \begin{pmatrix} x_1 \\ x_2 \\ x_3 \\ x_4 \end{pmatrix}, \qquad A = \begin{pmatrix} 0 & 1 & 0 & 0 \\ 0 & 0 & 0 & c \\ 0 & 0 & 0 & 1 \\ 0 & -c & 0 & 0 \end{pmatrix}, \qquad \mathcal{U} = \begin{pmatrix} 0 \\ u_1 \\ 0 \\ u_2 \end{pmatrix} \tag{1.22}$$

The fundamental matrix $X(\tau)$ of the linear part of Eq. (1.21) is given by

$$X(\tau) = \begin{pmatrix} 1 & \frac{1}{c}\sin c\tau & 0 & -\frac{1}{c}\cos c\tau + \frac{1}{c} \\ 0 & \cos c\tau & 0 & \sin c\tau \\ 0 & \frac{1}{c}\cos c\tau - \frac{1}{c} & 1 & \frac{1}{c}\sin c\tau \\ 0 & -\sin c\tau & 0 & \cos c\tau \end{pmatrix} \tag{1.23}$$

The relationship between an initial condition $\mathcal{X}^0$ of $\mathcal{X}$ and the duration of time intervals between switchings is given by [2]

$$\mathcal{X}^0 = \int_0^{-\tau_4} X(-\tau - s)\, \mathcal{U}_4 ds + \int_{-\tau_4}^{-\tau_4-\tau_3} X(-\tau - s)\, \mathcal{U}_3 ds + \int_{-\tau_4-\tau_3}^{-\tau+\tau_1} X(-\tau - s)\, \mathcal{U}_2 ds + \int_{-\tau+\tau_1}^{-\tau} X(-\tau - s)\, \mathcal{U}_1 ds \qquad (1.24)$$

where τ_j : time intervals between switchings, i.e., transition time between points S_{j-1} and S_j ($j = 1$ to 4) on the p_2p_4 plane (see Fig. 1.5)

$\mathcal{U}_j$: value of $\mathcal{U}$ during the time interval τ_j

$$\tau = \sum_{j=1}^{4} \tau_j$$

There are twelve possibilities for the mode of switching of $\bar{u}_1$ and $\bar{u}_2$ as listed in Table 1.2. The values of $\bar{u}_1$ and $\bar{u}_2$ are denoted, respectively, by the front and the rear number of the doublet in this table; for instance, 1, -1 means $\bar{u}_1 = 1$ and $\bar{u}_2 = -1$. Integral calculations of Eq. (1.24) are shown in Appendix I.1.

Numerical Example

The normalized angular velocity is chosen as $c = 0.1$.* Figure 1.6

---

* By way of an example, when

$$\Omega = 1.16 \times 10^{-3} \text{ rad/sec (90 min/cycle)}$$

$$A = 10 \text{ kg-m}^2 \qquad M_0 = 10^{-3} \text{ newton-m}$$

the time constant and the normalized angular velocity become

$$t_m = 10^2 \text{ sec} \qquad c = 0.116$$

shows the relationship between initial values x_1^0, x_3^0 and the possible shortest settling time τ to reduce x^0 to 0 in the case where $x_2^0 = 0$, $x_4^0 = 0$, i.e., both the initial velocities of deviations are zero. We see in the figure that τ is approximately proportional to the square of $\max(|x_1^0|, |x_3^0|)$. For initial conditions given in each of twelve regions in the figure, the optimal controls must follow the switching mode indicated in that region.

Table 1.2. Mode of switching of $\bar{u}_1(\tau)$ and $\bar{u}_2(\tau)$ for the time-optimal control

Mode	Time interval			
	τ_1	τ_2	τ_3	τ_4
I.1	1, -1	-1, -1	1, -1	1, 1
I.2	1, -1	-1, -1	-1, 1	1, 1
I.3	1, -1	1, 1	-1, 1	1, 1
II.1	1, 1	1, -1	1, 1	-1, 1
II.2	1, 1	1, -1	-1, -1	-1, 1
II.3	1, 1	-1, 1	-1, -1	-1, 1
III.1	-1, 1	1, 1	-1, 1	-1, -1
III.2	-1, 1	1, 1	1, -1	-1, -1
III.3	-1, 1	-1, -1	1, -1	-1, -1
IV.1	-1, -1	-1, 1	-1, -1	1, -1
IV.2	-1, -1	-1, 1	1, 1	1, -1
IV.3	-1, -1	1, -1	1, 1	1, -1

The regions I ~ IV are located $\pi/2$-symmetrically about the origin. Figure 1.7 shows the relationship between initial values x_2^0, x_4^0 and τ in the case where $x_1^0 = 0$, $x_3^0 = 0$, i.e., both the initial deviation angles are zero. In this case τ is approximately proportional to $\max(|x_2^0|, |x_4^0|)$.

Figure 1.8 illustrates iso- τ_j ($j = 1$ to 4) curves for Mode I on the $x_1^0 x_3^0$ plane ($x_2^0 = 0$, $x_4^0 = 0$). Rotating these curves by $\pi/2$, π, $3\pi/2$ radians in the counterclockwise direction yields iso- τ_j curves for Modes II, III, IV, respectively.

Application of the optimal controls thus obtained to the linearized systems (1.9) and (1.10) gives us the optimal phase trajectory leading to the origin for any initial state. The optimal controls for the linearized system are not optimal for the original nonlinear system (1.6). The corresponding trajectory for the nonlinear system can not lead to the origin but can reach the neighborhood of the origin. An example of the phase-plane trajectories of x_i ($i = 1$ to 6) is illustrated in Fig. 1.9, where the initial values are $x_1^0 = 0.087$, $x_3^0 = 0.099$, $x_5^0 = 0.090$, and $x_2^0 = x_4^0 = x_6^0 = 0$. The solid and the dotted curves are obtained for the nonlinear system (1.6) and the linearized systems (1.9) and (1.10), respectively.

1.6 Minimum-Fuel Control

In the preceding section, we investigated the time-optimal attitude control of an orbiting satellite. In space vehicles it is often important to minimize the amount of fuel or energy, instead of the settling time, allotted for the control requirement. This section deals with the minimum-fuel control in a reaction gas-jet system [3, 8, 9, 19, 23, 24, 34].

The thrust of jet T_J is approximately given by [35]

$$T_J = v_e \frac{dm}{dt} \tag{1.25}$$

where dm/dt is the mass flow rate of exhaust gas, and v_e is the exit velocity. If v_e is assumed to be constant, the rate of fuel consumption is proportional to control torque. Thus, the functional to be minimized may be taken in nondimensional quantities as

$$F = \int_0^T (|u_1| + |u_2| + |u_3|)d\tau \tag{1.26}$$

where T is a prescribed settling time. The time T must be larger than or equal to the possible minimum settling time which depends on an initial angular state.

The optimal controls for the system described by Eqs. (1.9) and (1.10) with the consideration of cost function (1.26) can be obtained by using the maximum principle. The Hamiltonian function of the problem is

$$\begin{aligned} H = {} & p_1 x_2 + cp_2 x_4 + p_3 x_4 - cp_4 x_2 + p_5 x_6 \\ & + (p_2 u_1 - |u_1|) + (p_4 u_2 - |u_2|) + (p_6 u_3 - |u_3|) \end{aligned} \tag{1.27}$$

Hence we obtain the optimal controls $\bar{u}_i$ (i = 1,2,3) as

$$\left.\begin{aligned} \bar{u}_1(\tau) &= \begin{cases} 0 & \text{for } |p_2(\tau)| \leq 1 \\ \operatorname{sgn} p_2(\tau) & \text{for } |p_2(\tau)| > 1 \end{cases} \\ \bar{u}_2(\tau) &= \begin{cases} 0 & \text{for } |p_4(\tau)| \leq 1 \\ \operatorname{sgn} p_4(\tau) & \text{for } |p_4(\tau)| > 1 \end{cases} \end{aligned}\right\} \tag{1.28}$$

$$\bar{u}_3(\tau) = \begin{cases} 0 & \text{for } |p_6(\tau)| \leq 1 \\ \operatorname{sgn} p_6(\tau) & \text{for } |p_6(\tau)| > 1 \end{cases} \tag{1.29}$$

Namely, the optimal controls are of an on-off type, assuming only the three values, ± 1 or 0.

The system of equations for the auxiliary variables p's was given by Eqs. (1.12) and (1.13) in Sec. 1.5.

(a) Control of the Pitch Motion (System of Two Variables)

As we observe in Eq. (1.17), p_6 is linear in time τ. Hence, by virtue of Eqs. (1.29), the value of $\bar{u}_3$ changes twice at most. Possible modes of switching are listed in Table 1.3.

The time intervals τ_j (j = 1,2,3) of Mode I are related to initial values x_5^0 and x_6^0 by

$$\left.\begin{aligned} x_5^0 &= -(\tau_2^2/2 + \tau_2\tau_3 + \tau_3^2) + (\tau_2 + 2\tau_3)T - T^2/2 \\ x_6^0 &= \tau_1 - \tau_3 \end{aligned}\right\} \qquad (1.30)$$

and

$$T = \tau_1 + \tau_2 + \tau_3$$

The signs of x_5^0 and x_6^0 are reversed for Mode II. If the initial velocity is zero, i.e., $x_6^0 = 0$, Eqs. (1.30) give

Table 1.3. Mode of switching of $\bar{u}_3(\tau)$ for the minimum-fuel control

Mode	Time interval		
	τ_1	τ_2	τ_3
I	-1	0	1
II	1	0	-1

$$\left.\begin{aligned} \tau_1 &= \tau_3 = [T - (T^2 - 4|x_5^0|)^{1/2}]/2 \\ \tau_2 &= (T^2 - 4|x_5^0|)^{1/2} \end{aligned}\right\} \tag{1.31}$$

Equations (1.31) require that

$$T \geq 2\sqrt{|x_5^0|} \tag{1.32}$$

We note that the right side of Eq. (1.32) is equal to the minimum settling time in this case [see Eq. (1.20)].

Figure 1.10 shows an optimal trajectory on the x_5x_6 plane in the case where $x_6^0 = 0$. The curve ℓ_1 indicates the locus of switching points from $\bar{u}_3 = -1$ to $\bar{u}_3 = 0$, and ℓ_2 is that of $\bar{u}_3 = 0$ to $+1$ switch points. These loci are given by

$$\left.\begin{aligned} \ell_1 &: \quad x_5 = -3x_6^2/2 - Tx_6 \\ \ell_2 &: \quad x_5 = x_6^2/2 \end{aligned}\right\} \tag{1.33}$$

The amount of consumed fuel may be calculated by using Eqs. (1.26) and (1.30). In the case of zero initial velocity the consumed fuel F_3 is given by

$$F_3 = \int_0^T |\bar{u}_3|\, d\tau = \tau_1 + \tau_3 = T - (T^2 - 4|x_5^0|)^{1/2} \tag{1.34}$$

The dependence of F_3 on the settling time T is illustrated in Fig. 1.11.

(b) Control of the Roll and Yaw Motion (System of Four Variables)

As we see in Eqs. (1.16), a representative point on the p_2p_4 plane moves along a circle at the uniform rate c. By virtue of Eqs. (1.28), the value of $\bar{u}_1$ must be switched at the instant in which the representative point traverses the lines $p_2 = \pm 1$; while $\bar{u}_2$ must be switched when the

point passes through the lines $p_4 = \pm 1$. By a consideration analogous to that of Sec. 1.5(b), we may conclude that switching of the values of $\bar{u}_1$ and $\bar{u}_2$ occurs six times at most. We may also conclude that four switchings are sufficient for most of the initial states; Table 1.4 shows the possible modes of switching in this case.

Table 1.4. Mode of switching of $\bar{u}_1(\tau)$ and $\bar{u}_2(\tau)$ for the minimum-fuel control

Mode	Time interval				
	τ_1	τ_2	τ_3	τ_4	τ_5
I.1	-1, -1	-1, 0	0, 0	1, 0	1, 1
I.2	-1, -1	0, -1	0, 0	1, 0	1, 1
I.3	-1, -1	0, -1	0, 0	0, 1	1, 1
I.4	1, -1	0, -1	0, 0	0, 1	1, 1
II.1	1, -1	0, -1	0, 0	0, 1	-1, 1
II.2	1, -1	1, 0	0, 0	0, 1	-1, 1
II.3	1, -1	1, 0	0, 0	-1, 0	-1, 1
II.4	1, 1	1, 0	0, 0	-1, 0	-1, 1
III.1	1, 1	1, 0	0, 0	-1, 0	-1, -1
III.2	1, 1	0, 1	0, 0	-1, 0	-1, -1
III.3	1, 1	0, 1	0, 0	0, -1	-1, -1
III.4	-1, 1	0, 1	0, 0	0, -1	-1, -1
IV.1	-1, 1	0, 1	0, 0	0, -1	1, -1
IV.2	-1, 1	-1, 0	0, 0	0, -1	1, -1
IV.3	-1, 1	-1, 0	0, 0	1, 0	1, -1
IV.4	-1, -1	-1, 0	0, 0	1, 0	1, -1

The time intervals τ_j (j = 1 to 5) in Table 1.4 are related to an initial value $\mathcal{X}^0$ by [2]

$$\left.\begin{aligned}\mathcal{X}^0 = &\int_0^{-\tau_5} X(-T-s)\,\mathcal{U}_5 ds + \int_{-\tau_5}^{-\tau_5-\tau_4} X(-T-s)\,\mathcal{U}_4 ds \\ &+ \int_{-\tau_5-\tau_4}^{-\tau_5-\tau_4-\tau_3} X(-T-s)\,\mathcal{U}_3 ds + \int_{-\tau_5-\tau_4-\tau_3}^{-T+\tau_1} X(-T-s)\,\mathcal{U}_2 ds \\ &+ \int_{-T+\tau_1}^{-T} X(-T-s)\,\mathcal{U}_1 ds \\ T = &\sum_{j=1}^{5} \tau_j\end{aligned}\right\} \qquad (1.35)$$

where vectors $\mathcal{X}$ and $\mathcal{U}$ are defined by Eqs. (1.22). $\mathcal{U}_j$ is the value of $\mathcal{U}$ during the time interval τ_j. The fundamental matrix $X(\tau)$ is given by Eq. (1.23). In Appendix I.2 is shown the relationship between $\mathcal{X}^0$ and τ_j for each mode in Table 1.4.

Numerical Example

Let us consider a case where c = 0.1 and T = 1. The object of control is to make all the state variables x_1 to x_4 zero at $\tau = T = 1$ in the minimum-fuel process. Figure 1.12 shows the relationship between initial values x_1^0, x_3^0 and the minimum-fuel consumption F in the case where $x_2^0 = 0$ and $x_4^0 = 0$. From the result of investigation of the time-optimal control (Fig. 1.6), it is known that any initial state located in the region inside the dotted lines can be restored to the origin in an interval of time less than or equal to unity. By making use of Eqs. (1.35), one may conclude that the square area bordered by the lines $|x_1^0| = 0.25$ and $|x_3^0| = 0.25$ is the region of initial states which can be restored to the origin by the minimum-fuel

controls of Table 1.4. The controls require generally four switchings. This region is divided into sixteen subregions as marked by I.1, I.2,..., IV.4. If an initial value is prescribed in one of the subregions, say I.1, the optimal control must be switched as indicated in Table 1.4 by the same number of mode. The regions I to IV are located $\pi/2$-symmetrically about the origin. The narrow areas bordered by the dotted lines and the lines $|x_1^0| = 0.25$ or $|x_3^0| = 0.25$ are the regions of initial states restored to the origin by five or six switchings of the control.

Figure 1.13 illustrates the iso- τ_j ($j = 1$ to 5) curves for Mode I on the $x_1^0 x_3^0$ plane ($x_2^0 = 0$, $x_4^0 = 0$). Rotating these curves by $\pi/2$, π, and $3\pi/2$ radians in the counterclockwise direction yields the iso- τ_j curves for Modes II, III, and IV, respectively.

The optimal controls for the linearized system of Eqs. (1.9) and (1.10) are not optimal for the nonlinear system of Eqs. (1.6). An example of the phase-plane trajectories of x_i ($i = 1$ to 6) is illustrated in Fig. 1.14, where the initial values are $x_1^0 = 0.103$, $x_3^0 = 0.100$, $x_5^0 = 0.100$, and $x_2^0 = x_4^0 = x_6^0 = 0$. The solid and the dotted curves are obtained for the original nonlinear system (1.6) and the linearized systems (1.9) and (1.10), respectively.

1.7 Attitude Oscillation of a Satellite in an Elliptic Orbit (Effect of Parametric Excitation)

For a satellite revolving along an elliptic orbit, angular velocity Ω of the earth-centered frame is approximately given by

$$\Omega = \overline{\Omega} [1 + 2\varepsilon \cos \overline{\Omega} (t - t_p)] \tag{1.36}$$

where $\bar{\Omega}$ is the mean value of Ω over one revolution along the orbit, and t_p denotes the time at which the satellite passes through the perigee. Under the assumption that the eccentricity ε is not so large, terms of order higher than the first in ε are discarded in Eq. (1.36). Periodical change of Ω produces terms with periodic coefficients in the attitude equations (1.7). Substituting Eq. (1.36) into (1.7) and solving for $M_1 = M_2 = M_3 = 0$ gives us

$$\left.\begin{aligned}
\psi &= r \sin(\tau + \alpha) + \psi_0 + \varepsilon[-2r \sin(\tau + \alpha) - \theta_0 \sin\tau \\
&\quad - 2\psi_0 \cos\tau - \psi_0 \tau \sin\tau + \theta_0 \tau \cos\tau \\
&\quad + r \sin(2\tau + \alpha) + r \sin\alpha + 2\psi_0] \\
\theta &= r \cos(\tau + \alpha) + \theta_0 + \varepsilon[-2r \cos(\tau + \alpha) + \psi_0 \sin\tau \\
&\quad - 2\theta_0 \cos\tau - \theta_0 \tau \sin\tau - \psi_0 \tau \cos\tau \\
&\quad + r \cos(2\tau + \alpha) + r \cos\alpha + 2\theta_0] \\
\phi &= \phi_1 \tau + \phi_0 - 2\varepsilon(\cos\tau - 1)
\end{aligned}\right\} \quad (1.37)$$

where r, α, ψ_0, θ_0, ϕ_0, and ϕ_1 are constants of integration, and $\tau = \bar{\Omega}(t - t_p)$. The oscillatory terms which grow up indefinitely with time t appear in ψ and θ.

The optimal control of a system with time-varying parameters is a rather complicated problem. If one could assume that $\bar{\Omega}t$ is small, the problem reduces to the control of a system with time-invariant parameters by replacing Ω with $\bar{\Omega}(1 + 2\varepsilon \cos\bar{\Omega}t_p)$.

1.8 Concluding Remarks

The optimization problems in the attitude control of an orbiting satellite are investigated. The gyrodynamical equations of a satellite contain

nonlinear terms, i.e., trigonometric functions of the angles. These equations are reduced to linear if one assumes that the angular deviations and their time rates are sufficiently small. The linearized equations (1.7) show that the pitch motion is independent of the roll and yaw motions. The former is characterized as the system of two variables, while the latter as that of four variables.

The torque-producing elements considered in this chapter are reaction gas jets. Most of modern gas-jet systems are characterized by on-off type behavior. In this case the normalized actuator torque is considered as a control function. The time-optimal control and the minimum-fuel control are discussed in this system. In time optimization, the optimal controls are of an on-off type, assuming the values ± 1. The control function for the system of two variables changes sign once at most; while, in the system of four variables, the reversal of the sign of controls occurs three times at most. In fuel minimization, the optimal controls are again of on-off type, but taking the third value 0 as well as ± 1. The controls require generally two switchings in the system of two variables, and six (usually four) switchings in the system of four variables, respectively. The shortest settling time and the minimum fuel consumption have been determined for various initial states of angular deviation. Control of the original nonlinear system has also been mentioned by illustrating particular numerical examples. Figures 1.9 and 1.14 show that the linearized system is a good approximation to the original one.

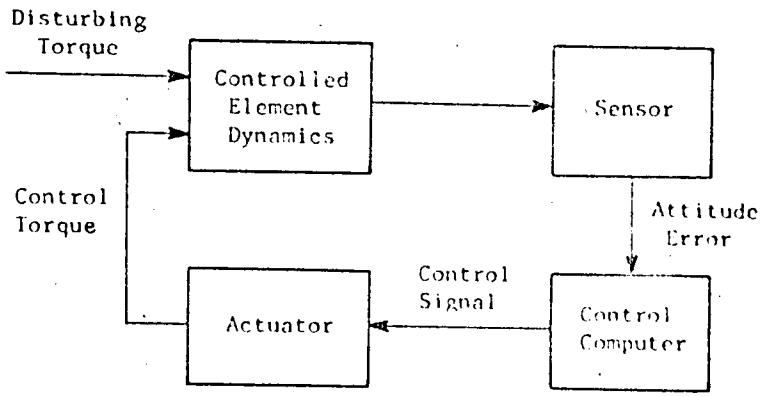

Fig. 1.1. Schematic diagram of an active attitude control system.

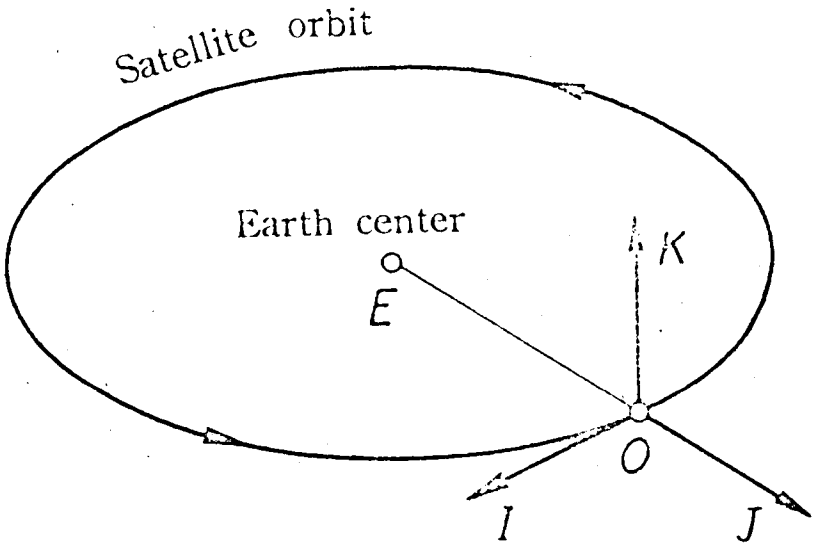

Fig. 1.2. Earth-centered reference frame.

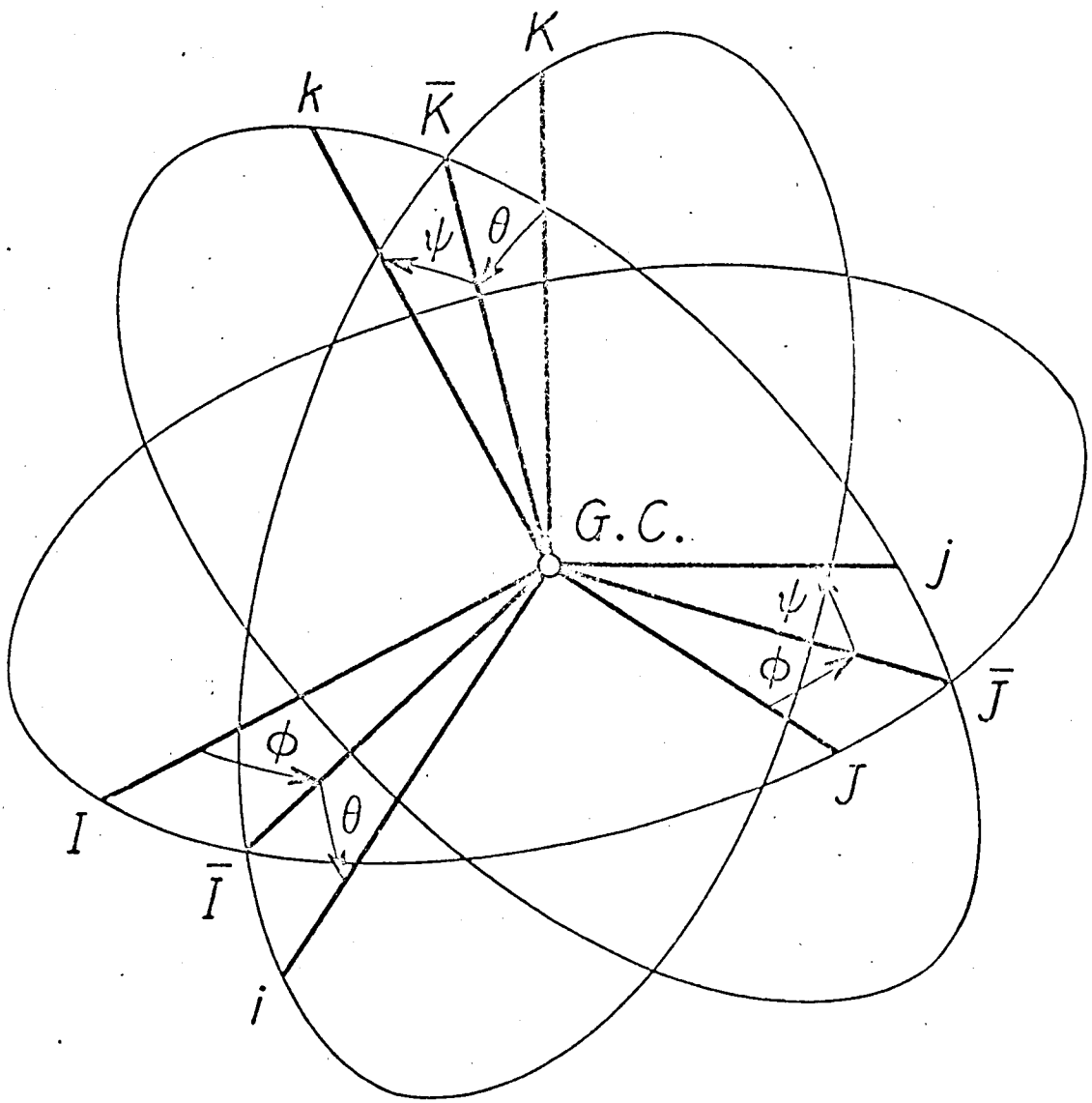

Fig. 1.3. Reference axes and body-fixed axes.

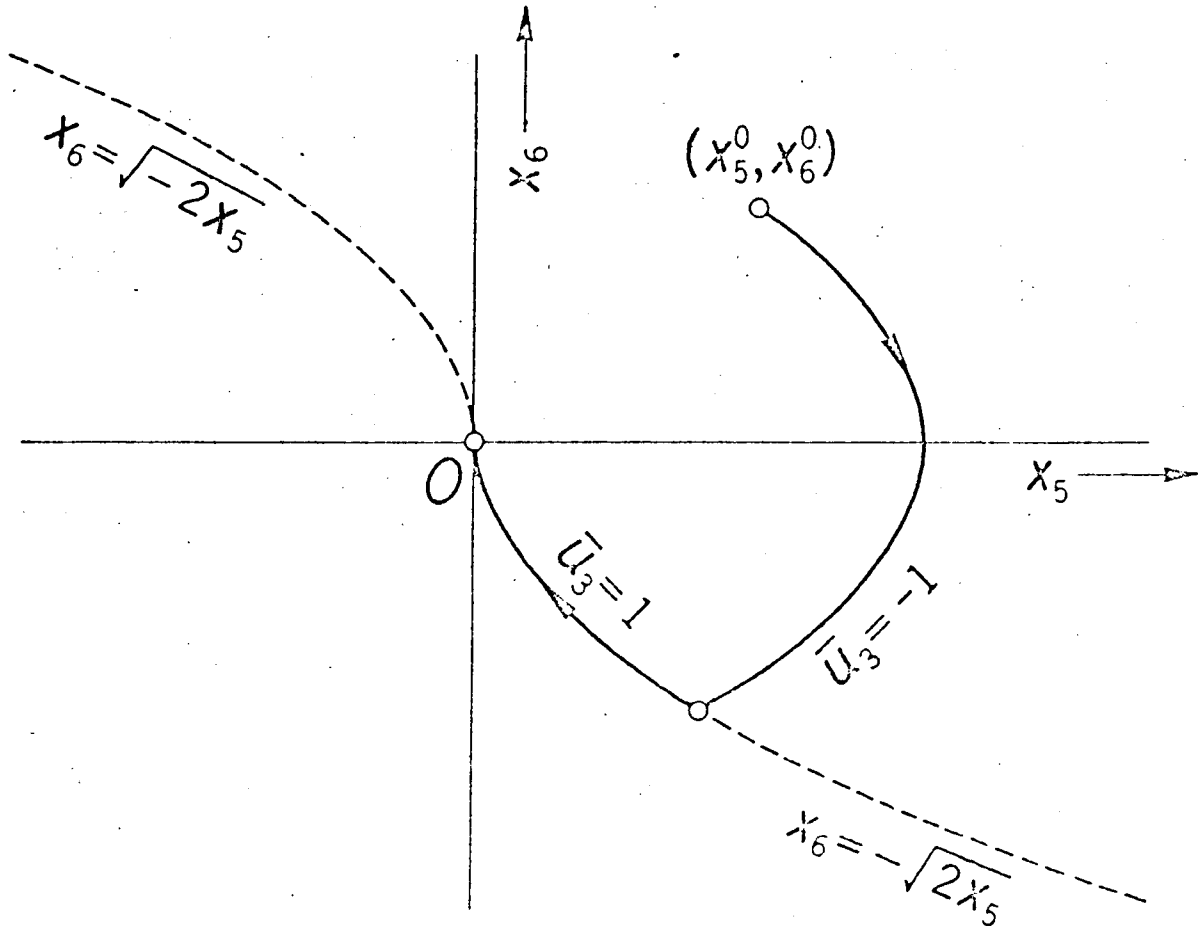

Fig. 1.4. Phase trajectory on the x_5x_6 plane for the time-optimal control.

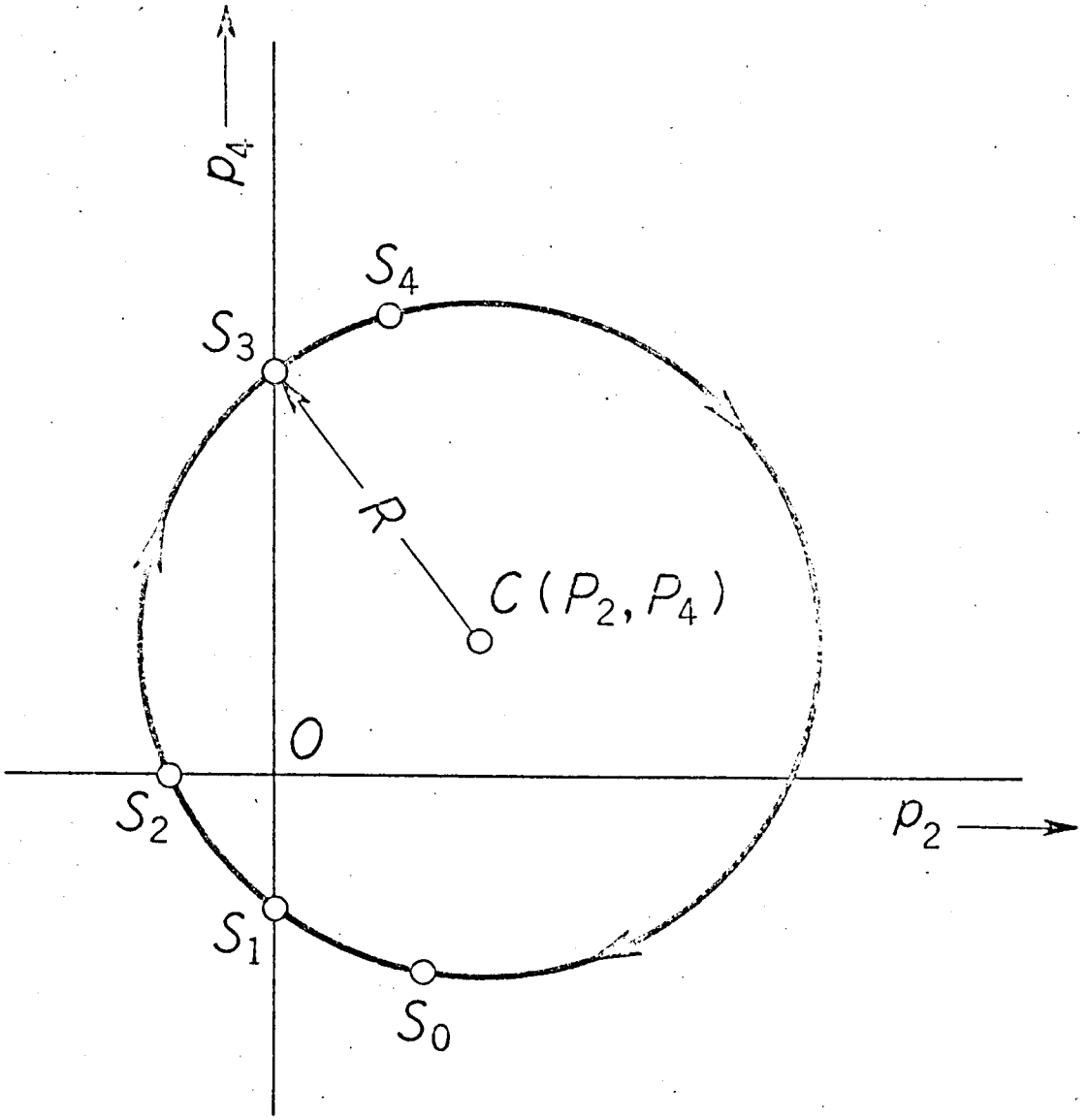

Fig. 1.5. Trajectory on the p_2p_4 plane.

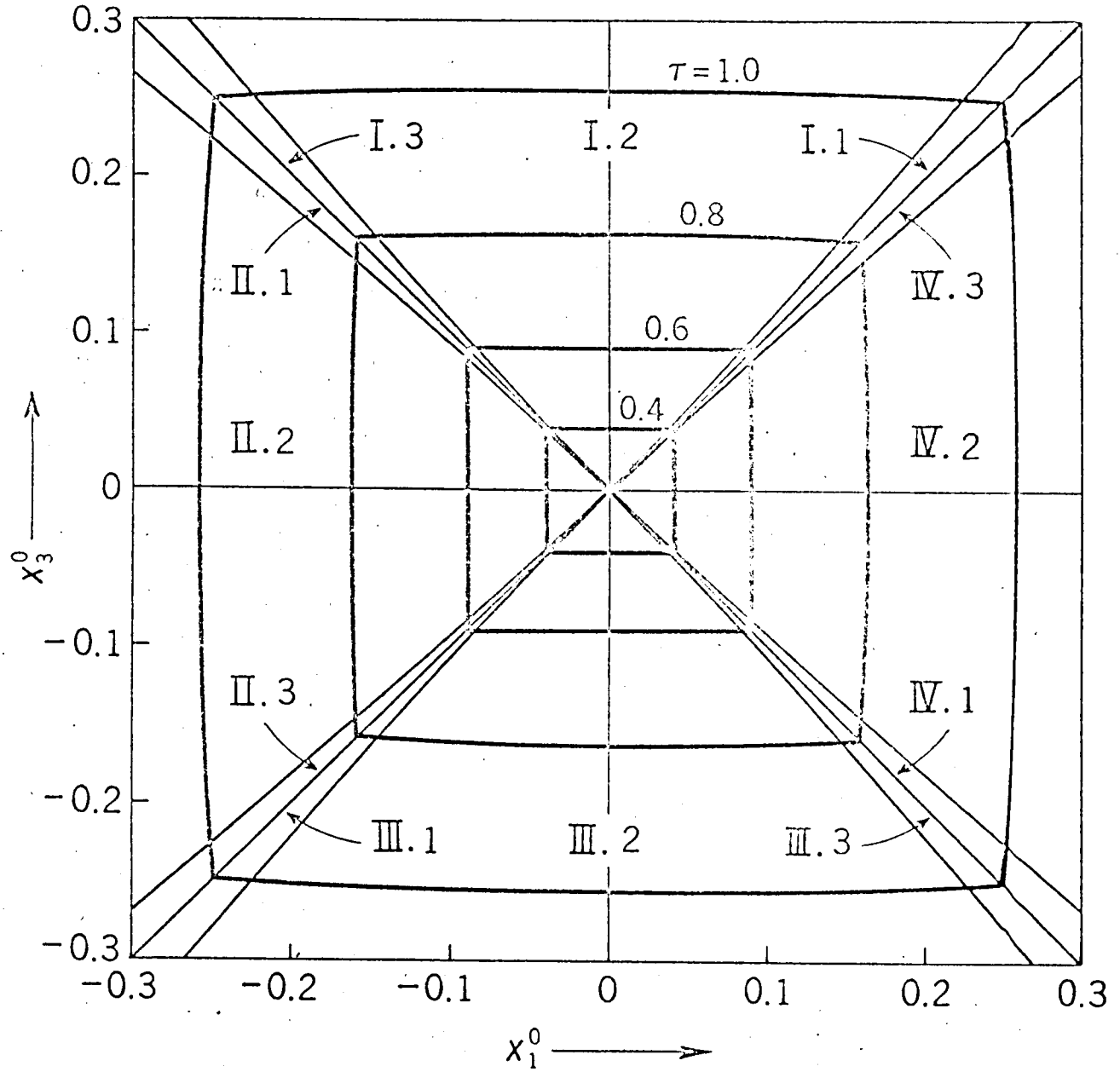

Fig. 1.6. Iso-τ curves on the $x_1^0 x_3^0$ plane ($x_2^0 = 0$ and $x_4^0 = 0$).

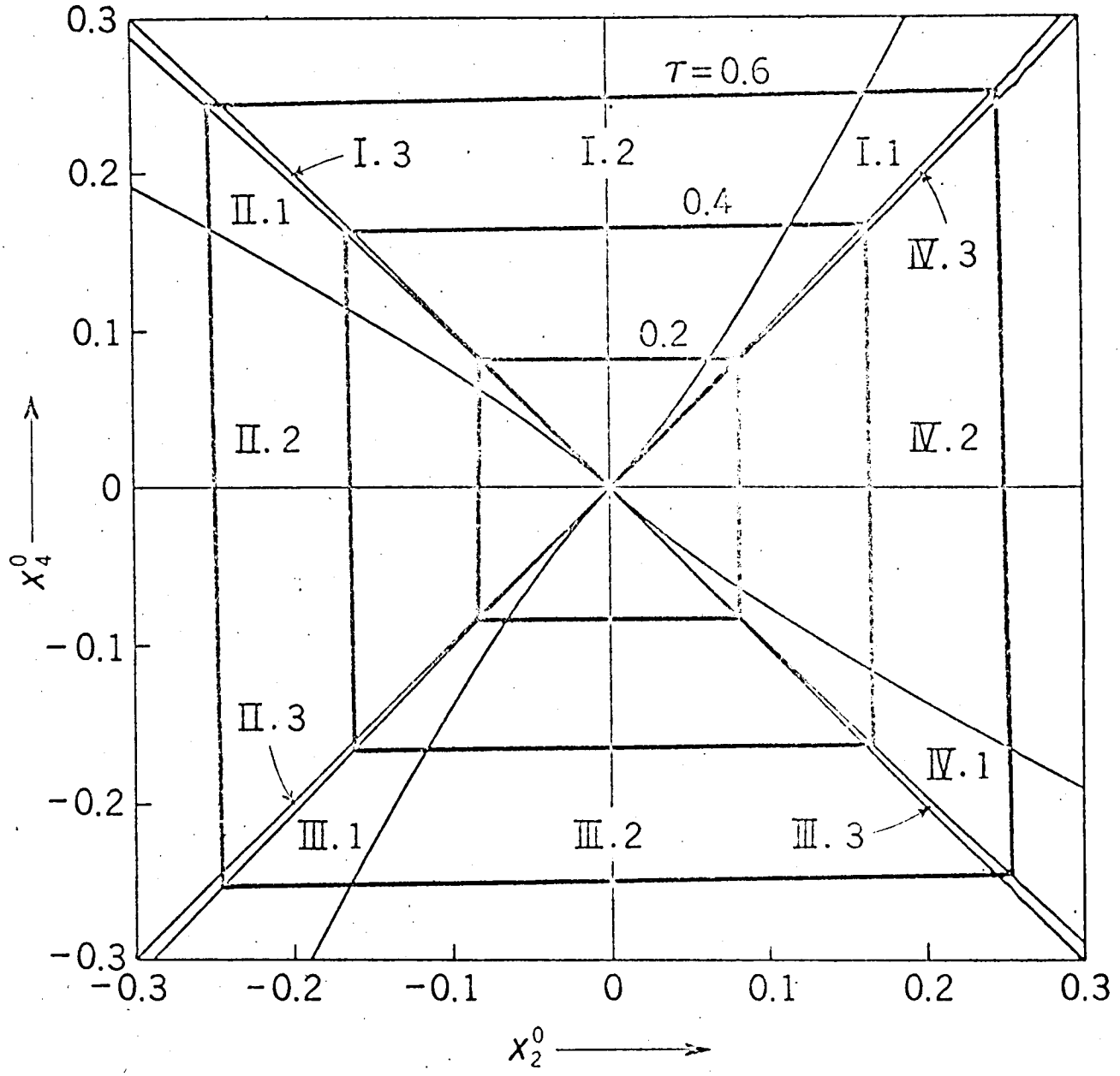

Fig. 1.7. Iso-τ curves on the $x_2^0 x_4^0$ plane ($x_1^0 = 0$ and $x_3^0 = 0$).

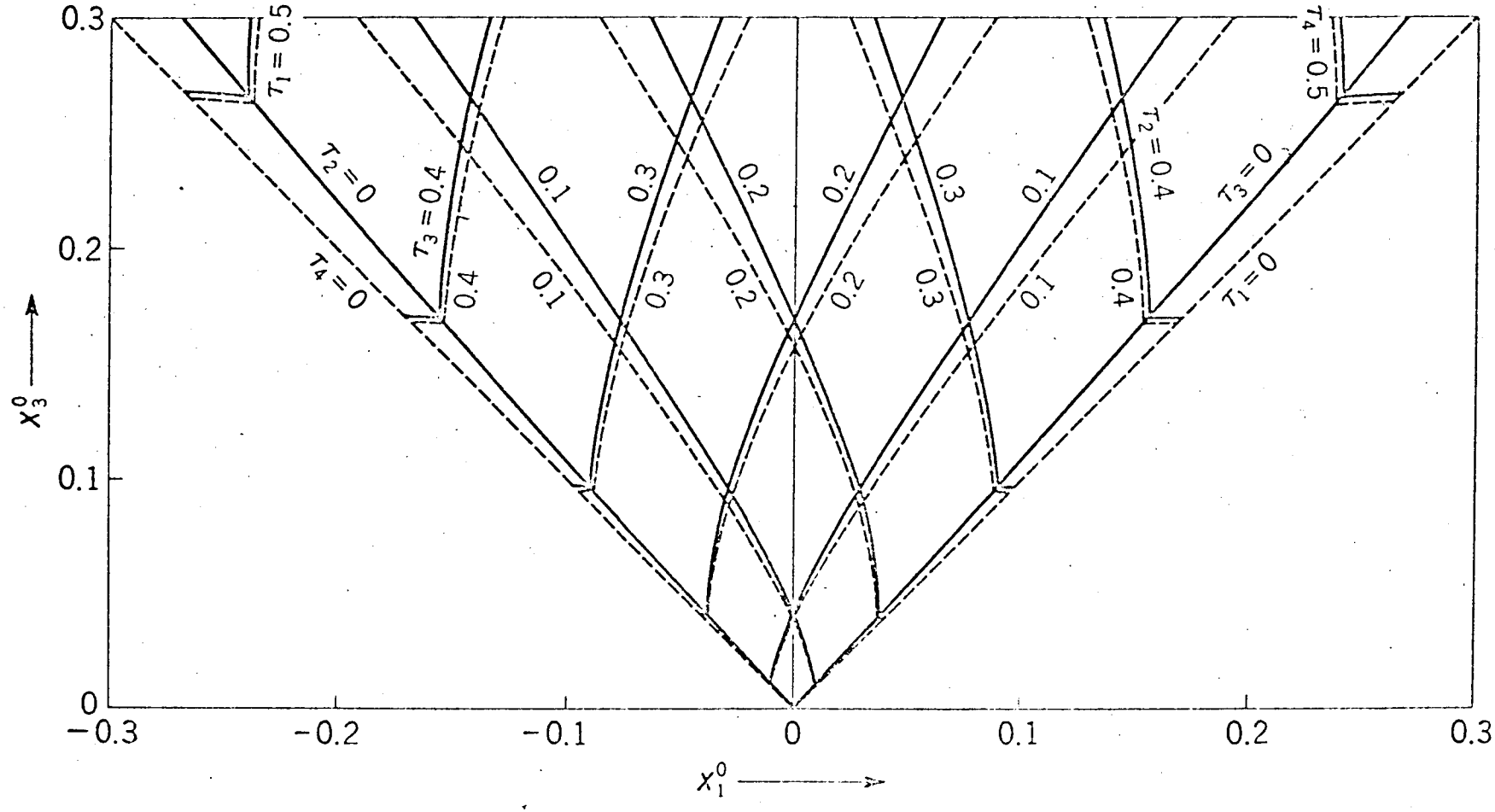

Fig. 1.8. Iso- τ_j curves for Mode I on the $x_1^0 x_3^0$ plane ($x_2^0 = 0$ and $x_4^0 = 0$).

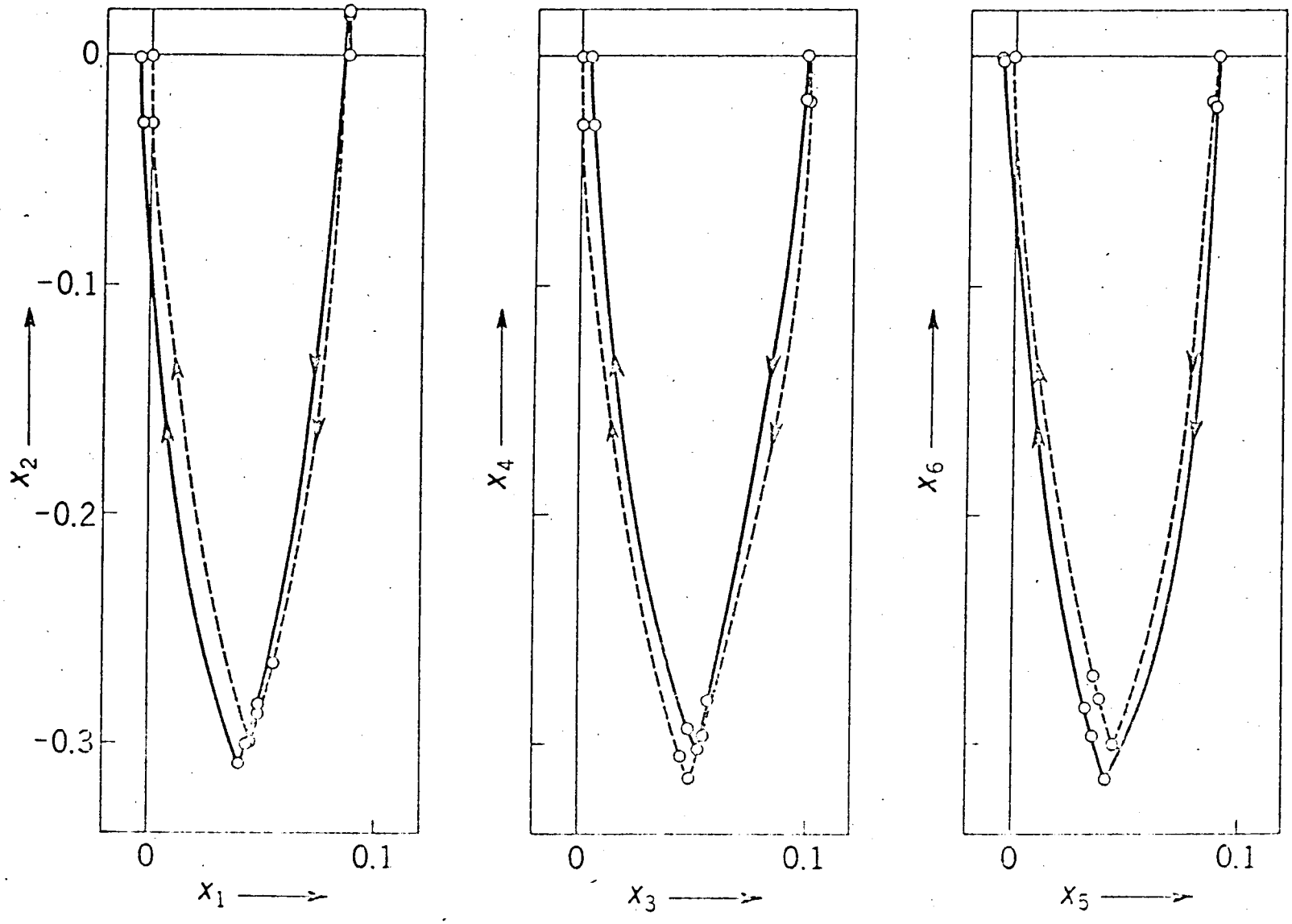

Fig. 1.9. Trajectories of the state variables $x_1 \sim x_6$ in the time-optimal control.

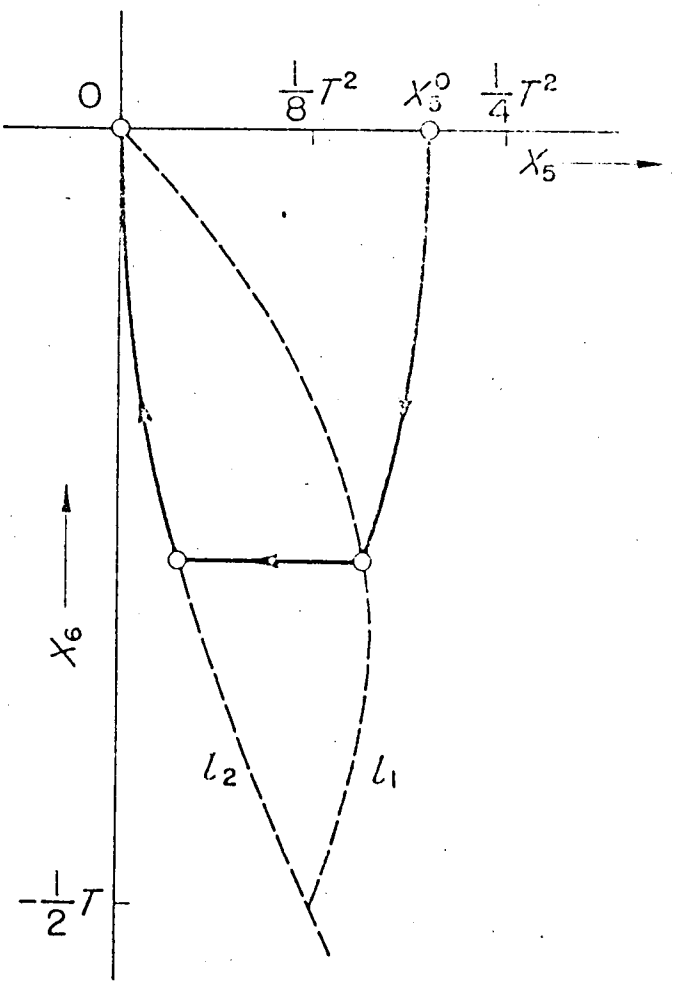

Fig. 1.10. Phase trajectory on the x_5x_6 plane for the minimum-fuel control.

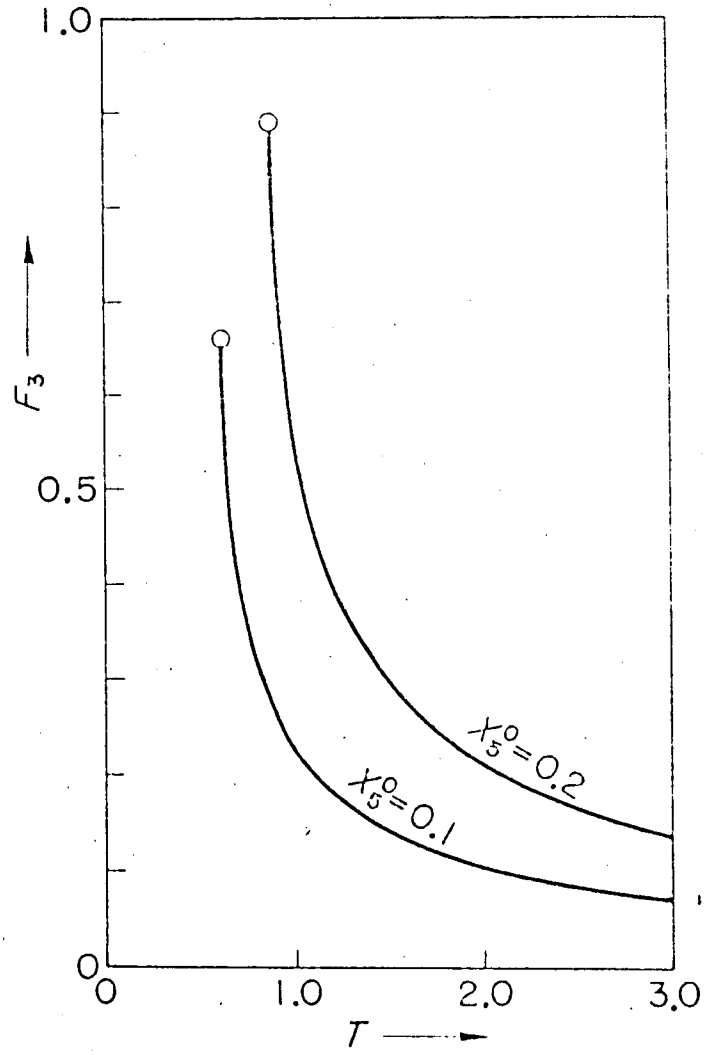

Fig. 1.11. Influence of the settling time on the fuel consumption ($x_6^0 = 0$).

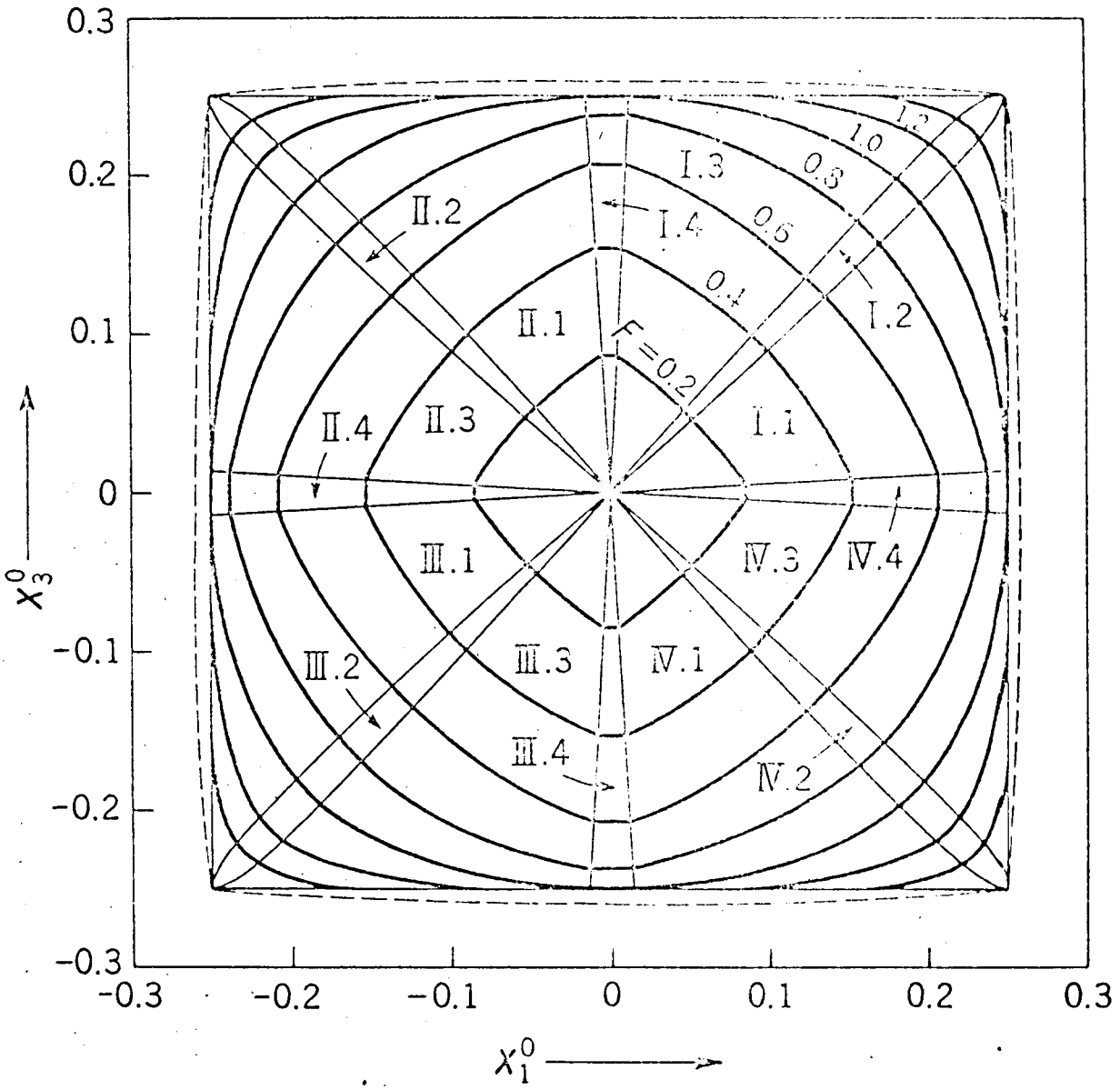

Fig. 1.12. Iso-F curves on the $x_1^0 x_3^0$ plane ($x_2^0 = 0$ and $x_4^0 = 0$).

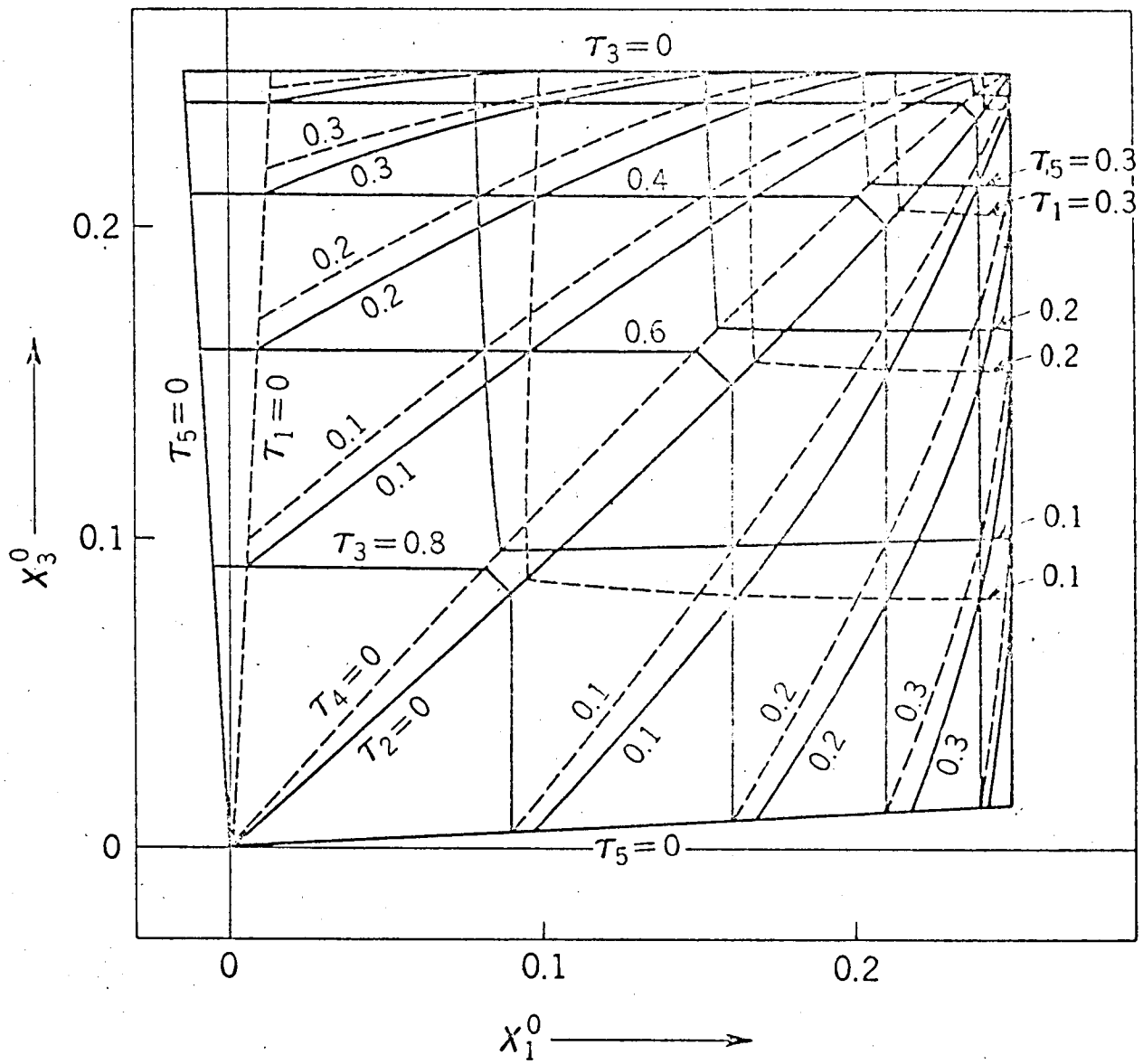

Fig. 1.13. Iso- τ_j curves for Mode I on the $x_1^0 x_3^0$ plane ($x_2^0 = 0$ and $x_4^0 = 0$).

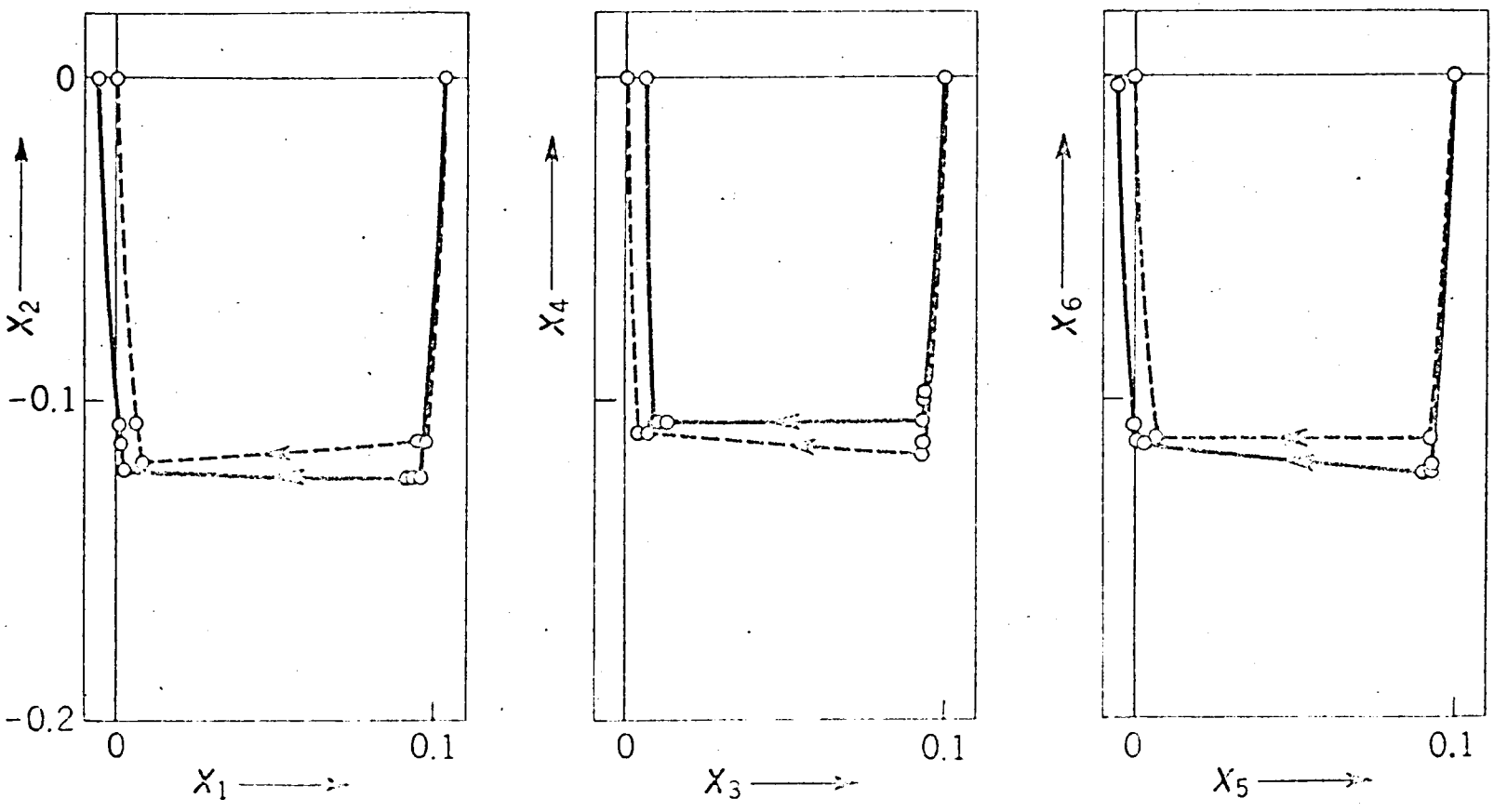

Fig. 1.14. Trajectories of the state variables $x_1 \sim x_6$ in the minimum-fuel control.

CHAPTER 2

OPTIMAL ATTITUDE CONTROL OF AN ORBITING SATELLITE USING REACTION WHEELS

2.1 Introduction

In the preceding chapter, we have investigated the optimal attitude control of a satellite by means of reaction jets. Another technique for effecting attitude control involves the use of reaction wheels. The ability of reaction wheels to control the attitude orientation of space vehicles stems from the basic law of action and reaction. If a reaction wheel mounted within the vehicle is accelerated about its axis of rotation, the vehicle is accelerated in the inertial space about the same axis, but in the opposite direction. In other words, exchange of angular momentum is made between the vehicle and the momentum storage element. In the presence of a cyclic disturbing torque, reaction wheels may be accelerated back and forth repeatedly; while, for a constant torque acting on the vehicle, the wheel system will get saturated attaining its maximum speed.* Therefore, the reaction wheel system is not suited for compensating secular changes of momentum, but is more effi-

---

* According to Ref. 32, the gravitational and the electromagnetic torques from the Earth's fields are regarded as time variables with major harmonics at orbital frequency. However, the solar radiation effect has a constant torque characteristic.

cient in counteracting cyclic momentum changes [4, 12, 16].

The present chapter deals with optimization problems in attitude control of an orbiting satellite using reaction wheels [23, 24]. The orbit is assumed to be circular. The satellite is a spherical rigid body. The earth-centered triad is taken as a reference frame of the attitude. The reaction wheel is accelerated with respect to the satellite body by an electric motor. The optimization criteria considered in this chapter are to minimize the settling time and the amount of input energy to the motors. The optimal switching policy of the control functions is determined for various initial states of angular deviation.

2.2 Reaction Wheel System

Reaction wheels are mounted in fixed bearings relative to the satellite frame, and are made to accelerate about those fixed axes. We assume that the driving torque is provided by armature-controlled, permanent-magnet d-c motors. The motors are driven by some voltage source. Three sets of wheels are disposed so that their spin axes are directed along the body axes. Then the satellite consists of a main body and a number of internal rotating parts (motors and wheels).

The following symbols are introduced to describe the motion of the satellite.

A : moment of inertia of the main body.

ω : angular velocity of the main body relative to the inertial space, ω^0 is its initial value.

M : torque on the main body produced from the internal rotating parts.

I_w : moment of inertia of the rotating part about its spin axis.

γ : angular velocity of the rotating parts relative to the main body, γ^0 is its initial value.

R_a : armature resistance of the motor.

K_t, K_s : torque and speed constants of the motor, respectively.

V_1, V_2, V_3: applied voltages to the motors disposed along the body axes i, j, k, respectively. The polarity of the applied voltage is taken to be positive when the motor rotates in the clockwise direction ($\gamma < 0$) at no load. For convenience, we denote $\mathbf{V} = V_1 \mathbf{i} + V_2 \mathbf{j} + V_3 \mathbf{k}$.

V_0 : maximum value of the applied voltage.

The torque $\mathbf{M}$ on the main body from the motor is given by

$$\mathbf{M} = \frac{K_t}{R_a} \left(\mathbf{V} + \frac{\boldsymbol{\gamma}}{K_s} \right) \tag{2.1}$$

In the absence of external torques, the angular momentum of the satellite about its center of mass remains constant [38, pp. 49-50]. Thus the following relation is approximately satisfied [31]:*

$$A\omega + I_w(\omega + \gamma) = A\omega^0 + I_w(\omega^0 + \gamma^0) \tag{2.2}$$

We further assume that $A \gg I_w$, and that the wheels are initially at rest relative to the main body, i.e., $\gamma^0 = 0$. Then Eq. (2.2) becomes

---

* It is here assumed that the center of mass and the axes of inertia of the composite system do not shift from those of the main body. The gyroscopic crosscoupling effects are neglected in Eq. (2.2).

$$\gamma = A(\omega^0 - \omega)/I_w \tag{2.3}$$

where ω is given in component forms by Eqs. (1.4).

The gyrodynamical equations of the main body are the same as those in the preceding chapter; namely, they are given by Eqs. (1.6) for the original nonlinear system and Eqs. (1.7) for the linearized system. Substituting Eq. (2.3) into Eq. (2.1) and using Eqs. (1.4) and (1.7) yields the differential equations

$$\left.\begin{aligned} \dot{x}_1 &= x_2 \qquad \dot{x}_2 = -kx_2 + kcx_3 + cx_4 + kb_1 + u_1 \\ \dot{x}_3 &= x_4 \qquad \dot{x}_4 = -kcx_1 - cx_2 - kx_4 + kb_2 + u_2 \end{aligned}\right\} \tag{2.4}$$

$$\dot{x}_5 = x_6 \qquad \dot{x}_6 = -kx_6 + kb_3 + u_3 \tag{2.5}$$

where

$$\left.\begin{aligned} &x_1 = \psi \quad x_2 = \dot{\psi} \quad x_3 = \theta \quad x_4 = \dot{\theta} \quad x_5 = \phi \quad x_6 = \dot{\phi} \\ &u_i = V_i/V_0 \ (i = 1,2,3) \quad \tau = t/t_m \quad c = t_m\Omega \quad k = t_m K_t/K_s I_w R_a \\ &b_1 = t_m\omega_1^0 \quad b_2 = t_m\omega_2^0 \quad b_3 = t_m(\omega_3^0 - \Omega) \quad t_m = (AR_a/K_t V_0)^{1/2} \end{aligned}\right\} \tag{2.6}$$

In the above equations a dot over a quantity denotes differentiation with respect to the dimensionless time τ. b_1, b_2, and b_3 correspond to the i, j, and k components of the initial velocity of deviation from the reference frame, respectively. As one sees from Eqs. (1.4), b_i (i = 1,2,3) are approximately related to the initial values x_i^0 (i = 1 to 6) of the state variables by

$$\left.\begin{aligned} b_1 &= x_2^0 - cx_3^0 \\ b_2 &= x_4^0 + cx_1^0 \end{aligned}\right\} \tag{2.7}$$

$$b_3 = x_6^0 \tag{2.8}$$

2.3 Time-Optimal Control

Time-optimal controls for the system described by Eqs. (2.4) and (2.5) can be obtained by using the maximum principle. The system of equations for the auxiliary variables p's is given by

$$\left.\begin{aligned} \dot{p}_1 &= kcp_4 & \dot{p}_2 &= -p_1 + kp_2 + cp_4 \\ \dot{p}_3 &= -kcp_2 & \dot{p}_4 &= -cp_2 - p_3 + kp_4 \end{aligned}\right\} \tag{2.9}$$

$$\dot{p}_5 = 0 \qquad \dot{p}_6 = -p_5 + kp_6 \tag{2.10}$$

By applying the maximum principle, we obtain the necessary conditions for the optimal controls $\bar{u}_i$ (i = 1,2,3) [30, pp. 9-21]:

$$\left.\begin{aligned} \bar{u}_1(\tau) &= \operatorname{sgn} p_2(\tau) \\ \bar{u}_2(\tau) &= \operatorname{sgn} p_4(\tau) \end{aligned}\right\} \tag{2.11}$$

$$\bar{u}_3(\tau) = \operatorname{sgn} p_6(\tau) \tag{2.12}$$

Solving Eqs. (2.9) and (2.10) yields

$$\left.\begin{aligned} p_2(\tau) &= R \sin(c\tau + \Theta) + P_2 e^{k\tau} \\ p_4(\tau) &= R \cos(c\tau + \Theta) + P_4 e^{k\tau} \end{aligned}\right\} \tag{2.13}$$

$$p_6(\tau) = P_6 e^{k\tau} + P_5 \tag{2.14}$$

where R, Θ, P_2, P_4, P_5, and P_6 are constants to be determined by initial conditions.

(a) Control of the Pitch Motion (System of Two Variables)

Let us consider for system (2.5) the problem of getting to the desired state (0, 0) from a given initial state (x_5^0, x_6^0) in the shortest time [8].

As we see in Eq. (2.14), p_6 varies monotonously with time τ ; therefore, the optimal control $\bar{u}_3$ changes sign once at most. Possible modes of switching are shown in Table 1.1 in Sec. 1.5(a).

By following the procedure mentioned in Sec. 1.5(a), the time intervals τ_1 and τ_2 of Mode I are related to initial values x_5^0 and x_6^0 by

$$\left.\begin{aligned} x_5^0 &= \frac{\alpha[k(1 - \tau_1 + \tau_2) + k^2(\tau_1^2 - 2\tau_1\tau_2 - \tau_2^2)/2] + k^2(1 - \tau_1 + \tau_2)(\tau_1 - \tau_2)}{k^2[k(1 - \tau_1 + \tau_2) - \alpha]} \\ x_6^0 &= \frac{\alpha}{\alpha - k(1 - \tau_1 + \tau_2)} \end{aligned}\right\} \tag{2.15}$$

where

$$\alpha = e^{k(\tau_1 + \tau_2)} - 2e^{k\tau_1} + 1$$

The signs of x_5^0 and x_6^0 should be reversed for Mode II. If the initial velocity is zero, Eqs. (2.15) give

$$\left.\begin{aligned} \tau_1 &= \frac{1}{k}\left[\, k^2|x_5^0| + \log\left(1 + \sqrt{1 - e^{-k^2|x_5^0|}}\right)\right] \\ \tau_2 &= \frac{1}{k}\log\left(1 + \sqrt{1 - e^{-k^2|x_5^0|}}\right) \end{aligned}\right\} \tag{2.16}$$

Consequently, the shortest settling time τ is given by

$$\tau = \tau_1 + \tau_2 = \frac{1}{k}\left[\, k^2|x_5^0| + 2\log\left(1 + \sqrt{1 - e^{-k^2|x_5^0|}}\right)\right] \tag{2.17}$$

(b) Control of the Roll and Yaw Motion (System of Four Variables)

We consider the time-optimal control for the system described by Eqs. (2.4) with the initial conditions (2.7). From Eqs. (2.13), a representative point on p_2p_4 plane moves at the uniform rate c along the circle whose center is moving along a line. As seen from Eqs. (2.11), the optimal controls $\bar{u}_1$ and $\bar{u}_2$ are of a bang-bang type. The signs of $\bar{u}_1$ and $\bar{u}_2$ are reversed when the representative point traverses p_2 and p_4 axes, respectively. By a consideration analogous to that of Sec. 1.5(b), we may conclude that the reversal of the signs of $\bar{u}_1$ and $\bar{u}_2$ occurs three times at most, and that twelve switching modes as listed in Table 1.2 are possible. The time intervals between switchings of the controls are related to the initial values of the state variables as will be shown in Appendix II.1.

Numerical Example

We put c = 0.1 and k = 1.0 in Eqs. (2.4). The object of control is to make all the state variables x_1 to x_4 zero in the shortest time. Figure 2.1 illustrates the relationship between initial values x_1^0, x_3^0 and the possible shortest settling time τ in the case where $b_1 = 0$ and $b_2 = 0$, i.e., both the initial angular velocities of the main body are zero. In this case, iso-τ_j (j = 1 to 4) curves for Mode I are shown in Fig. 2.2. Rotating these curves about the origin by $\pi/2$, π, $3\pi/2$ radians in the counterclockwise direction yields iso-τ_j curves for Modes II, III, IV, respectively. Figure 2.3 shows the relationship between x_1^0, x_3^0 and τ in the case where $b_1 = 0.2$, $b_2 = 0.2$. We see in these figures that all switching modes indicated in Table 1.2 are not always used. An open question is which modes of switching

of $\bar{u}_1$ and $\bar{u}_2$ are required in order to restore any initial state to the origin. Of course, it depends on the values of b_1 and b_2. The detailed discussion will be mentioned in Appendix II.2.

Figure 2.4 illustrates an example of phase-plane trajectories of x_i (i = 1 to 6), where the initial values are $x_1^0 = 0.074$, $x_2^0 = 0.013$, $x_3^0 = 0.134$, $x_4^0 = -0.007$, $x_5^0 = 0.100$, and $x_6^0 = 0.000$. The solid and the dotted curves are obtained for the original nonlinear system and the linearized system, respectively.

2.4 Minimum-Energy Control

In this section we assume, for simplicity, that the angular velocity of the vehicle does not deviate initially from that of the reference frame, i.e., $b_1 = b_2 = b_3 = 0$. Then the initial conditions (2.7) and (2.8) are rewritten as

$$\left.\begin{aligned} x_2^0 - cx_3^0 &= 0 \\ x_4^0 + cx_1^0 &= 0 \end{aligned}\right\} \tag{2.18}$$

$$x_6^0 = 0 \tag{2.19}$$

The quantity to be minimized in the control is input energy to the motors [8, 23, 24]. The power W_i supplied to each motor is

$$W_i = V_i\,(V_i + \gamma_i/K_s)/R_a \qquad (i = 1,2,3) \tag{2.20}$$

Then the energy is expressed by the nondimensional variables as

$$E = \int_0^T \left\{u_1[u_1 - k(x_2 - cx_3)] + u_2[u_2 - k(x_4 + cx_1)] + u_3(u_3 - kx_6)\right\} d\tau \tag{2.21}$$

where T is a prescribed transition time.

The system of equations for the auxiliary variables p's is given by [30, pp. 9-21]

$$\left.\begin{aligned} \dot{p}_1 &= kcp_4 - kcu_2 & \dot{p}_2 &= -p_1 + kp_2 + cp_4 - ku_1 \\ \dot{p}_3 &= -kcp_2 + kcu_1 & \dot{p}_4 &= -cp_2 - p_3 + kp_4 - ku_2 \end{aligned}\right\} \tag{2.22}$$

$$\dot{p}_5 = 0 \qquad \dot{p}_6 = -p_5 + kp_6 - ku_3 \tag{2.23}$$

Hence, by use of the maximum principle, we obtain the necessary conditions for the optimal controls $\bar{u}_i$ (i = 1,2,3):

$$\left.\begin{aligned} \bar{u}_1 &= \begin{cases} q_2 & \text{for} \quad |q_2| \leq 1 \\ \operatorname{sgn} q_2 & \text{for} \quad |q_2| > 1 \end{cases} \\ \bar{u}_2 &= \begin{cases} q_4 & \text{for} \quad |q_4| \leq 1 \\ \operatorname{sgn} q_4 & \text{for} \quad |q_4| > 1 \end{cases} \end{aligned}\right\} \tag{2.24}$$

$$\bar{u}_3 = \begin{cases} q_6 & \text{for} \quad |q_6| \leq 1 \\ \operatorname{sgn} q_6 & \text{for} \quad |q_6| > 1 \end{cases} \tag{2.25}$$

where

$$\left.\begin{aligned} q_2 &= [p_2 + k(x_2 - cx_3)]/2 \qquad q_4 = [p_4 + k(x_4 + cx_1)]/2 \\ q_6 &= (p_6 + kx_6)/2 \end{aligned}\right\} \tag{2.26}$$

The minimum-energy control functions $\bar{u}_1$, $\bar{u}_2$, and $\bar{u}_3$ vary continuously between and including ± 1.

(a) Control of the Pitch Motion (System of Two Variables)

First, we assume that the optimal control $\bar{u}_3$ does not saturate at any time during the transition. By virtue of Eqs. (2.25) and (2.26), the optimal

control is given by

$$\bar{u}_3 = (p_6 + kx_6)/2 \tag{2.27}$$

Substituting Eq. (2.27) into Eqs. (2.5) and (2.23) yields a set of differential equations in x_5, x_6, p_5, and p_6. By solving the equations thus obtained with boundary conditions

$$\left.\begin{aligned} x_5(0) &= x_5^0 \qquad & x_6(0) &= 0 \\ x_5(T) &= 0 \qquad & x_6(T) &= 0 \end{aligned}\right\} \tag{2.28}$$

we obtain

$$\left.\begin{aligned} x_5 &= x_5^0\,[2(\tau/T)^3 - 3(\tau/T)^2 + 1] \\ x_6 &= (6x_5^0/T)[(\tau/T)^2 - \tau/T] \\ p_5 &= -24\,x_5^0/T^3 \\ p_6 &= (6x_5^0/T^2)[k\tau^2/T + (4/kT - 1)k\tau - 2] \end{aligned}\right\} \tag{2.29}$$

The optimal control does not saturate, i.e., $|\bar{u}_3| < 1$, if the following condition is satisfied:

$$|x_5^0| \leq \begin{cases} \dfrac{1}{6}T^2 & \text{for} \quad T \leq \dfrac{2}{k} \\[2ex] \dfrac{2}{3k^2}\cdot\dfrac{kT}{1 + 4/k^2T^2} & \text{for} \quad T > \dfrac{2}{k} \end{cases} \tag{2.30}$$

The minimum energy consumption depends on the settling time T. For the nonsaturating control, the energy E_3 is obtained by substitution of Eqs. (2.27) and (2.29) into Eq. (2.21), i.e.,

$$\begin{aligned} E_3 &= \int_0^T \bar{u}_3(\bar{u}_3 - kx_6)\,d\tau \\ &= 0.25\int_0^T [p_6^2 - (kx_6)^2]\,d\tau = 12(x_5^0)^2/T^3 \end{aligned} \tag{2.31}$$

As mentioned in Sec. 2.3(a), the relationship between the initial state and the shortest settling time is given by Eq. (2.17). It is seen from this relation that any initial state satisfying the condition

$$|x_5^0| \leq (2/k^2) \cdot \log [\cosh(kT/2)] \equiv (x_5^0)_{max} \tag{2.32}$$

can be restored to the origin in the interval of time T. Hence we see that, given an initial value satisfying the condition (2.32) but not satisfying (2.30), the optimal control saturates in certain intervals of the transition.

Second, we deal with the process in which $\bar{u}_3$ saturates in certain intervals. For convenience, we consider the following two cases separately.

Case 1. $kT \leq 2$

In the time-optimal process, the optimal control is switched from -1 to +1 if $x_5^0 > 0$, and from +1 to -1 if $x_5^0 < 0$. In the nonsaturating minimum-energy process above mentioned, $\bar{u}_3$ increases monotonously for $x_5^0 > 0$ and decreases monotonously for $x_5^0 < 0$. Hence we may infer the modes of switching of $\bar{u}_3$ as listed in Table 2.1.

Substituting the value of $\bar{u}_3$ in Table 2.1 into Eqs. (2.5) and (2.23) yields a set of differential equations in x_5, x_6, p_5, and p_6. By solving the equations thus obtained with the boundary conditions (2.28), we obtain the optimal trajectory and the time intervals between switchings of $\bar{u}_3$. The time intervals τ_1, τ_2, and τ_3 are related to an initial value x_5^0 by

$$\left.\begin{aligned} |x_5^0| &= \frac{1}{6k^2}\left\{(e^{k\tau_3})[(k\tau_2)^2 + 4k\tau_2 + 6 - 2e^{k(\tau_2-T)}(k\tau_2 - 3)] \right. \\ &\qquad \left. + 2k(3T - 4\tau_2 - 6\tau_3) - 12\right\} \\ \tau_3 &= -\frac{1}{k}\log\left\{\frac{1}{4}[(2 + k\tau_2) + (2 - k\tau_2)e^{k(\tau_2-T)}]\right\} \end{aligned}\right\} \tag{2.33}$$

$$\tau_1 = T - \tau_2 - \tau_3 \qquad \Big)$$

The minimum energy consumption is calculated by inserting the value of $\bar{u}_3$ in Table 2.1 into Eq. (2.21). For the control of Mode I.2, the energy E_3 is given by

$$E_3 = \int_0^{\tau_1} (1 + kx_6)d\tau + 0.25\int_{\tau_1}^{\tau_1+\tau_2} [p_6^2 - (kx_6)^2]d\tau + \int_{\tau_1+\tau_2}^{T} (1 - kx_6)d\tau$$

$$= \frac{e^{k\tau_3}}{12k}[k\tau_2(e^{k(\tau_2-T)} + 1)^2 e^{k\tau_3} - 12e^{-k(T-\tau_2)} + 12] \qquad (2.34)$$

where τ_2 and τ_3 are to be determined by Eqs. (2.33). For the control of Mode II.2, we have the same result as Eq. (2.34).

Table 2.1 Mode of switching of $\bar{u}_3(\tau)$ for the partly saturating control ($kT \leq 2$)

Mode	Time interval τ_1	τ_2	τ_3	Initial value
I.2	-1	q_6	1	$T^2/6 \leq x_5^0 \leq (x_5^0)_{max}$
II.2	1	q_6	-1	$-T^2/6 \geq x_5^0 \geq -(x_5^0)_{max}$

Case 2. $kT > 2$

In this case, we encounter a somewhat complicated situation. If x_5^0 takes a value between $(2/3k^2)[kT/(1 + 4/k^2T^2)] \equiv (x_5^0)_1$ and $(1/3k^2)[3kT - 5 + e^{(2-kT)}] \equiv (x_5^0)_2$, the optimal control $\bar{u}_3$ does not vary monotonously; while, if x_5^0 is between $(x_5^0)_2$ and $(x_5^0)_{max}$, $\bar{u}_3$ varies monotonously like as in Case 1. We may summarize the modes of switching as listed in Table 2.2.

By proceeding as in Case 1, the time intervals τ_1, τ_2, and τ_3 in Mode I.1 or II.1 are related to an initial value x_5^0 by

$$\left.\begin{aligned} x_5^0 &= \frac{e^{k\tau_2}[(k\tau_3)^3 - 4] + (k\tau_3)^3 - 12k\tau_3 + 20}{3k^2[(k\tau_3 - 2)^2 + (k\tau_3)^2(e^{k\tau_2})]} + \frac{(T - \tau_3)}{k} \\ \tau_3 &= (1/2k)[k(T - \tau_2) + 2] \\ \tau_1 &= T - \tau_2 - \tau_3 \end{aligned}\right\} \qquad (2.35)$$

Table 2.2 Mode of switching of $\bar{u}_3(\tau)$ for the partly saturating control ($kT > 2$)

Mode	Time interval τ_1	τ_2	τ_3	Initial value
I.1	q_6	-1	q_6	$(x_5^0)_1 \leq x_5^0 \leq (x_5^0)_2$
I.2	-1	q_6	1	$(x_5^0)_2 \leq x_5^0 \leq (x_5^0)_{max}$
II.1	q_6	1	q_6	$-(x_5^0)_1 \geq x_5^0 \geq -(x_5^0)_2$
II.2	1	q_6	-1	$-(x_5^0)_2 \geq x_5^0 \geq -(x_5^0)_{max}$

The energy consumption E_3 is given by

$$E_3 = \frac{4}{3k[(k\tau_3)^2(e^{k\tau_2}) + (k\tau_3 - 2)^2]^2}\Big\{6(k\tau_3 - 1)[(k\tau_3 - 3)(e^{2k\tau_2} - 1) + 2(e^{k\tau_2} - 1)^2 - 4] + (e^{k\tau_2} + 1)^2[(k\tau_3)^3 + (k\tau_3 - 2)^3]\Big\} \qquad (2.36)$$

where τ_2 and τ_3 are determined by Eqs. (2.35).

The time intervals in Mode I.2 or II.2 are given by Eqs. (2.33) in Case 1, and E_3 by Eq. (2.34).

Numerical Example

Case 1. $k = 1$ and $T = 1$ $(kT = 1)$

Figure 2.5 shows a number of optimal trajectories which start with various initial values x_3^0. The control $\bar{u}_3$ does not saturate on the trajectories shown in solid lines. It saturates on the broken-line trajectories. $\bar{u}_3$ does not saturate in the case of curve A where $x_3^0 = 0.100$. Curve B corresponds to a special case in which $x_3^0 = T^2/6 = 0.167$. Curve C corresponds to a partly saturating control of Mode I.2 in which $x_3^0 = 0.221$ and $\tau_3 = 0.5$. Curve D coincides with the time-optimal trajectory, i.e., $x_3^0 = (x_3^0)_{max} = 0.241$. Since $kT = 1 < 2$, the optimal control of Mode I.1 does not appear. A switching curve is shown dotted in the figure. Figure 2.6 shows the time responses of the optimal control in each case above mentioned.

The influence of T on the energy E_3 is illustrated in Fig. 2.7, where the solid lines correspond to nonsaturating control and the broken lines to partly saturating control.

Case 2. $k = 1$ and $T = 3$ $(kT = 3)$

See the optimal trajectories in Fig. 2.8. Curve A corresponds to a

nonsaturating control where $x_5^0 = 1$. Curves B and C correspond to special cases where initial values are $x_5^0 = (x_5^0)_1 = 1.385$ and $x_5^0 = (x_5^0)_2 = 1.456$, respectively. For an initial state existing between those of trajectories B and C, $\bar{u}_5$ follows the switching mode of I.1. Curve D corresponds to a control of Mode I.2 in which $x_5^0 = 1.634$ and $\tau_2 = 1$. Curve E coincides with the time-optimal trajectory where $x_5^0 = (x_5^0)_{max} = 1.711$. The dotted line in Fig. 2.8 shows the switching curve in this case. Time responses of the optimal control is illustrated in Fig. 2.9.

(b) Control of the Roll and Yaw Motion (System of Four Variables)

For the sake of simplicity, we confine our consideration to the nonsaturating control. Also for convenience, the parameter k is set equal to unity.* As shown in Eqs. (2.24) and (2.26), the optimal controls are given by

$$\left.\begin{aligned} \bar{u}_1 &= (p_2 + x_2 - cx_3)/2 \\ \bar{u}_2 &= (p_4 + x_4 + cx_1)/2 \end{aligned}\right\} \tag{2.37}$$

Substitution of Eqs. (2.37) into (2.4) and (2.22) yields a set of differential equations in x's and p's. By solving the equations thus obtained with boundary conditions [see Eqs. (2.18)]

$$\left.\begin{aligned} x_2^0 - cx_3^0 &= x_4^0 + cx_1^0 = 0 \\ \text{and} \qquad x_1(T) &= x_2(T) = x_3(T) = x_4(T) = 0 \end{aligned}\right\} \tag{2.38}$$

---

* In the linear system (2.4), this assumption does not lose the generality of the problem.

we obtain the solution

$$\left.\begin{aligned}
x_1 &= -c\beta(\tau - T)^4 - 2(\alpha + cT\beta)(\tau - T)^3 - T(6\alpha + cT\beta)(\tau - T)^2/2 \\
x_2 &= -4c\beta(\tau - T)^3 - 6(\alpha + cT\beta)(\tau - T)^2 - T(6\alpha + cT\beta)(\tau - T) \\
x_3 &= c\alpha(\tau - T)^4 - 2(\beta - cT\alpha)(\tau - T)^3 - T(6\beta - cT\alpha)(\tau - T)^2/2 \\
x_4 &= 4c\alpha(\tau - T)^3 - 6(\beta - cT\alpha)(\tau - T)^2 - T(6\beta - cT\alpha)(\tau - T) \\
p_1 &= -6[c\beta(\tau - T)^2 + cT\beta(\tau - T) - 4\alpha] \\
p_2 &= -2c\beta(\tau - T)^3 - 3[2\alpha + c(T + 4)\beta](\tau - T)^2 \\
&\quad - [6(T + 4)\alpha + cT(T + 12)\beta](\tau - T) - 2T(6\alpha + cT\beta) \\
p_3 &= 6[c\alpha(\tau - T)^2 + cT\alpha(\tau - T) + 4\beta] \\
p_4 &= 2c\alpha(\tau - T)^3 - 3[2\beta - c(T + 4)\alpha](\tau - T)^2 \\
&\quad - [6(T + 4)\beta - cT(T + 12)\alpha](\tau - T) - 2T(6\beta - cT\alpha)
\end{aligned}\right\} \qquad (2.39)$$

The terms of order higher than the first in c are neglected in the above equations. In Eqs. (2.39) α and β are constants determined by the initial conditions other than as given by Eqs. (2.38). The condition for nonsaturating control ($|u_1| < 1$ and $|u_2| < 1$) requires that the parameters α and β satisfy the following inequalities during the transition:

$$\left.\begin{aligned}
&\left| 2c\beta\tau^3 + 3[2\alpha - c(T - 2)\beta]\tau^2 \right. \\
&\qquad \left. - [6(T - 2)\alpha - cT(T - 6)\beta]\tau - T(6\alpha - cT\beta) \right| \leq 1 \\
&\left| 2c\alpha\tau^3 - 3[2\beta + c(T - 2)\alpha]\tau^2 \right. \\
&\qquad \left. + [6(T - 2)\beta + cT(T - 6)\alpha]\tau + T(6\beta + cT\alpha) \right| \leq 1
\end{aligned}\right\} \qquad (2.40)$$

The minimum energy consumption E is obtained by substituting Eqs. (2.37) and (2.39) into Eq. (2.21), i.e.,

$$E = \int_0^T \left\{ u_1[u_1 - (x_2 - cx_3)] + u_2[u_2 - (x_4 + cx_1)] \right\} d\tau$$

$$= 0.25 \int_0^T [p_2^2 - (x_2 - cx_3)^2 + p_4^2 - (x_4 + cx_1)^2]\, dT$$

$$= 12[(x_1^0)^2 + (x_3^0)^2]/T^3 \qquad (2.41)$$

Numerical Example

Taking the parameters c = 0.1 and T = 1 in the conditions (2.40) gives

$$\left.\begin{array}{ll} |60\alpha + \beta| \leq 10 & \\ |60\beta + \alpha| \leq 10 & \text{for} \quad \alpha\beta > 0 \\ |60\alpha - \beta| \leq 10 & \\ |60\beta - \alpha| \leq 10 & \text{for} \quad \alpha\beta < 0 \end{array}\right\} \qquad (2.42)$$

Equations (2.39) and the inequalities (2.42) determine the region of initial states which can be restored to the origin by the nonsaturating controls. Since the initial values x_1^0, x_3^0 and x_2^0, x_4^0 are interrelated by Eqs. (2.38), an initial state $(x_1^0, x_2^0, x_3^0, x_4^0)$ may be given by prescribing only two of them, say x_1^0 and x_3^0. The area shown bordered by the heavy line in Fig. 2.10 is the region of x_1^0 and x_3^0 which give the initial states restored to the origin by the nonsaturating controls. The iso-E curves are shown in this region.

The broken line shows the boundary of the region of initial states which can be restored in an interval of time less than or equal to unity.* Hence, if an initial state is given in the area lying between the heavy line and the broken line, the controls may saturate in certain intervals of the tran-

---

* This boundary is obtained from the investigation of the time-optimal control, as shown in Fig. 2.1.

sition. The optimal switching policy of the partly saturating controls is omitted, because the computation becomes too laborious.

Figure 2.11 illustrates an example of the optimal trajectories, where the initial values are $x_1^0 = 0.100$, $x_2^0 = 0.010$, $x_3^0 = 0.100$, and $x_4^0 = -0.010$. Figure 2.12 shows the time responses of the optimal controls in this case.

2.5 Concluding Remarks

Optimization problems in the attitude control system using reaction wheels are discussed. This system is more complicated than the reaction gas-jet system in Chap. 1 because of the gyroscopic coupling of the rotating parts with the rotation of the satellite body. For simplicity, we assume that the expression for this gyroscopic coupling is given by Eq. (2.3). The control torque is considered to be provided by armature-controlled d-c motors. The input voltage to the motor is taken as the manipulated variable, or the control function.

The time-optimal control of the reaction wheel system is of the same type as that of the reaction gas-jet system, that is, of a bang-bang type. On the other hand, the condition of energy minimization necessitates that the optimal controls take not only the saturated values but any values between them; hence the controls are of continuous type. The optimal switching policy has been shown in several tables and charts for various initial states. The energy consumption under the action of the optimal controls has also been determined.

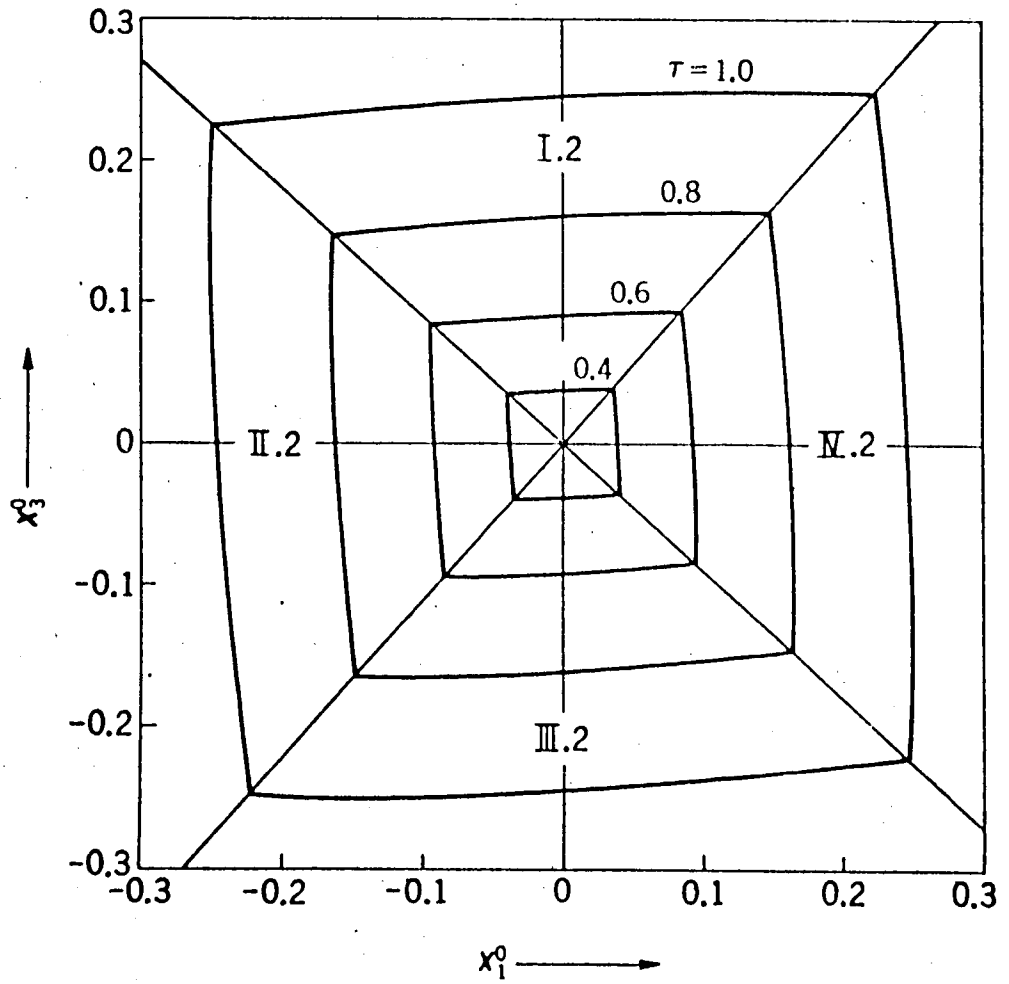

Fig. 2.1. Iso-τ curves on the $x_1^0 x_3^0$ plane ($b_1 = 0$ and $b_2 = 0$).

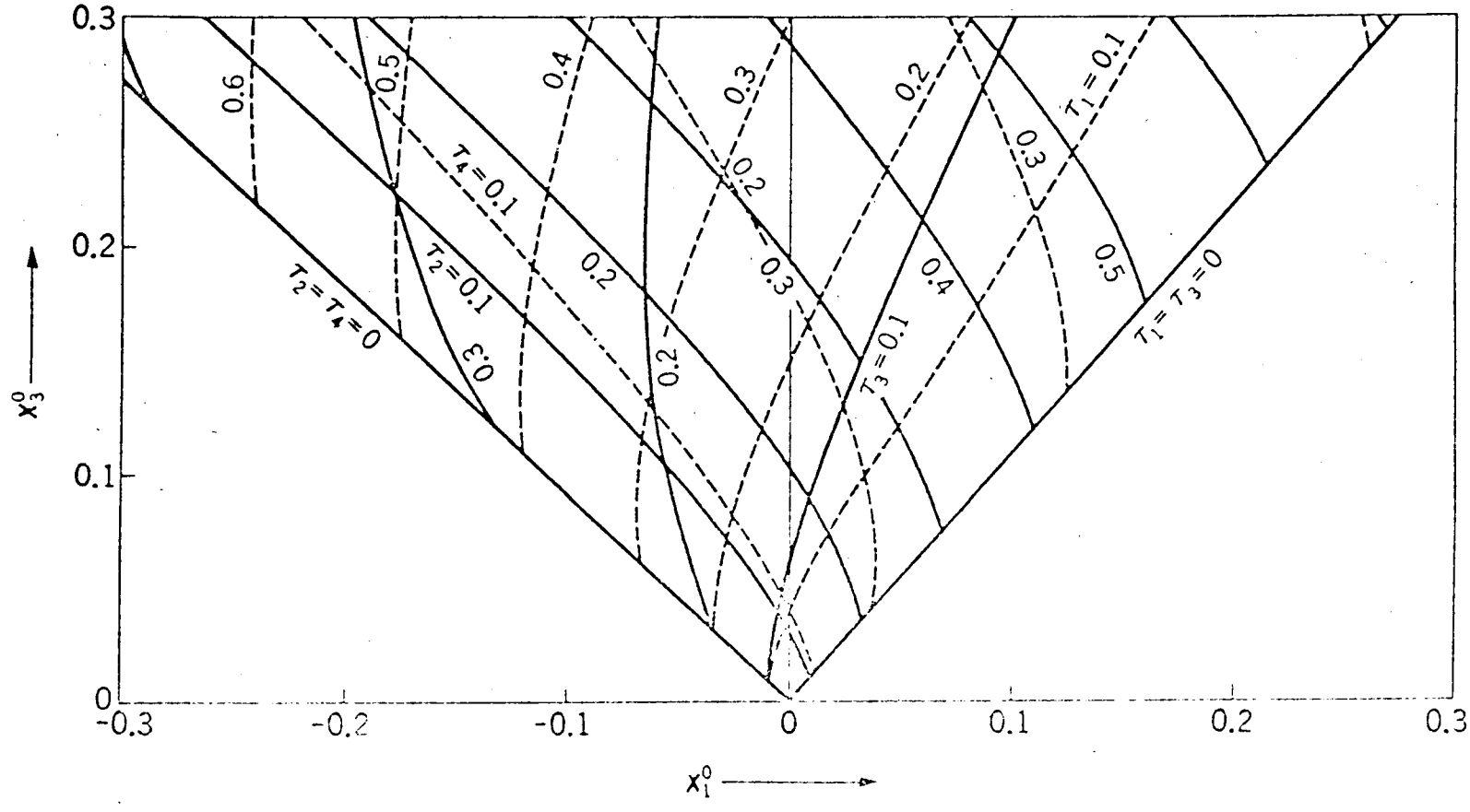

Fig. 2.2. Iso- τ_j curves for Mode I on the $x_1^0 x_3^0$ plane ($b_1 = 0$ and $b_2 = 0$).

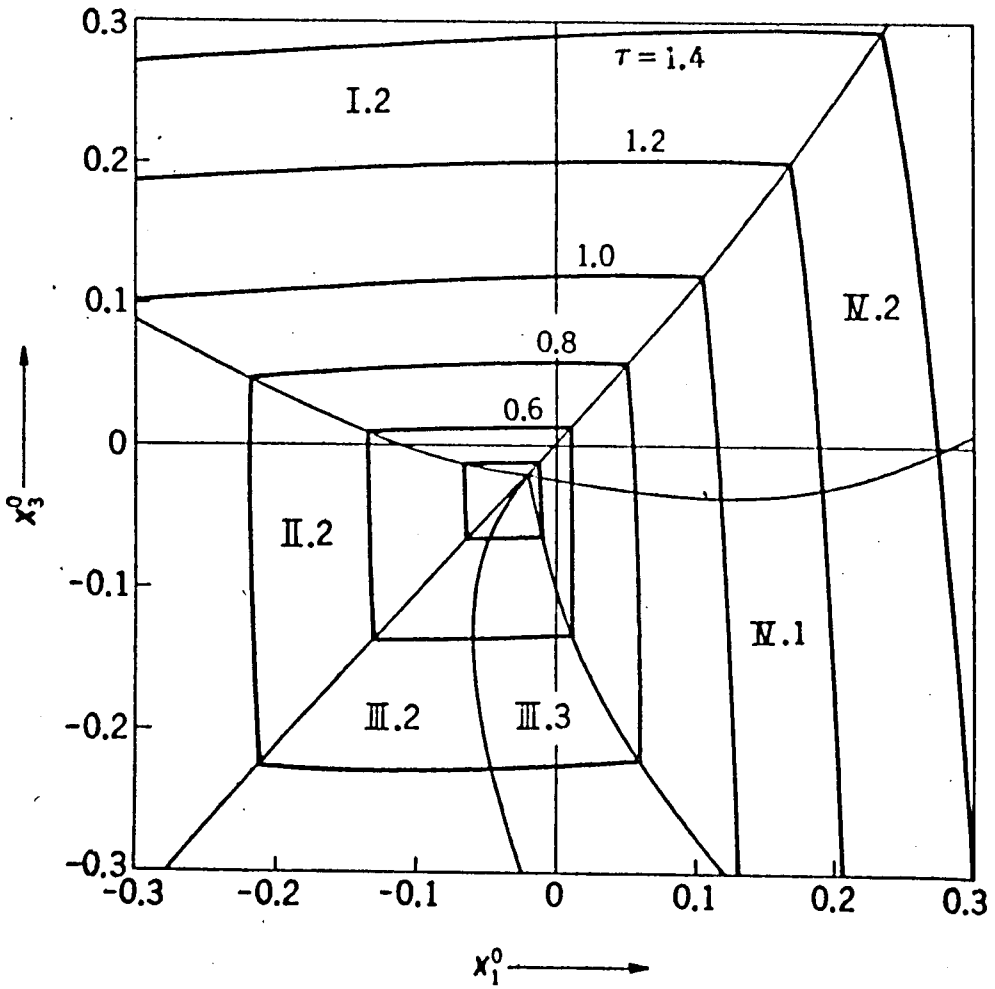

Fig. 2.3. Iso-τ curves on the $x_1^0 x_3^0$ plane ($b_1 = 0.2$ and $b_2 = 0.2$).

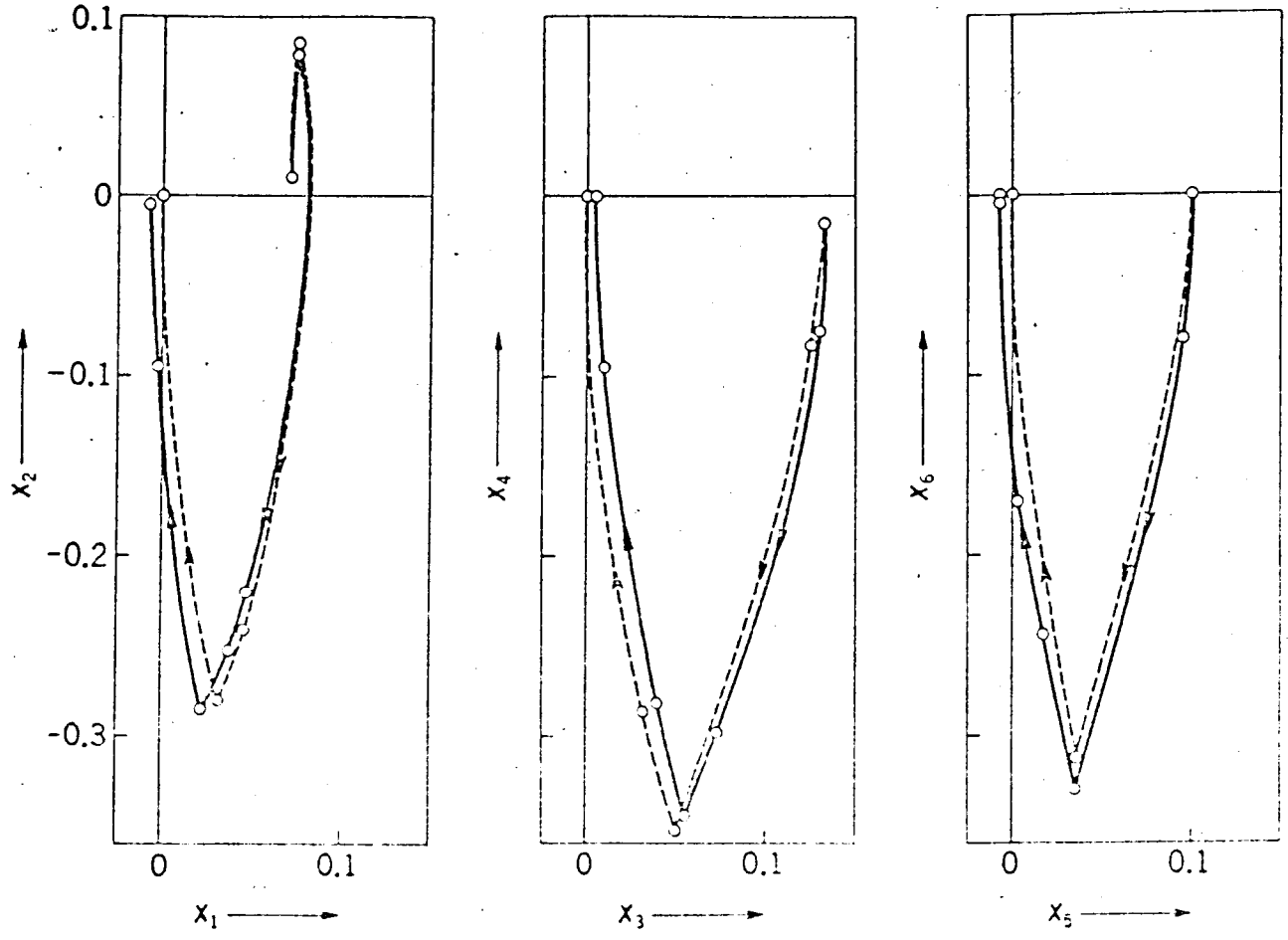

Fig. 2.4. Trajectories of the state variables $x_1 \sim x_6$ in the time-optimal control.

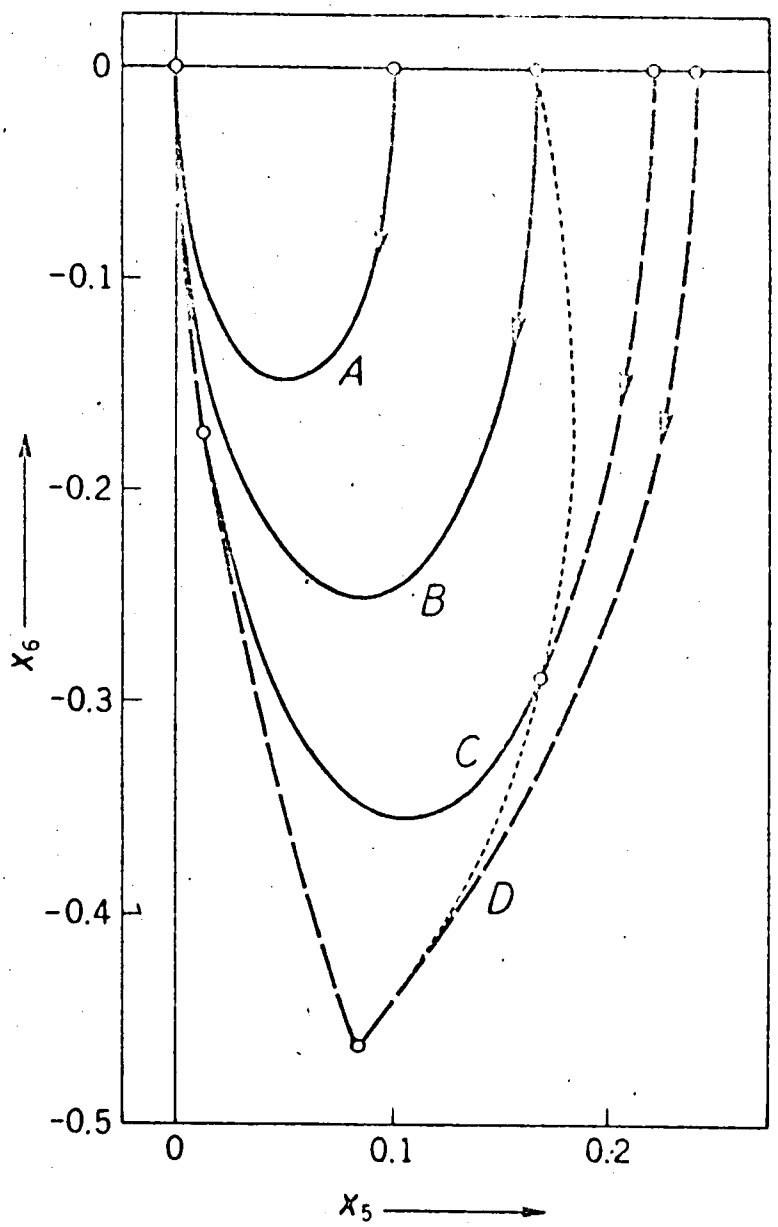

Fig. 2.5. Phase trajectories on the x_5x_6 plane for the minimum-energy control (k = 1 and T = 1).

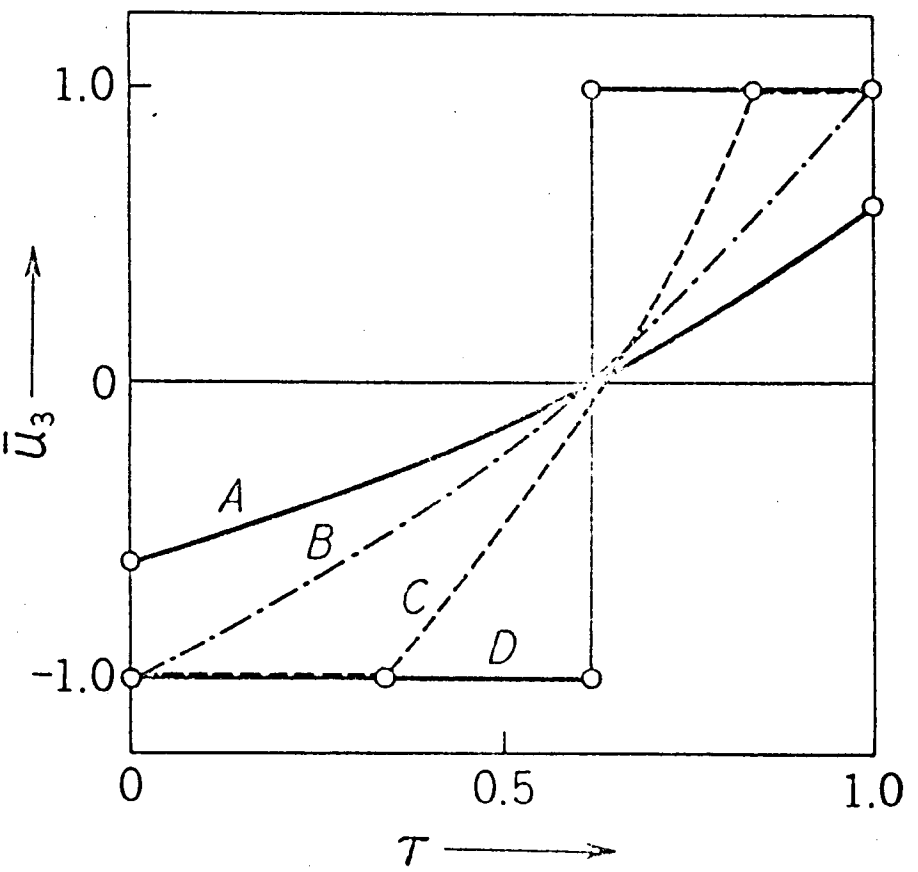

Fig. 2.6. Time responses of the optimal control (k = 1 and T = 1).

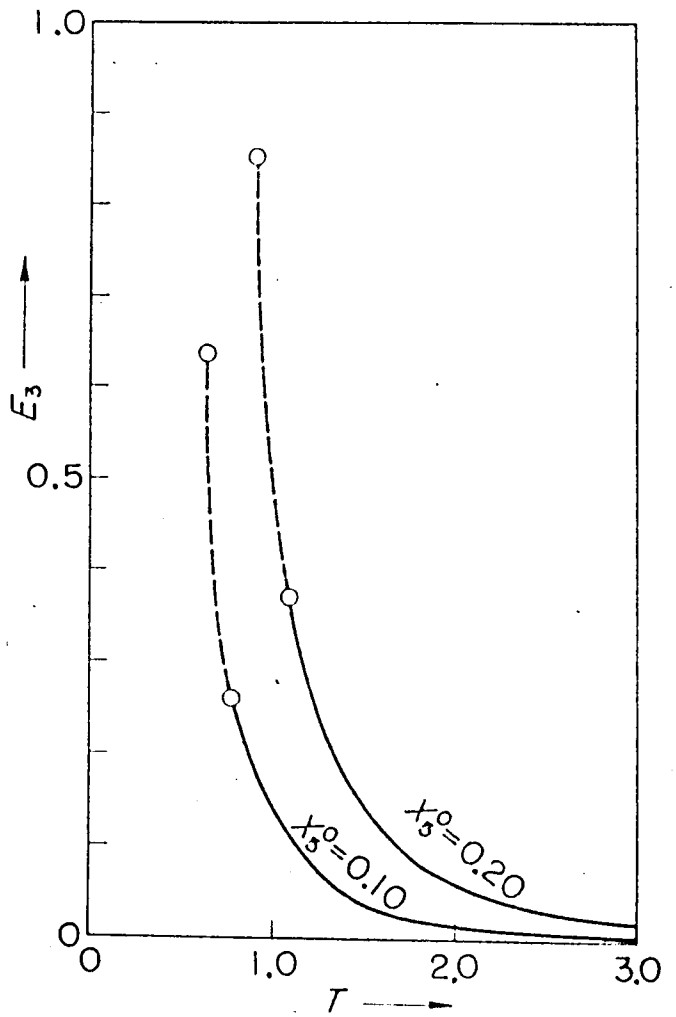

Fig. 2.7. Influence of the settling time on the energy consumption ($k = 1$ and $x_6^0 = 0$).

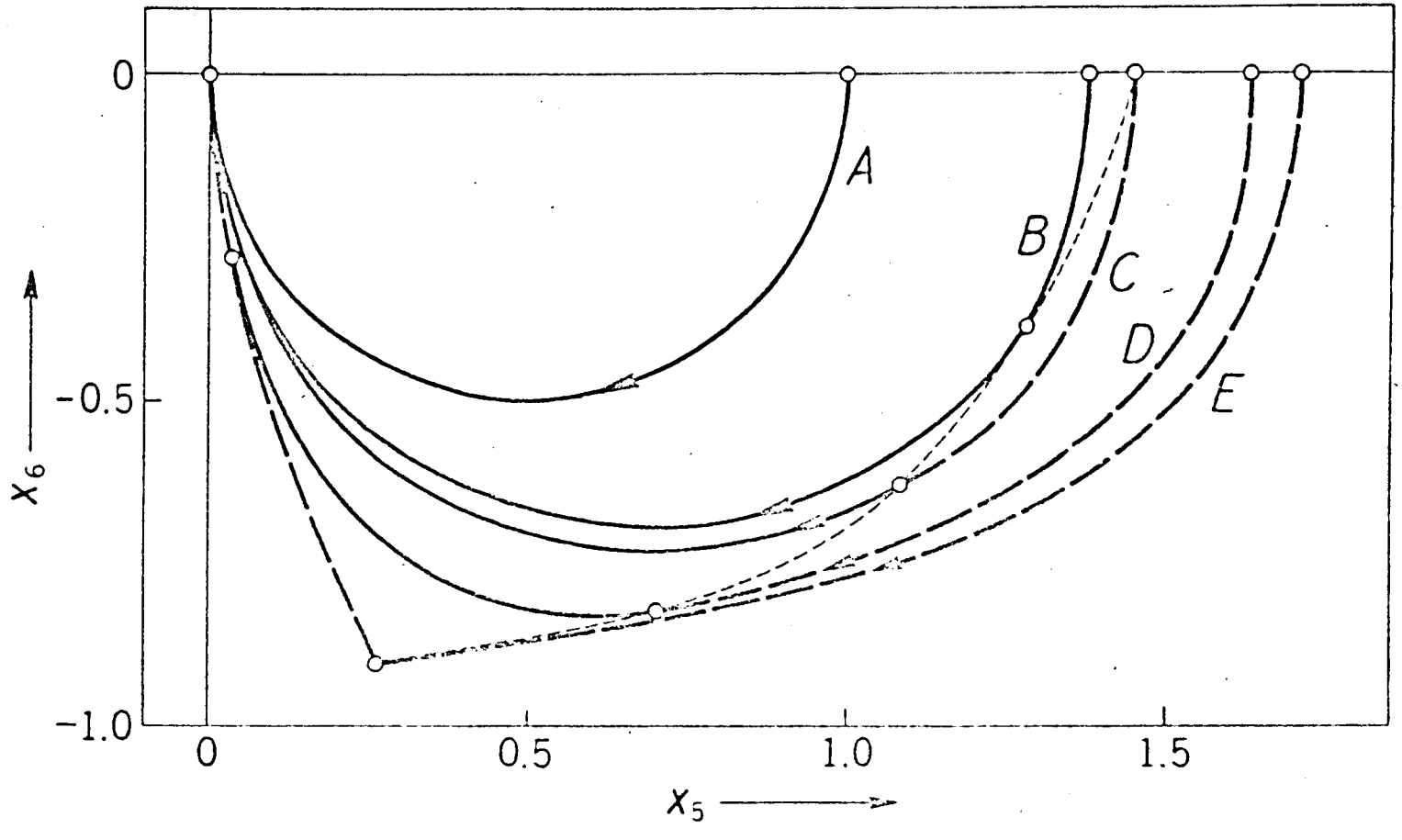

Fig. 2.8. Phase trajectories on the x_5x_6 plane for the minimum-energy control (k = 1 and T = 3).

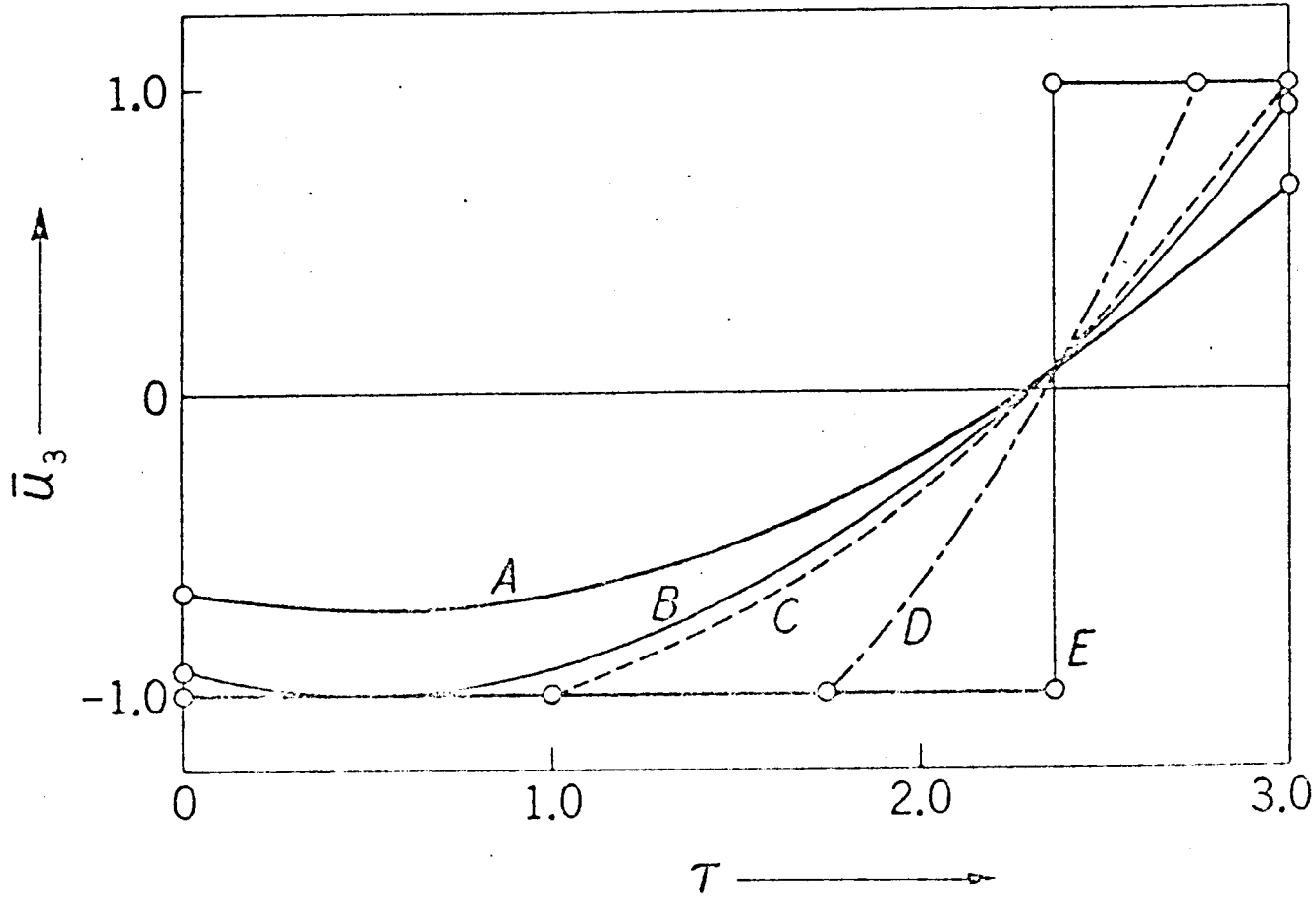

Fig. 2.9. Time responses of the optimal control (k = 1 and T = 3).

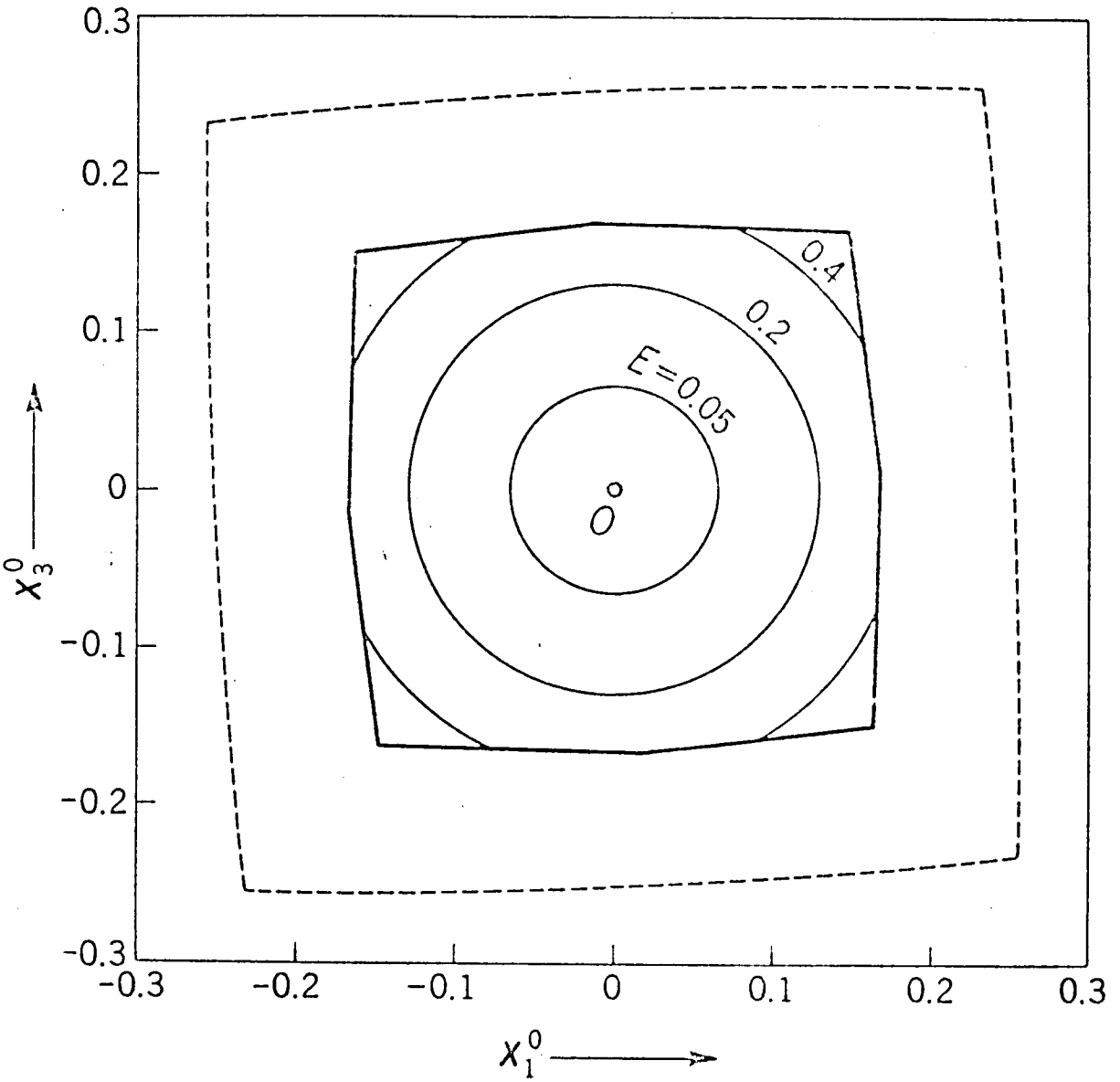

Fig. 2.10. Region of initial values for the nonsaturating control and iso-E curves on the $x_1^0 x_3^0$ plane.

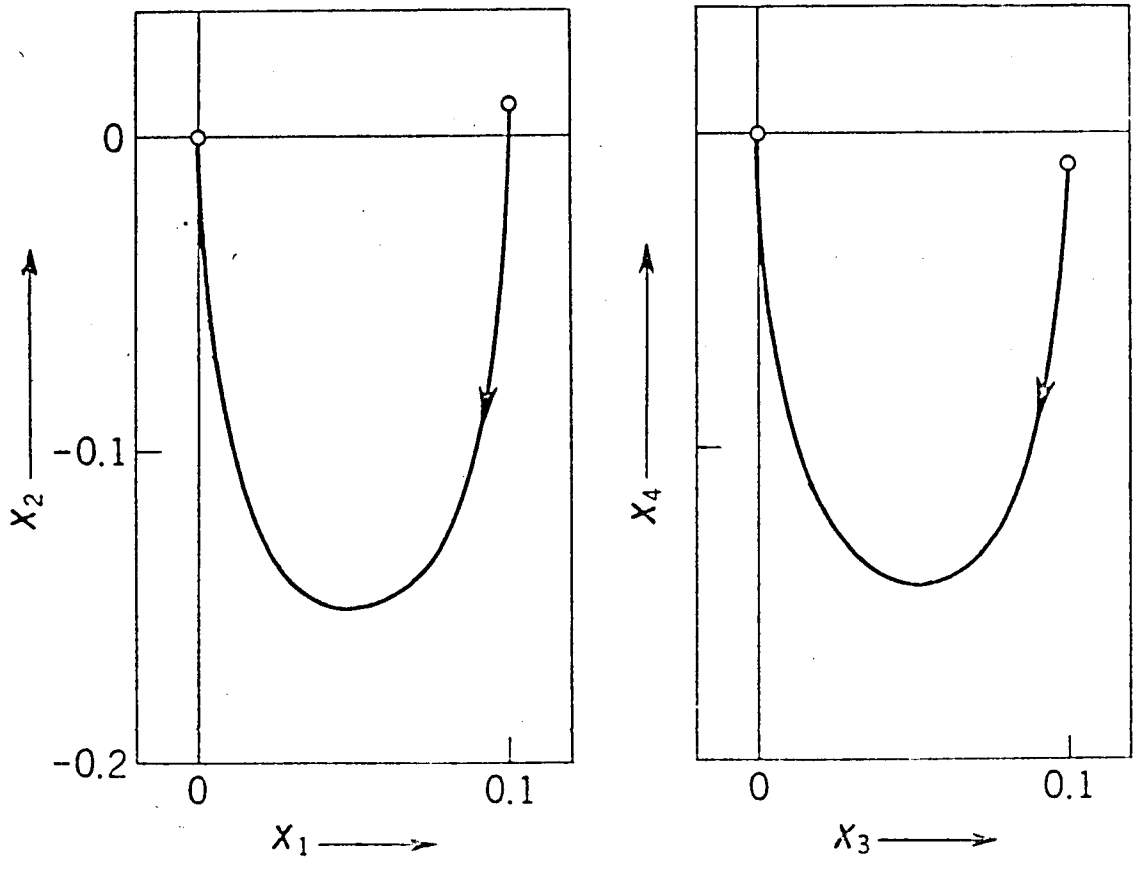

Fig. 2.11. Trajectories of the state variables $x_1 \sim x_4$ in the minimum-energy control.

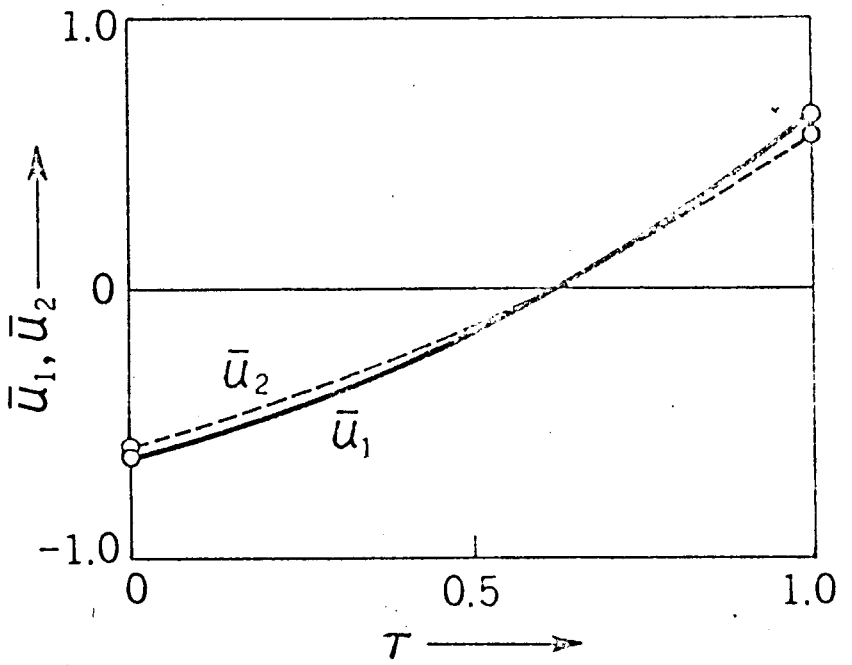

Fig. 2.12. Time responses of the optimal controls.

CHAPTER 3

OPTIMAL VARIABLE-THRUST TRANSFER BETWEEN NEIGHBORING ELLIPTIC ORBITS

3.1 Introduction

It is well known that free-flight trajectories of space vehicles in an inverse-square gravitational force field are conic sections. Thrust forces are often required to act on a vehicle in order to correct its perturbed trajectory or to transfer its orbit on account of some specified mission. In most cases, optimization of thrust program with respect to propellant expenditure may be desired, since this permits the largest payload to be delivered for a given size of vehicle.

The present chapter is concerned with the minimum-fuel transfer between neighboring elliptic orbits for a low-thrust power-limited propulsion system. There have been a number of previous papers on trajectory optimization for power-limited propulsion system [5-7, 10, 11, 18, 20, 33]. Among them, F. W. Gobetz has treated the variable-thrust transfer between neighboring circular orbits and obtained an exact solution analytically [10]. This chapter extends the work of Gobetz and deals with the optimal thrust program for transfer between neighboring elliptic orbits [14, 25-28].

Since an initial orbit and a target orbit are assumed to be located close to each other, the inclination between orbit planes is small and the radial separation between orbits is also small relative to the semilatus rectum of either orbit. It is furthermore assumed that the terminal ellipses are of

small eccentricities. In the case of circular terminal orbits, the symmetry of the orbits about their common center allows arbitrary choice of the optimal point of departure from the initial orbit. The orbital velocity of a vehicle revolving along an elliptic orbit varies periodically in time. This variation produces terms with periodic coefficients in the equation of motion; furthermore, it results in the variation of fuel consumption depending upon the point of departure.

The analysis is carried out in two sets of state variables. First, the equation of motion of a vehicle is expressed in terms of the coordinates of a rotating rectangular system with the origin moving in an initial orbit about the earth. If the motion in the transfer does not deviate significantly from the terminal orbits, the gravitational terms in the equation of motion may be linearized. However, terms with time-varying coefficients appear in the equation. When the eccentricities of the orbits are small, the time-varying terms are also small. The small parameter method is applied for obtaining an approximate solution of the differential equation with periodic coefficients. This method of analysis is investigated in Secs. 3.2 through 3.5.

Secondly, another set of state variables, i.e., orbital elements of a space vehicle, are introduced in order to treat the same problem. The orbital elements are constant if there is no force other than the inverse-square gravitational force. The values of elements, however, change under the influence of the thrust force. If the thrust force is small compared with the gravitational force, the instantaneous values of the elements change slowly with time. Consequently, another form of the linearized equation of motion is obtained. Sections 3.6 through 3.10 deal with this method of analysis.

The results obtained are compared with those of the former analysis (Secs. 3.2-3.5).

The optimal thrust program is investigated by using the maximum principle. The motion of the vehicle and the fuel consumption under the action of the optimal thrust are calculated. The dependence of fuel consumption on the transfer time and on the position of departure from the initial orbit is also studied.

3.2 System Description

(a) Coordinate System

One of the basic problems for describing dynamical behavior of a space vehicle is the choice of a reference coordinate system. We choose a rotating rectangular system, as shown in Fig. 3.1. The origin O revolves along the initial orbit in the direction of the arrow on the trajectory. The vehicle S is coincident with the origin O when no thrust acceleration is applied. Axis j is directed outward along the local vertical and axis i is perpendicular to axis j in the initial orbit plane. Axis k is normal to the orbit plane and directed so as to form the coordinates i, j, k a right-handed triad.

The distance r of the origin O from the center of the earth E is related to the true anomaly θ by

$$r = \frac{\ell}{1 + \varepsilon \cos \theta} \tag{3.1}$$

where ℓ and ε denote the semilatus rectum and the eccentricity of the initial orbit, respectively. The time variation of the anomaly θ is approximately given by

$$\theta = \bar{n}t + 2\varepsilon \sin \bar{n}t \tag{3.2}$$

where $\bar{n}$ is the mean value of angular velocity n of the origin O over one revolution along the orbit. The time origin is chosen as t = 0 when the point O passes through the perigee P of the orbit. Under the assumption that the eccentricity ε is not so large, terms of order higher than the first in ε are discarded in Eq. (3.2).

The reference coordinate system is rotating about axis k. The angular velocity ω of the system i, j, k relative to the inertial space may be written as

$$\omega = 0\,\mathring{i} + 0\,\mathring{j} - \theta' \mathring{k} \tag{3.3}$$

where $\mathring{i}$, $\mathring{j}$, and $\mathring{k}$ are the unit vectors along axes i, j, and k, respectively. The prime denotes differentiation with respect to time t.

(b) Equations of Motion of the Vehicle

Let x, y, and z be the i, j, and k components of the vehicle displacement in the reference frame, respectively. The position vector R of the vehicle with respect to the center of the earth may be expressed as

$$R = x\,\mathring{i} + (r + y)\,\mathring{j} + z\,\mathring{k} \tag{3.4}$$

The gravitational force G acting on a unit mass of the vehicle is

$$G = -\frac{\mu}{R^3}\left[x\,\mathring{i} + (r + y)\,\mathring{j} + z\,\mathring{k}\right] \tag{3.5}$$

where μ is the product of the universal gravitational constant times the mass of the gravitational source, i.e., the earth, and R is the magnitude of

the vector $\mathbb{R}$. Since the initial and target orbits are located close to each other, we may assume that the displacements x, y, and z are sufficiently small relative to the distance r (or R). Hence, by neglecting terms of order higher than the first in x/r, y/r, and z/r in Eq. (3.5), we obtain

$$\mathbb{G} = -\frac{\mu}{r^3}[x\mathring{i} + (r - 2y)\mathring{j} + z\mathring{k}] \tag{3.6}$$

The thrust acceleration vector $\mathbb{A}$ of the vehicle may be represented as

$$\mathbb{A} = A_1\mathring{i} + A_2\mathring{j} + A_3\mathring{k} \tag{3.7}$$

where A_1, A_2, and A_3 are the circumferential, radial, and normal components of the thrust acceleration, respectively.

The equation of motion of the vehicle is given by [38, pp. 20-23]

$$\mathbb{R}'' + \omega \times (\omega \times \mathbb{R}) + \omega' \times \mathbb{R} + 2\omega \times \mathbb{R}' = \mathbb{G} + \mathbb{A} \tag{3.8}$$

where the primes denote time derivatives in the reference frame. The component forms of Eq. (3.8) can be immediately obtained by substitution of Eqs. (3.1) through (3.4) and (3.6), (3.7) into Eq. (3.8), i.e.,

$$\left.\begin{aligned} &x'' + 2\bar{n}(1 + 2\varepsilon\cos\bar{n}t)y' \\ &\qquad - \varepsilon\bar{n}^2(\cos\bar{n}t\cdot x + 2\sin\bar{n}t\cdot y) - A_1 = 0 \\ &y'' - 2\bar{n}(1 + 2\varepsilon\cos\bar{n}t)x' \\ &\qquad + \bar{n}^2(2\varepsilon\sin\bar{n}t\cdot x - 3y - 10\varepsilon\cos\bar{n}t\cdot y) - A_2 = 0 \\ &z'' + \bar{n}^2(1 + 3\varepsilon\cos\bar{n}t)z - A_3 = 0 \end{aligned}\right\} \tag{3.9}$$

The first and second equations are mutually related; while the third equation is independent of the first two. In other words, the out-of-plane motion is decoupled from the in-plane motion in the linearized system.

For convenience, we introduce dimensionless quantities defined by

$$\left.\begin{aligned} x_1 &= x/\ell \qquad x_2 = \dot{x}/\ell \qquad x_3 = y/\ell \\ x_4 &= \dot{y}/\ell \qquad x_5 = z/\ell \qquad x_6 = \dot{z}/\ell \\ u_i &= A_i/\ell\,\bar{n}^2 \quad (i = 1, 2, 3) \qquad \tau = \bar{n}t \end{aligned}\right\} \tag{3.10}$$

where a dot over a quantity denotes differentiation with respect to the normalized time τ. By use of these quantities, we rewrite Eqs. (3.9) as

$$\left.\begin{aligned} \dot{x}_1 &= x_2 \\ \dot{x}_2 &= -2x_4 \\ &\quad + \varepsilon\,(\cos\tau\cdot x_1 + 2\sin\tau\cdot x_3 - 4\cos\tau\cdot x_4) + u_1 \\ \dot{x}_3 &= x_4 \\ \dot{x}_4 &= 2x_2 + 3x_3 \\ &\quad - 2\varepsilon\,(\sin\tau\cdot x_1 - 2\cos\tau\cdot x_2 - 5\cos\tau\cdot x_3) + u_2 \end{aligned}\right\} \tag{3.11}$$

and

$$\left.\begin{aligned} \dot{x}_5 &= x_6 \\ \dot{x}_6 &= -x_5 - 3\varepsilon\cos\tau\cdot x_5 + u_3 \end{aligned}\right\} \tag{3.12}$$

(c) Power-Limited Propulsion System

Electrical propulsion systems are characterized by the use of electric energy for the ejection of the propellant mass [17]. The accelerating forces may be exerted upon the propellant particles by electric fields, magnetic fields, or a combination of both; or the heat energy contained in an electric arc discharge. In such systems, the propellant exhaust velocity and the rate of mass flow may be controlled independently. If there are no restrictions on the mass flow rate and the exhaust velocity, there is no limitation on the magnitude of the thrust that can be produced. However, the available power

must be limited depending on the source of electric power aboard the vehicle.

The acceleration A due to thrust is given by

$$A = \frac{\text{Thrust}}{\text{Mass}} = \frac{cM'}{M} \tag{3.13}$$

where M' and c are the rate of change of mass and the exhaust velocity, respectively. The exhaust power P(t) is given by

$$P(t) = -\frac{1}{2} M'c^2 \tag{3.14}$$

In electrical propulsion system, we have the restriction that the total power P(t) must at all times be less than or equal to the total useful power available, P_{max}:

$$P(t) \leq P_{max} \tag{3.15}$$

Eliminating c between Eqs. (3.13) and (3.14) becomes

$$\frac{A^2}{2\,P(t)} = -\frac{M'}{M^2} = \frac{d}{dt}\left(\frac{1}{M}\right) \tag{3.16}$$

If the subscripts 0 and T are used to denote initial and terminal values, an integration yields

$$\frac{1}{M_T} = \frac{1}{M_0} + \frac{1}{2}\int_0^T \frac{A^2}{P(t)}\,dt \tag{3.17}$$

Since the integrand of Eq. (3.17) is nowhere negative, the terminal mass M_T can be maximized by at all times choosing $P(t) = P_{max}$. Then Eq. (3.17) reduces to

$$\frac{1}{M_T} = \frac{1}{M_0} + \frac{1}{2P_{max}}\int_0^T A^2\,dt \tag{3.18}$$

Thus, if

$$J = \frac{1}{2}\int_0^T A^2\,dt \tag{3.19}$$

then the maximum payload and, consequently, the minimum fuel consumption is obtained by minimizing J.

3.3 Optimal Control Functions

The optimization problem is to derive the optimal control functions for the minimum-fuel transfer of a power-limited rocket with unbounded thrust acceleration in a prescribed time. From Eq. (3.19), this requires minimization of the integral

$$J = \frac{1}{2}\int_{\tau_0}^{\tau_0+T} (u_1^2 + u_2^2 + u_3^2)\, d\tau \tag{3.20}$$

subject to constraints imposed by the equations of motion, i.e., Eqs. (3.11) and (3.12). The control functions to be optimized are the normalized components u_1, u_2, and u_3 of the thrust acceleration. In Eq. (3.20), T is a prescribed transfer time and τ_0 denotes the instant of departure of the vehicle from the initial orbit.*

The optimal control functions can be obtained by using the maximum principle. The Hamiltonian function of the problem is given by [30, pp. 9-21]

$$\begin{aligned} H = {} & (p_2u_1 - \tfrac{1}{2}u_1^2) + (p_4u_2 - \tfrac{1}{2}u_2^2) + (p_6u_3 - \tfrac{1}{2}u_3^2) + p_1x_2 \\ & - p_2[2x_4 - \varepsilon(\cos\tau\cdot x_1 + 2\sin\tau\cdot x_3 - 4\cos\tau\cdot x_4)] \\ & + p_3x_4 + p_4[2x_2 + 3x_3 - 2\varepsilon(\sin\tau\cdot x_1 \\ & - 2\cos\tau\cdot x_2 - 5\cos\tau\cdot x_3)] + p_5x_6 \\ & - p_6(x_5 + 3\varepsilon\cos\tau\cdot x_5) \end{aligned} \tag{3.21}$$

---

* See Sec. 3.2(a) for the time origin.

where the auxiliary variables p's satisfy the set of differential equations

$$\left.\begin{aligned}
\dot{p}_1 &= -\varepsilon\,(\cos\tau\cdot p_2 - 2\sin\tau\cdot p_4)\\
\dot{p}_2 &= -p_1 - 2p_4 - 4\varepsilon\cos\tau\cdot p_4\\
\dot{p}_3 &= -3p_4 - 2\varepsilon\,(\sin\tau\cdot p_2 + 5\cos\tau\cdot p_4)\\
\dot{p}_4 &= 2p_2 - p_3 + 4\varepsilon\cos\tau\cdot p_2
\end{aligned}\right\} \qquad (3.22)$$

$$\left.\begin{aligned}
\dot{p}_5 &= p_6 + 3\varepsilon\cos\tau\cdot p_6\\
\dot{p}_6 &= -p_5
\end{aligned}\right\} \qquad (3.23)$$

By using the maximum principle, we obtain the necessary conditions for the optimal controls $\bar{u}_i\,(i = 1,2,3)$:

$$\bar{u}_1 = p_2, \qquad \bar{u}_2 = p_4, \qquad \text{and} \qquad \bar{u}_3 = p_6 \qquad (3.24)$$

Since Eqs. (3.22) and (3.23) are linear equations with periodic coefficients, it is not possible to obtain the exact solution. We here apply the small parameter method for obtaining an approximate solution. According to the principle of the small parameter method, first we develop the desired solutions in power series with respect to the small parameter ε [13]:

$$p_i(\tau) = p_i^0(\tau) + \varepsilon\, p_i^1(\tau) + \varepsilon^2 p_i^2(\tau) + \cdots \qquad (3.25)$$

$$(i = 1 \text{ to } 6)$$

where the functions p_i with superscript n are the coefficients of the n-th order terms in the expansions. Secondly, upon substituting Eqs. (3.25) into Eqs. (3.22) and (3.23) and collecting the terms with like powers of ε, the sequence of linear differential equations with constant coefficients is obtained, i.e.,

$$\varepsilon^0: \quad \left.\begin{aligned} \dot{p}_1^0 &= 0 \\ \dot{p}_2^0 &= -p_1^0 - 2p_4^0 \\ \dot{p}_3^0 &= -3p_4^0 \\ \dot{p}_4^0 &= 2p_2^0 - p_3^0 \end{aligned}\right\} \tag{3.26}$$

$$\left.\begin{aligned} \dot{p}_5^0 &= p_6^0 \\ \dot{p}_6^0 &= -p_5^0 \end{aligned}\right\} \tag{3.27}$$

$$\varepsilon^n: \quad \left.\begin{aligned} \dot{p}_1^n &= -\cos\tau\cdot p_2^{n-1} + 2\sin\tau\cdot p_4^{n-1} \\ \dot{p}_2^n &= -p_1^n - 2p_4^n - 4\cos\tau\cdot p_4^{n-1} \\ \dot{p}_3^n &= -3p_4^n - 2\sin\tau\cdot p_2^{n-1} - 10\cos\tau\cdot p_4^{n-1} \\ \dot{p}_4^n &= 2p_2^n - p_3^n + 4\cos\tau\cdot p_2^{n-1} \end{aligned}\right\} \tag{3.28}$$

$$\left.\begin{aligned} \dot{p}_5^n &= p_6^n + 3\cos\tau\cdot p_6^{n-1} \\ \dot{p}_6^n &= -p_5^n \end{aligned}\right\} \tag{3.29}$$

$$(n = 1, 2, 3, \cdots)$$

Solving Eqs. (3.26) through (3.29) in ascending order of n yields p_i^0, $p_i^1, \cdots$, successively. The solutions p_2, p_4, and p_6 of Eqs. (3.22) and (3.23), up to terms of the first order in ε, are

$$\left.\begin{aligned} \bar{u}_1 &= p_2 = p_2^0 + \varepsilon\, p_2^1 \\ \bar{u}_2 &= p_4 = p_4^0 + \varepsilon\, p_4^1 \\ \bar{u}_3 &= p_6 = p_6^0 + \varepsilon\, p_6^1 \end{aligned}\right\} \tag{3.30}$$

where

$$
\left.
\begin{aligned}
p_2^0 &= -3c_4^0 - 3c_1^0\tau - 4c_3^0 \sin\tau + 4c_2^0 \cos\tau \\
p_4^0 &= 2c_1^0 + 2c_2^0 \sin\tau + 2c_3^0 \cos\tau \\
p_6^0 &= -c_9^0 \sin\tau + c_{10}^0 \cos\tau \\
p_2^1 &= -27c_2^0 + 21c_4^0 - 3c_4^1 + 3(c_1^0 + 2c_3^0 - c_1^1)\tau \\
&\quad - 4(2c_1^0 + 2c_3^0 + c_3^1) \sin\tau + (24c_2^0 - 21c_4^0 + 4c_2^1) \cos\tau \\
&\quad - 3c_1^0\tau \cos\tau - 3c_3^0 \sin 2\tau + 3c_2^0 \cos 2\tau \\
p_4^1 &= -2c_1^0 - 6c_3^0 + 2c_1^1 \\
&\quad + 2(6c_2^0 - 6c_4^0 + c_2^1) \sin\tau \\
&\quad + 2(c_1^0 + 2c_3^0 + c_3^1) \cos\tau \\
&\quad - 3c_1^0\tau \sin\tau + 2c_2^0 \sin 2\tau + 2c_3^0 \cos 2\tau \\
p_6^1 &= -1.5c_{10}^0 + (c_9^0 - c_9^1) \sin\tau + (c_{10}^0 + c_{10}^1) \cos\tau \\
&\quad - 0.5c_9^0 \sin 2\tau + 0.5c_{10}^0 \cos 2\tau
\end{aligned}
\right\} \qquad (3.31)
$$

In the above equations c_j^0 and c_j^1 ($j = 1$ to 4, and 9, 10) are constants of integration; they are determined by initial values of p_i^0 and p_i^1, respectively.

By substituting Eqs. (3.30) into Eq. (3.20), we obtain the cost function up to the first order in ε as

$$
\begin{aligned}
J &= J^0 + \varepsilon J^1 \\
&= \frac{1}{2} \int_{\tau_0}^{\tau_0+T} [(p_2^0)^2 + (p_4^0)^2 + (p_6^0)^2] \, d\tau \\
&\quad + \varepsilon \int_{\tau_0}^{\tau_0+T} (p_2^0 p_2^1 + p_4^0 p_4^1 + p_6^0 p_6^1) \, d\tau
\end{aligned} \qquad (3.32)
$$

Similarly, the solutions of the equations of motion, Eqs. (3.11) and

(3.12), are sought in the form

$$x_i(\tau) = x_i^0(\tau) + \varepsilon\, x_i^1(\tau) + \varepsilon^2 x_i^2(\tau) + \cdots \qquad (3.33)$$

$$(i = 1 \text{ to } 6)$$

Substitution of Eqs. (3.30), (3.31), and (3.33) into Eqs. (3.11), (3.12) and collection of like powers of ε gives a set of simultaneous equations, i.e.,

$$\varepsilon^0: \quad \left.\begin{aligned} \dot{x}_1^0 &= x_2^0 \\ \dot{x}_2^0 &= -2x_4^0 + p_2^0 \\ \dot{x}_3^0 &= x_4^0 \\ \dot{x}_4^0 &= 2x_2^0 + 3x_3^0 + p_4^0 \end{aligned}\right\} \qquad (3.34)$$

$$\left.\begin{aligned} \dot{x}_5^0 &= x_6^0 \\ \dot{x}_6^0 &= -x_5^0 + p_6^0 \end{aligned}\right\} \qquad (3.35)$$

$$\varepsilon^n: \quad \left.\begin{aligned} \dot{x}_1^n &= x_2^n \\ \dot{x}_2^n &= -2x_4^n + p_2^n + \cos\tau \cdot x_1^{n-1} + 2\sin\tau \cdot x_3^{n-1} - 4\cos\tau \cdot x_4^{n-1} \\ \dot{x}_3^n &= x_4^n \\ \dot{x}_4^n &= 2x_2^n + 3x_3^n + p_4^n - 2\sin\tau \cdot x_1^{n-1} + 4\cos\tau \cdot x_2^{n-1} + 10\cos\tau \cdot x_3^{n-1} \end{aligned}\right\} \qquad (3.36)$$

$$\left.\begin{aligned} \dot{x}_5^n &= x_6^n \\ \dot{x}_6^n &= -x_5^n + p_6^n - 3\cos\tau \cdot x_5^{n-1} \end{aligned}\right\} \qquad (3.37)$$

$$(n = 1, 2, 3, \cdots)$$

The solutions of Eqs. (3.11) and (3.12), up to the first order in ε, are given by

$$x_i(\tau) = \sum_{j=1}^{8} c_j^0 X_{ij}^0(\tau) + \varepsilon \sum_{j=1}^{8} [c_j^1 X_{ij}^0(\tau) + c_j^0 X_{ij}^1(\tau)] \qquad (3.38)$$

$$(i = 1, 2, 3, 4)$$

$$x_i(\tau) = \sum_{j=9}^{12} c_j^0 X_{ij}^0(\tau) + \varepsilon \sum_{j=9}^{12} [c_j^1 X_{ij}^0(\tau) + c_j^0 X_{ij}^1(\tau)] \qquad (3.39)$$

$$(i = 5, 6)$$

where $X_{ij}^0(\tau)$ and $X_{ij}^1(\tau)$ are definite functions of time τ, the details of which will be shown in Appendix III. The constants of integration c_j^0 and c_j^1 ($j = 5$ to 8, and 11, 12) may be determined by initial values of x_i^0 and x_i^1, respectively.

3.4 Boundary Conditions

In order to determine the values of c_j^0 and c_j^1 ($j = 1$ to 12) which minimize the cost function J under a prescribed condition, the boundary conditions of the transfer orbit and the transversality conditions of the problem must be investigated.

Figure 3.2 gives a schematic presentation of a transfer between two elliptic orbits. Let α be the inclination of the target orbit plane with respect to the initial orbit plane. ϕ_1 and $\phi_2 = \phi_1 - \psi$ are the true anomalies of the line of intersection of the orbit planes as measured from the points P_1 and P_2 respectively, where P_1 and P_2 are the perigees of the corresponding ellipses. The parameter ψ stands exactly for the angle between the apse lines of the two ellipses when the terminal orbits are coplanar, i.e., $\alpha = 0$; and it does approximately when the inclination α is small.

The eccentricity and the semilatus rectum of the target ellipse are denoted by εE and $\ell + \Delta\ell \equiv \ell(1 + \lambda)$, respectively. In other words, the parameter E denotes the ratio of eccentricities of the two ellipses, and $\lambda\ell$ is the increment in the semilatus rectum.

Point 1 in Fig. 3.2 shows the point of departure from the initial orbit, i.e., the point at which the thrust acceleration begins to act. Points 2 and 3 represent, respectively, the position of the origin O of the reference frame and the position of the vehicle S at the final time of transfer.

Prior to the application of the thrust acceleration, the vehicle S is coincident with the origin O. Hence all the state variables are zero at $\tau = \tau_0$, i.e.,

$$x_i(\tau_0) = 0 \qquad (i = 1 \text{ to } 6) \tag{3.40}$$

Let us consider the boundary condition at the final point of transfer. The position of the vehicle at the final time $\tau = \tau_0 + T \equiv \tau_f$ may be defined by the angle $\Delta\theta = \angle 2E3$ in the figure. The final velocity of the vehicle must agree with the orbital velocity along the target ellipse at point 3. This condition demands the following relations:

$$\left.\begin{aligned}
x_1(\tau_f) &= \Delta\theta\,[1 - \varepsilon E \cos(\tau_f - \psi)] \\
x_2(\tau_f) &= -1.5\lambda - \varepsilon\{\Delta\theta\, E \sin(\tau_f - \psi) + \lambda[2\cos\tau_f \\
&\qquad - 0.5E\cos(\tau_f - \psi)] + 2\cos\tau_f - 2E\cos(\tau_f - \psi)\} \\
x_3(\tau_f) &= \lambda + \varepsilon[\Delta\theta\, E \sin(\tau_f - \psi) - \lambda E\cos(\tau_f - \psi) \\
&\qquad + \cos\tau_f - E\cos(\tau_f - \psi)] \\
x_4(\tau_f) &= \varepsilon\{\Delta\theta\,[2\cos\tau_f - E\cos(\tau_f - \psi)] \\
&\qquad - 0.5\lambda E \sin(\tau_f - \psi) - \sin\tau_f + E\sin(\tau_f - \psi)\}
\end{aligned}\right\} \tag{3.41}$$

$$
\left.
\begin{aligned}
x_5(\tau_f) &= \alpha\{\sin(\tau_f - \phi_1) + \varepsilon[\sin\phi_1 + 0.5E\sin\phi_2 \\
&\quad - 0.5E\sin(2\tau_f - 2\phi_1 + \phi_2) + \sin(2\tau_f - \phi_1)]\} \\
x_6(\tau_f) &= \alpha\{\cos(\tau_f - \phi_1) + \varepsilon[-\cos\phi_1 + E\cos\phi_2 \\
&\quad + \cos(2\tau_f - \phi_1)]\}
\end{aligned}
\right\} \quad (3.42)
$$

Since the quantities α, λ, and, consequently, $\Delta\theta$ are small, terms of order higher than the first in those quantities are discarded in Eqs. (3.41) and (3.42).* Linearization in those parameters results in the separation of the boundary conditions into the conditions for the in-plane components, Eqs. (3.41), and those for the out-of-plane components, Eqs. (3.42).

We substitute Eqs. (3.38), (3.39) into Eqs. (3.40), (3.41), and (3.42), and collect terms with the zero and first powers of ε. Then we obtain twenty four relations which serve to determine as many integration constants c_j^0 and c_j^1 (j = 1 to 12). Those relations contain the parameters τ_0 and $\Delta\theta$ which represent the points of departure and arrival respectively. Those parameters must be determined so as to minimize the fuel consumption for a given transfer time. In other words, transversality conditions with respect to τ_0 and $\Delta\theta$ must be satisfied. The transversality condition with respect to $\Delta\theta$ is given by [30, pp. 45-50]

$$
\sum_{i=1}^{6} p_i(\tau_f)\cdot\frac{\partial}{\partial\Delta\theta}x_i(\tau_f) = 0 \qquad (3.43)
$$

Substituting the solutions $p_i(\tau_f)$ of Eqs. (3.22), (3.23) and $x_i(\tau_f)$ of

---

* The process for deriving Eqs. (3.41) and (3.42) will be shown in Appendix IV.

Eqs. (3.41), (3.42) into Eq. (3.43) leads to

$$\left.\begin{aligned} c_1^0 &= 0 \\ c_1^1 + 2c_2^0 E \sin\psi + 2c_3^0(E\cos\psi - 2) &\\ + 3c_4^0[E\sin(\tau_f - \psi) - \sin\tau_f] &= 0 \end{aligned}\right\} \qquad (3.44)$$

The transversality condition with respect to τ_0 leads to a complicated relation. Therefore, we directly calculate the cost function J for various values of τ_0 and fix a value of τ_0 which minimizes the cost function.

The procedure for obtaining the optimal control may be summarized as follows. Let $\Delta\theta^0$ and $\varepsilon\,\Delta\theta^1$ be the zero- and first-order terms in the power series expansion of $\Delta\theta$. For given values of τ_0 and T, twenty-six unknown quantities c_j^0, c_j^1 (j = 1 to 12) and $\Delta\theta^0$, $\Delta\theta^1$ are determined by solving the system of linear algebraic equations (3.40), (3.41), (3.42), and (3.44). Upon substituting the values of c_j^0 and c_j^1 thus obtained into Eqs. (3.30) and (3.31), we obtain the optimal control functions $\bar{u}_1$, $\bar{u}_2$, and $\bar{u}_3$. The cost function and the transfer trajectory under the action of the optimal thrust acceleration are calculated from Eqs. (3.32) and (3.38), (3.39), respectively, by using the same integration constants.

3.5 Numerical Examples

(a) Transfer between Coplanar Ellipses of a Same Eccentricity Whose Axes Are Aligned and Oriented in the Same Sense

Let us consider a case in which the terminal orbits are coplanar, i.e., $\alpha = 0$. In this case we may infer that the motion of a vehicle is confined

only in the plane of initial orbit.

First, we assume that the terminal ellipses have a same eccentricity and are coaxial with each other, and that their axes are oriented in the same sense, i.e., $E = 1$ and $\psi = 0$. Then the boundary conditions, Eqs. (3.40), (3.41), and the transversality condition, Eqs. (3.44), become

$$\sum_{j=1}^{8} c_j^0 X_{ij}^0(\tau_0) = 0 \qquad (i = 1 \text{ to } 4) \tag{3.45}$$

$$\sum_{j=1}^{8} [c_j^0 X_{ij}^1(\tau_0) + c_j^1 X_{ij}^0(\tau_0)] = 0 \qquad (i = 1 \text{ to } 4) \tag{3.46}$$

$$\left.\begin{aligned} \sum_{j=1}^{8} c_j^0 X_{1j}^0(\tau_f) - \Delta\theta^0 &= 0 \\ \sum_{j=1}^{8} c_j^0 X_{2j}^0(\tau_f) &= -1.5\lambda \\ \sum_{j=1}^{8} c_j^0 X_{3j}^0(\tau_f) &= \lambda \\ \sum_{j=1}^{8} c_j^0 X_{4j}^0(\tau_f) &= 0 \end{aligned}\right\} \tag{3.47}$$

$$\left.\begin{aligned} \sum_{j=1}^{8} [c_j^0 X_{1j}^1(\tau_f) + c_j^1 X_{1j}^0(\tau_f)] + \Delta\theta^0 \cos\tau_f - \Delta\theta^1 &= 0 \\ \sum_{j=1}^{8} [c_j^0 X_{2j}^1(\tau_f) + c_j^1 X_{2j}^0(\tau_f)] + \Delta\theta^0 \sin\tau_f &= -1.5\lambda\cos\tau_f \\ \sum_{j=1}^{8} [c_j^0 X_{3j}^1(\tau_f) + c_j^1 X_{3j}^0(\tau_f)] - \Delta\theta^0 \sin\tau_f &= -\lambda\cos\tau_f \\ \sum_{j=1}^{8} [c_j^0 X_{4j}^1(\tau_f) + c_j^1 X_{4j}^0(\tau_f)] - \Delta\theta^0 \cos\tau_f &= -0.5\lambda\sin\tau_f \end{aligned}\right\} \tag{3.48}$$

$$\left.\begin{aligned} c_1^0 &= 0 \\ c_1^1 - 2c_3^0 &= 0 \end{aligned}\right\} \tag{3.49}$$

By solving the system of linear algebraic equations (3.45) through (3.49), c_j^0, c_j^1 (j = 1 to 8) and $\Delta\theta^0$, $\Delta\theta^1$ are obtained. They include terms of the first order in λ. Then substitution of the values of c_j^0 and c_j^1 thus obtained into Eq. (3.32) gives us the cost function including terms of the second order in λ.

Figure 3.3 shows variations of the cost function J with respect to τ_0 for various values of T. As in Eq. (3.32), the cost function is developed in power series with respect to ε. The zero-order term J^0 (represented by the dotted line) is constant with respect to τ_0 and agrees, as a matter of course, with the cost function for the transfer between circular orbits [10]. The first-order term J^1 (represented by the solid line) varies periodically in τ_0 with period 2π. This is a plausible result because the orbital velocity varies periodically in τ with the same period; see Eq. (3.2). Hence τ_0 corresponding to the minimum point of J^1 gives the optimal point of departure. When the transfer time T is $2n\pi$ (n being a positive integer), J does not change with τ_0; when $T \neq 2n\pi$, the optimal τ_0 is given by

$$\tau_0 = -(T/2) + (n-1)\pi \qquad \text{for} \qquad 2(n-1)\pi < T < 2n\pi \tag{3.50}$$

Equation (3.50) indicates that the optimal point of departure is located on the semi-ellipse traced by the vehicle moving toward the perigee from the apogee.

Let J_{opt} be the minimum value of J with respect to τ_0. The dependence of J_{opt} on the transfer time T is illustrated in Fig. 3.4, where the eccentricity is assumed to be $\varepsilon = 0.2$. As illustrated in the figure, the cost function J_{opt} decreases as T increases.

Figures 3.5 and 3.6 show time variations of the circumferential and

radial components of the optimal thrust acceleration, respectively. The circumferential components $\bar{u}_1^0$ and $\bar{u}_1^1$ are symmetrical about the midline in time; while the radial components $\bar{u}_2^0$ and $\bar{u}_2^1$ are symmetrical about the midpoint.

Figure 3.7 shows typical examples of the transfer orbit under the optimal acceleration.

(b) Transfer between Coplanar Ellipses of a Same Eccentricity Whose Axes Are Aligned and Oriented in the Opposite Senses

Secondly, we are concerned with the terminal ellipses which are coplanar, coaxial and of the same eccentricity, but are oriented in the opposite senses with each other ,i.e., $\alpha = 0$, $E = 1$, and $\psi = \pi$. In this case, the boundary conditions given by Eqs. (3.40) and (3.41) become Eqs. (3.45), (3.47), and the following equations:

$$\sum_{j=1}^{8} c_j^1 X_{ij}^0(\tau_0) = 0 \qquad (i = 1 \text{ to } 4) \tag{3.51}$$

$$\left.\begin{aligned} \sum_{j=1}^{8} c_j^1 X_{1j}^0(\tau_f) - \Delta\theta^1 &= 0 \\ \sum_{j=1}^{8} c_j^1 X_{2j}^0(\tau_f) &= -4\cos\tau_f \\ \sum_{j=1}^{8} c_j^1 X_{3j}^0(\tau_f) &= 2\cos\tau_f \\ \sum_{j=1}^{8} c_j^1 X_{4j}^0(\tau_f) &= -2\sin\tau_f \end{aligned}\right\} \tag{3.52}$$

where terms of order $\varepsilon\lambda$ are omitted in the above equations. From Eqs.

(3.44), the transversality condition becomes

$$c_1^0 = c_1^1 = 0 \tag{3.53}$$

with neglect of terms of order $\varepsilon\lambda$.

The unknown constants c_j^0, c_j^1 (j = 1 to 8) and $\Delta\theta^0$, $\Delta\theta^1$ are determined by solving the system of linear equations (3.45), (3.47), and (3.51) to (3.53). c_j^0 and $\Delta\theta^0$ are of the first order in λ, while c_j^1 and $\Delta\theta^1$ of the zero order in λ. Substituting the values of c_j^0 and c_j^1 thus obtained into Eq. (3.32) gives us the cost function $J = J^0 + \varepsilon J^1$, where J^0 is of order λ^2 but J^1 of order λ.*

Figure 3.8 shows variations of the cost functions J^0 and J^1 with respect to τ_0 for various values of T. As in the preceding case, J^0 is constant with respect to τ_0, and J^1 varies periodically in τ_0 with period 2π. However, in this case the optimal τ_0 is given by

$$\tau_0 = \begin{cases} -(T/2) + n\pi & \text{for} \quad 2(n-1)\pi < T < 2n\pi \\ \text{arbitrary} & \text{for} \quad T = 2n\pi \end{cases} \tag{3.54}$$

$$(n = 1, 2, 3, \cdots)$$

In other words, the optimal point of departure is located on the semi-ellipse traced by the vehicle moving toward the apogee from the perigee.

Figure 3.9 shows an example of the optimal transfer orbit.

---

* A term $\varepsilon^2 J^2$, where J^2 is of the zero order in λ, may be calculated in the same way, but the details are omitted here.

(c) Transfer between Non-Coplanar Ellipses

Lastly, let us assume that the target orbit is inclined with respect to the initial orbit at a small angle α. We may discuss the out-of-plane motion of a vehicle independently of the in-plane motion.

The out-of-plane component J_3 of the cost function is given by [see Eq. (3.32)]

$$J_3 = J_3^0 + \varepsilon J_3^1$$

$$= \frac{1}{2}\int_{\tau_0}^{\tau_0+T} (p_6^0)^2 \, d\tau + \varepsilon \int_{\tau_0}^{\tau_0+T} p_6^0 p_6^1 \, d\tau \qquad (3.55)$$

J_3^0, the optimal value of the cost function for a transfer between circular orbits, can be obtained exactly and written as

$$J_3^0 = \alpha^2 \frac{T - \sin T \cdot \cos [2(\phi_1 - \tau_0) - T]}{T^2 - \sin^2 T} \qquad (3.56)$$

Equation (3.56) indicates that, in the case of a transfer between non-coplanar circles, J_3 varies periodically in τ_0 with period π, namely, half the period of the orbital motion along the initial orbit.

Let $\phi_1 = \phi_2 = 0.5\pi$ (consequently $\psi = 0$) and $E = 1$. Figure 3.10 shows variations of J_3 with respect to τ_0 for various values of T. J_3^0 and J_3^1 are represented by the dotted line and the solid line, respectively.

Figure 3.11 shows time variation of the out-of-plane component of the optimal thrust acceleration.

In general, the optimal point of departure for a transfer between non-coplanar ellipses may be decided by finding out τ_0 which corresponds to the minimum point of J, where J is given by summing up the in-plane and the out-

of-plane component of the cost function. As an example, Figure 3.12 illustrates the dependence of J on τ_0, where the parameters of the terminal orbits are assumed to be $\alpha = \lambda$, $E = 1$, and $\phi_1 = \phi_2 = 0.5\pi$ (consequently $\psi = 0$).* The zero-order term J^0 in the power series expansion of J with respect to ε is represented in the figure by the dotted line, while the first-order term J^1 is shown by the solid line.

3.6 Method of Analysis by Using Orbital Elements of a Space Vehicle

In the preceding sections, the rotating rectangular coordinate system was applied in order to describe the equation of motion of the vehicle. We now introduce another set of state variables, i.e., the elements of an orbit. The orbital elements are constant if there is no force other than the inverse-square central gravitational force. The values of elements, however, change with time under the influence of any perturbing force. If the perturbing force is small compared with the central force, the instantaneous values of the elements will change slowly.

The following sections are concerned with a method for analyzing the minimum-fuel change of orbital elements of a space vehicle which transfers between neighboring elliptic orbits [6, 11, 27, 28]. As in the foregoing investigations, both the terminal ellipses are assumed to be of small eccentricities. The propulsion system that effects the change of the orbital elements is considered to be power-limited and thrust-variable. The analysis

---

* In this case the cost function J is obtained by summing up the in-plane component as shown in Fig. 3.3 and the out-of-plane component as in Fig. 3.10.

is carried out under the assumption that the thrust acceleration is small compared with the gravity acceleration and that the perturbations of the orbital elements due to thrust are small.

The optimal thrust program is determined and the fuel consumption under the action of this thrust program is calculated. The results obtained are compared with those of the preceding sections.

3.7 Orbital Elements and Their Perturbation

In celestial mechanics, an orbit and the position of a body in that orbit are defined by six constants called orbital elements [1, pp. 17-19]. Three of them define the spatial orientation of the orbit, and two of them specify the size and shape of the orbit. The sixth orbital element is required for the angular position of the body.

Figure 3.13 illustrates a typical elliptic orbit of a space vehicle. The reference plane is a plane which includes the center E of gravitational force and a reference line EL. The line of intersection of the orbital plane and the reference plane is called the line of nodes. If the direction of motion of the vehicle is as indicated by the arrow, the point N is referred to as the ascending node. Then the longitude of the ascending node Ω is given by the angle LEN. The angle of inclination of the orbit plane to the reference plane is denoted by i. These two elements orient the orbital plane. The third element orients the orbit within the orbital plane. Namely, the argument of perigee ω is the angle between the lines EN and EP.* It is

---

* The perigee and the apogee are denoted by the points P and A in Fig. 3.13, respectively.

customary to denote the sum $\Omega + \omega$ by $\bar{\omega}$, called the longitude of perigee.* The size of the orbit is specified by the semimajor axis a and the shape by the eccentricity ε. The sixth element, which may be defined in several ways, specifies the angular position of the vehicle S in its orbit at a particular time, or the time at which it passes a particular point.

The orbital elements are constant if there is no force other than the earth gravitation; however, if a perturbing force is applied to the vehicle S, the values of elements will change with time. This change is called perturbation of the orbital elements. In celestial mechanics, there have been a number of investigations which deal with the perturbation of an orbit. According to Ref. 36 the rates of changes of the orbital elements are given by the following equations:

$$
\left.
\begin{aligned}
\frac{da}{dt} &= 2\sqrt{\frac{a^3}{\mu(1-\varepsilon^2)}}\left[(1+\varepsilon\cos\eta)\alpha_1 + \varepsilon\sin\eta\cdot\alpha_2\right] \\
\frac{d\varepsilon}{dt} &= \sqrt{\frac{a(1-\varepsilon^2)}{\mu}}\left[\frac{2\cos\eta + \varepsilon(1+\cos^2\eta)}{1+\varepsilon\cos\eta}\alpha_1 + \sin\eta\cdot\alpha_2\right] \\
\frac{d\bar{\omega}}{dt} &= \sqrt{\frac{a(1-\varepsilon^2)}{\mu\varepsilon^2}}\left[\frac{\sin\eta\cdot(2+\varepsilon\cos\eta)}{1+\varepsilon\cos\eta}\alpha_1 - \cos\eta\cdot\alpha_2\right. \\
&\qquad \left. - \frac{\varepsilon\tan(i/2)\cdot\sin(\eta+\bar{\omega}-\Omega)}{1+\varepsilon\cos\eta}\alpha_3\right] \\
\frac{di}{dt} &= -\sqrt{\frac{a(1-\varepsilon^2)}{\mu}}\cdot\frac{\cos(\eta+\bar{\omega}-\Omega)}{1+\varepsilon\cos\eta}\alpha_3 \\
\frac{d\Omega}{dt} &= -\sqrt{\frac{a(1-\varepsilon^2)}{\mu}}\cdot\frac{\sin(\eta+\bar{\omega}-\Omega)}{\sin i\cdot(1+\varepsilon\cos\eta)}\alpha_3
\end{aligned}
\right\} \qquad (3.57)
$$

---

* It should be noted that this is not a longitude in the ordinary sense because it is measured in two different planes.

In Eqs. (3.57), α_1, α_2, and α_3 are, respectively, the circumferential, radial, and normal components of the vehicle acceleration due to a perturbing force (see Fig. 3.13). The constant μ is the product of the universal gravitational constant and the mass of the earth, and η denotes the true anomaly of the vehicle, i.e., the angle between lines EP and ES.

3.8 Equations of Motion of the Vehicle

Our problem is to change the elements of the initial orbit to those of a given target orbit with use of a suitable controlling thrust. For convenience of calculation we choose the initial orbit plane as a reference plane, and the line of apsides EP_0 of the initial orbit as a reference line (see Fig. 3.14). Furthermore, in order to define the position of the vehicle during transfer, we consider the same rectangular coordinate system as defined in Sec. 3.2(a). That is, the origin O of the coordinate system revolves along the initial orbit in the direction of the arrow on the trajectory. Axis j is directed outward along the local vertical and axis i is perpendicular to axis j in the initial orbit plane. Axis k is normal to the orbit plane and directed so as to form the coordinates i, j, k a right-handed triad. The time origin is chosen as $t = 0$ when the point O passes through the perigee P_0 of the initial orbit. Let x, y, and z be the i, j, and k-components of the vehicle displacement relative to the origin O, respectively.

At any instant of time, the position and velocity vectors of the vehicle may be used to define an instantaneous conic path, i.e., an osculating orbit.*

---

* The osculating orbit is the orbit which the vehicle would follow if at any time all perturbing forces suddenly vanished [1, pp. 188-190].

Then the displacements x, y, z and their time derivatives are related to the osculating elements by the following equations:

$$\left.\begin{aligned} x &= (\eta + \bar{\omega} - \theta)a_0 \\ \frac{dx}{dt} &= -\sqrt{\frac{\mu}{a_0}}\left[1.5\,\frac{a - a_0}{a_0} - 2\varepsilon\cos(\theta - \bar{\omega}) + 2\varepsilon_0\cos\theta\right] \\ y &= a - a_0\left[1 + \varepsilon\cos(\theta - \bar{\omega}) - \varepsilon_0\cos\theta\right] \\ \frac{dy}{dt} &= \sqrt{\frac{\mu}{a_0}}\left[\varepsilon\sin(\theta - \bar{\omega}) - \varepsilon_0\sin\theta\right] \\ z &= -i\,a_0\sin(\theta - \Omega) \\ \frac{dz}{dt} &= -i\sqrt{\frac{\mu}{a_0}}\cos(\theta - \Omega) \end{aligned}\right\} \qquad (3.58)$$

where the subscript 0 denotes the value of elements of the initial orbit. θ is the true anomaly of the origin O in the initial orbit plane (see Fig. 3.14). In the derivation of Eqs. (3.58), quantities of order higher than the first in ε, ε_0, i, $(a - a_0)/a_0$, and $\eta + \bar{\omega} - \theta$ are neglected.

In the present study, a set of state variables $x_1, x_2, \ldots, x_6$ consist of six variables defined by the following combinations of the orbital elements a, ε, $\bar{\omega}$, i, Ω, and the displacement x:

$$\left.\begin{aligned} x_1 &= (a - a_0)/a_0 & x_2 &= x/a_0 \\ x_3 &= \varepsilon\sin\bar{\omega} & x_4 &= \varepsilon\cos\bar{\omega} \\ x_5 &= \sin i \cdot \sin\Omega & x_6 &= \sin i \cdot \cos\Omega \end{aligned}\right\} \qquad (3.59)$$

Note that these state variables are dimensionless quantities. The control variables A_1, A_2, A_3 are orthogonal i, j, k-components of the thrust acceler-

ation vector $\mathbb{A}$. For convenience we introduce the dimensionless controls u_1, u_2, u_3 and the dimensionless time τ defined by

$$u_j = A_j/a_0\bar{n}^2 \qquad (j = 1,2,3) \qquad\qquad \tau = \bar{n}t \tag{3.60}$$

where $\bar{n}$ is the mean angular velocity of the initial orbital motion, i.e.,

$$\bar{n} = \sqrt{\mu/a_0^3} \tag{3.61}$$

The true anomaly θ of the point O can be expressed as

$$\theta = \bar{n}t + 2\,\varepsilon_0 \sin \bar{n}t \tag{3.62}$$

with neglect of terms of order higher than the first in ε_0.* Substitution of Eq. (3.62) into the first equation of (3.58) gives

$$\eta = \bar{n}t - \bar{\omega} + x/a_0 + 2\,\varepsilon_0 \sin \bar{n}t \tag{3.63}$$

The two sets of components α_1, α_2, α_3 and A_1, A_2, A_3 of the vehicle acceleration due to controlling thrust are related to each other by

$$\begin{pmatrix} \alpha_1 \\ \alpha_2 \\ \alpha_3 \end{pmatrix} = \begin{pmatrix} 1 & -(\eta+\bar{\omega}-\theta) & -i\cos(\eta+\bar{\omega}-\Omega) \\ \eta+\bar{\omega}-\theta & 1 & -i\sin(\eta+\bar{\omega}-\Omega) \\ i\cos(\theta-\Omega) & i\sin(\theta-\Omega) & 1 \end{pmatrix} \begin{pmatrix} A_1 \\ A_2 \\ A_3 \end{pmatrix} \tag{3.64}$$

Terms of order higher than the first in i and $\eta + \bar{\omega} - \theta$ are neglected in

---

* It should be noted that, throughout the foregoing investigations in Secs. 3.2 to 3.5, the eccentricity of the initial orbit was denoted by ε instead of ε_0.

Eq. (3.64).

Under the assumption that the thrust acceleration is small compared with the gravity acceleration and, consequently, the perturbations of the orbital elements due to thrust are small, x_i and u_j defined by Eqs. (3.59) and (3.60) may be regarded as small quantities. Substituting Eqs. (3.59) through (3.64) into Eqs. (3.57) and the second equation of (3.58), and thereupon disregarding quantities of order higher than the first in x_i and u_j yields the following equations for the state variables:

$$\left.\begin{aligned}
\dot{x}_1 &= 2u_1 \\
\dot{x}_2 &= -1.5x_1 + 2\sin\tau \cdot x_3 + 2\cos\tau \cdot x_4 - 2\varepsilon_0\cos\tau \\
\dot{x}_3 &= 2\sin\tau \cdot u_1 - \cos\tau \cdot u_2 \\
\dot{x}_4 &= 2\cos\tau \cdot u_1 + \sin\tau \cdot u_2 \\
\dot{x}_5 &= -\sin\tau \cdot u_3 \\
\dot{x}_6 &= -\cos\tau \cdot u_3
\end{aligned}\right\} \qquad (3.65)$$

where a dot over a quantity denotes differentiation with respect to τ.

The last two equations of (3.65), representing the out-of-plane motion, are independent of the first four equations of the in-plane motion.

3.9 Optimal Control Functions in Terms of Orbital Elements

Now the problem is to obtain the optimal controls for the minimum-fuel transfer of a power-limited rocket with unbounded thrust acceleration in a prescribed time. Mathematically, it requires that the following functional

is to be minimized:*

$$J = \frac{1}{2}\int_{\tau_0}^{\tau_0+T} (u_1^2 + u_2^2 + u_3^2)\, d\tau \tag{3.66}$$

The controls to be optimized are the dimensionless components u_1, u_2, and u_3 of the thrust acceleration. In Eq. (3.66) T is a prescribed transfer time and τ_0 denotes the instant of departure of the vehicle from the initial orbit.

By proceeding in the same manner as in Sec. 3.3, the optimal controls can be obtained by using the maximum principle. The Hamiltonian of the problem is given by [30, pp. 9 - 21]

$$\begin{aligned} H = {} & [(2p_1 + 2\sin\tau\cdot p_3 + 2\cos\tau\cdot p_4)u_1 - \tfrac{1}{2}u_1^2] \\ & - [(\cos\tau\cdot p_3 - \sin\tau\cdot p_4)u_2 + \tfrac{1}{2}u_2^2] \\ & - [(\sin\tau\cdot p_5 + \cos\tau\cdot p_6)u_3 + \tfrac{1}{2}u_3^2] \\ & - p_2(1.5x_1 - 2\sin\tau\cdot x_3 - 2\cos\tau\cdot x_4 + 2\varepsilon_0\cos\tau) \end{aligned} \tag{3.67}$$

where the auxiliary variables p's satisfy the set of differential equations

$$\left.\begin{aligned} \dot{p}_1 &= 1.5p_2 & \dot{p}_2 &= 0 \\ \dot{p}_3 &= -2\sin\tau\cdot p_2 & \dot{p}_4 &= -2\cos\tau\cdot p_2 \\ \dot{p}_5 &= 0 & \dot{p}_6 &= 0 \end{aligned}\right\} \tag{3.68}$$

From Eq. (3.67), the optimal controls $\bar{u}_j$ are obtained, as functions of the variables p_i, as

---

* See Eq. (3.19).

$$\left.\begin{aligned} \bar{u}_1 &= 2p_1 + 2\sin\tau\cdot p_3 + 2\cos\tau\cdot p_4 \\ \bar{u}_2 &= -\cos\tau\cdot p_3 + \sin\tau\cdot p_4 \\ \bar{u}_3 &= -\sin\tau\cdot p_5 - \cos\tau\cdot p_6 \end{aligned}\right\} \qquad (3.69)$$

Constants introduced by integrating Eqs. (3.65) and (3.68) must be determined so as to satisfy the boundary conditions and transversality conditions of the problem. Prior to application of the thrust acceleration, all the orbital elements are equivalent to those of the initial orbit. Hence we have

$$x_1 = x_2 = x_3 = x_5 = x_6 = 0 \quad \text{and} \quad x_4 = \varepsilon_0 \qquad (3.70)$$

at $\tau = \tau_0$. At the instant of arrival to the target orbit $\tau = \tau_0 + T \equiv \tau_f$, we have the conditions

$$\left.\begin{aligned} x_1 &= \lambda \qquad x_3 = \varepsilon_0 E \sin\bar{\omega}_f \qquad x_4 = \varepsilon_0 E \cos\bar{\omega}_f \\ x_5 &= i_f \sin\Omega_f \qquad\qquad x_6 = i_f \cos\Omega_f \end{aligned}\right\} \qquad (3.71)$$

where $\lambda = (a_f - a_0)/a_0$, $E = \varepsilon_f/\varepsilon_0$.* In a problem of orbit transfer the position of the vehicle on the target orbit is not specified, that is, the value of x_2 at $\tau = \tau_f$ is free. Consequently, transversality condition at $\tau = \tau_f$ requires that [30, pp. 45 - 50]

$$p_2 = 0 \qquad \text{at} \quad \tau = \tau_f \qquad (3.72)$$

We can carry out integration of Eqs. (3.65) and (3.68) with consideration of the conditions (3.70), (3.71), and (3.72). By substitution of the

---

* The subscript f denotes the value of elements of the target orbit.

results thus obtained into Eqs. (3.69), we have the following expressions for the optimal controls:

$$\left.\begin{aligned}
\bar{u}_1 &= \frac{1}{(5T - 3\sin T)[\,5T^2 + 3T\sin T - 32\sin^2(T/2)]} \\
&\quad \times \Big\{\lambda(5T - 3\sin T)[\tfrac{1}{2}(5T + 3\sin T) - 8\sin\tfrac{T}{2}\cdot\cos(\tau - \tau_0 - \tfrac{T}{2})] \\
&\quad - 4\,\varepsilon_0(E\cos\bar{\omega}_f - 1)[2(5T - 3\sin T)\sin\tfrac{T}{2}\cdot\cos(\tau_0 + \tfrac{T}{2}) \\
&\quad - (5T^2 - 16\sin^2\tfrac{T}{2})\cos\tau + (3T\sin T - 16\sin^2\tfrac{T}{2})\cos(\tau - 2\tau_0 - T)]\Big\} \\
\bar{u}_2 &= \frac{-1}{(5T - 3\sin T)[5T^2 + 3T\sin T - 32\sin^2(T/2)]} \\
&\quad \times \Big\{4\lambda(5T - 3\sin T)\sin\tfrac{T}{2}\cdot\sin(\tau - \tau_0 - \tfrac{T}{2}) \\
&\quad + 2\,\varepsilon_0 E\sin\bar{\omega}_f[(5T^2 - 16\sin^2\tfrac{T}{2})\cos\tau + (3T\sin T - 16\sin^2\tfrac{T}{2}) \\
&\quad \times\cos(\tau - 2\tau_0 - T)] - 2\varepsilon_0(E\cos\bar{\omega}_f - 1)[(5T^2 - 16\sin^2\tfrac{T}{2})\sin\tau \\
&\quad - (3T\sin T - 16\sin^2\tfrac{T}{2})\sin(\tau - 2\tau_0 - T)]\Big\} \\
\bar{u}_3 &= \frac{2\,i_f}{T^2 - \sin^2 T}\,[\sin T\cos(\tau - 2\tau_0 - T + \Omega_f) - T\cos(\tau - \Omega_f)]
\end{aligned}\right\} \tag{3.73}$$

Further, by substituting Eqs. (3.73) into Eq. (3.66), the value of the cost function J may be written as

$$J = \frac{1}{2(5T - 3\sin T)[5T^2 + 3T\sin T - 32\sin^2(T/2)]}$$

$$\times\Big\langle \frac{\lambda^2}{4}(25T^2 - 9\sin^2 T) - 8\varepsilon_0\lambda \sin\frac{T}{2}\,(5T - 3\sin T)$$

$$\times\Big[E\cos(\tau_0 - \bar{\omega}_f + \frac{T}{2}) - \cos(\tau_0 + \frac{T}{2})\Big]$$

$$+ 2\varepsilon_0^2\Big\{(5T^2 - 16\sin^2\frac{T}{2})(1 - 2E\cos\bar{\omega}_f + E^2)$$

$$- (3T\sin T - 16\sin^2\frac{T}{2})\Big[\cos(2\tau_0 + T)$$

$$- 2E\cos(2\tau_0 + T - \bar{\omega}_f) + E^2\cos(2\tau_0 + T - 2\bar{\omega}_f)\Big]\Big\}\Big\rangle$$

$$+ i_f^2\ \frac{T - \sin T\cdot\cos(2\tau_0 + T - 2\Omega_f)}{T^2 - \sin^2 T} \qquad (3.74)$$

where λ, ε_0, E, Ω_f, i_f, $\bar{\omega}_f$, and T are given quantities. The value of τ_0 which minimizes J of Eq. (3.74) gives the optimal point for departure from the initial orbit. Note that J of Eq. (3.74) is a quantity of order second in λ, ε_0, and i_f.

3.10 Numerical Examples

(a) Transfer between Coplanar and Coaxial Ellipses of a Same Eccentricity

Let us examine a case in which the terminal orbits are coplanar, i.e., $i_f = 0$. In this case we may infer that the motion of a vehicle is confined in the plane of initial orbit.

First, we assume that the terminal ellipses are of a same eccentricity and coaxial with each other, and that their axes are oriented in the same sense, i.e., E = 1 and $\bar{\omega}_f = 0$. Then the cost function J given by Eq. (3.74) reduces to

$$J = \frac{\lambda^2(5T + 3 \sin T)}{8[5T^2 + 3T \sin T - 32 \sin^2(T/2)]} \tag{3.75}$$

which is independent of the parameter τ_0. In the previous analysis (see Sec. 3.5a), we have developed J in a power series with respect to ε_0:

$$J = J^0 + \varepsilon_0 J^1 \tag{3.76}$$

The value of J obtained by the present analysis, Eq. (3.75), is equivalent to J^0 in Eq. (3.76), which is in turn equivalent to J for circle-to-circle transfer. A term corresponding to $\varepsilon_0 J^1$ is disregarded in the present analysis because it is a quantity of order $\varepsilon_0 \lambda^2$. In other words, the method of the present analysis cannot account for the effect of small eccentricity in case of this example.

Secondly, we are concerned with the terminal ellipses which have a same eccentricity and a common apse line, but are directed in the opposite senses with each other, i.e., E = 1 and $\bar{\omega}_f = \pi$.

Figure 3.15 shows the dependence of J on τ_0 calculated by Eq. (3.74). J consists of terms containing λ^2, $\varepsilon_0\lambda$, and ε_0^2. On the other hand, the dependence of J^0 and J^1 in Eq. (3.76) was already shown in Fig. 3.8 in Sec. 3.5(b). J^0 is a quantity of order λ^2, while J^1 is a quantity of order λ. The discrepancy between J of Eq. (3.74) and that of Eq. (3.76) is due to disregard of terms of order ε_0^2 in the calculation of the previous analysis.

Figure 3.16 illustrates time history of the optimal controls $\bar{u}_1$ (solid line) and $\bar{u}_2$ (broken line). Figure 3.17 shows the corresponding time history of the orbital elements $(a - a_0)/a_0\lambda$ (solid line), $\varepsilon/\varepsilon_0$ (broken line), and $\bar{\omega}/\pi$ (chain line).

(b) Transfer between Non-Coplanar Ellipses

Let us consider a case in which the target orbit is inclined with respect to the initial orbit at a small angle i_f. The out-of-plane component of the cost function is given by the last term of the right side of Eq. (3.74). This value is of order i_f^2 and identical with J_3^0 given by Eq. (3.56) in Sec. 3.5(c), which is the value of the cost function for transfer between circular orbits.* A term corresponding to order $\varepsilon_0 i_f^2$ is disregarded in the present analysis because it is a quantity of order higher than the second in the small parameters.

Let us consider an example in which the terminal orbit parameters are given by

$$i_f = \lambda \qquad \Omega_f = 0.5\pi \qquad \bar{\omega}_f = 0 \qquad E = 1 \qquad \text{and} \qquad \varepsilon_0 = 0.2$$

The dependence of the cost function J on τ_0 is shown dotted in Fig. 3.18. The solid line represents the result obtained by the foregoing analysis which takes account of the effect of small eccentricity.†

(c) Transfer from Earth to Mars

Thus far, the problems have been confined to the transfer from one satellite orbit of the earth to another one, but the method of analysis can be

---

* There are some differences in the notation of the terminal orbit parameters between the cases of the foregoing analysis (Secs. 3.2-3.5) and the present one (Secs. 3.6-3.10). Namely, parameters α, ϕ_1, ϕ_2, and ε in the foregoing analysis correspond, respectively, to i_f, Ω_f, $\Omega_f - \bar{\omega}_f$, and ε_0 in the present analysis.

† See Fig. 3.12.

applied, without difficulty, to interplanetary orbit transfer. We now calculate the optimal Earth-Mars flight. The result obtained is compared with the numerical solutions which have been obtained by W. G. Melbourne [20] and C. Saltzer [33].

The orbital elements of the earth and Mars are listed in Table 3.1 [1, pp. 377-379]. If we choose the Mars orbit as an initial orbit and the earth orbit as a target orbit, the following numerical values are given to the parameters:

$$\lambda = -0.344 \qquad \varepsilon_0 = 0.093 \qquad E \cong 0 \qquad i_f \cong 0 \tag{3.77}$$

By substitution of Eqs. (3.77) into Eq. (3.74), the cost function is given, in a dimensionless quantity, by

$$J^* = \frac{1}{(5T - 3\sin T)[5T^2 + 3T\sin T - 32\sin^2(T/2)]}$$
$$\times \{0.413T^2 - 0.133\sin^2 T - 0.138\sin^2(T/2)$$
$$- 0.128(5T - 3\sin T)\cdot\sin(T/2)\cdot\cos(\tau_0 + T/2)$$

Table 3.1 Orbital elements of the earth and Mars

	Earth	Mars
Semimajor axis a	1.0000 A.U.*	1.5237 A.U.
Eccentricity ε	0.0167	0.0934
Inclination i	0.0°	1.850°
Longitude of perihelion $\bar{\omega}$	102.3°	335.3°
Longitude of node Ω	0.0°	49.2°

* 1 A.U. (astronomical unit) = 1.495×10^{11} m

$$- 0.009[3T \sin T - 16 \sin^2(T/2)]\cos(2\tau_0 + T)\} \qquad (3.78)$$

In the M.K.S. system of units we have

$$J = \mu^{3/2} a_0^{-5/2} J^* = 0.06175\, J^* \quad \text{(kwatt/kg)} \qquad (3.79)$$

where μ is the product of the universal gravitational constant and the mass of the sun, and a_0 denotes the semimajor axis of Mars orbit.†

There have been a number of calculations of a heliocentric transfer between the orbits of the earth and Mars. The difficulty of the general problem lies in the fact that the optimal thrust program is the solution of a boundary value problem for a system of nonlinear differential equations subject to nonlinear constraints. A numerical result was obtained by W. G. Melbourne [20]. His procedure consists of generating repeated numerical solutions of the Euler-Lagrange equations on a large digital computer, varying the assumed initial conditions until the desired terminal conditions are approximately matched. In order to overcome this two-point boundary value problem, he has developed an iterative routine designed to efficiently conduct parametric analyses. Application of this method was given to an Earth-Mars flight. The orbit of the earth was assumed circular. The orbit of Mars possesses an eccentricity of 0.09337 and an inclination of 1.850° to the

---

† Constants μ and a_0 are as follows:

$$\mu = (6.670 \times 10^{-11}\ m^3/kg \cdot sec^2) \times (1.991 \times 10^{30}\ kg)$$
$$= 1.328 \times 10^{20}\ m^3/sec^2$$
$$a_0 = (1.524\ A.U.) \times (1.495 \times 10^{11}\ m)$$
$$= 2.278 \times 10^{11}\ m$$

ecliptic plane. The result due to W. G. Melbourne is illustrated by the full line in Fig. 3.19. The variation of the cost function is plotted against the heliocentric angle from the line of nodes to the rendezvous point. The result by linear analysis, which is given by Eq. (3.79), is shown dashed in this figure.

An alternative approach to this variational problem is presented by C. Saltzer and C. W. Fetheroff [33]. Following them, it is postulated to approximate the system by a discrete version. That is, the time interval is subdivided into N equal intervals and the trapezoidal rule is used in evaluation of the integral in each subinterval. Consequently, the problem is posed in the form of minimizing a function of 2(N + 1) variables subject to constraints expressed by the linear algebraic equations. A gradient technique is applicable in order to solve this problem.* The numerical results for an Earth-Mars mission have been presented. It has been assumed that the orbits of the earth and Mars are coplanar and that the earth's orbit is circular. The results obtained are shown in Fig. 3.20. In this figure the variation of the cost function for the Earth-Mars transfer is plotted against the heliocentric angle between the rendezvous point and the perihelion of Mars for several flight durations. The results obtained by linear analysis is also included in Fig. 3.20. The discrepancy in the cost function is less than few percents.

---

* According to Ref. 33, this method has been programmed for a medium-size electronic digital computer, and satisfactory results have been obtained for N equal to 10 or 20.

3.11 Concluding Remarks

The minimum-fuel transfer between neighboring elliptic orbits for a low-thrust power-limited propulsion system has been discussed. The motion of a space vehicle can be described by either of two sets of variables:

1. displacements and their time derivatives in a rotating coordinate system with the origin moving in an initial orbit about the earth,
2. instantaneous values of orbital elements of the vehicle.

In the first case, the analysis has been based on the assumption that only small deviations of the vehicle from an initial orbit are allowed; therefore the gravitational terms in the equation of motion may be linearized. The orbital velocity of the vehicle revolving along an elliptic orbit varies periodically in time. This variation brings terms with periodic coefficients into the equation of motion of the vehicle. If the variation is not so large, the small parameter method is applicable for obtaining an approximate solution of the equation. Then, we have developed the equation of motion, control functions, cost function, and so forth in power series with respect to the small parameter, that is, the eccentricity ε_0 of the initial orbit. Their first approximations up to and including terms of the first order in ε_0 have been obtained. The zero-order terms show the values for transfer between circular orbits, while the first-order terms characterize transfer between elliptic orbits. In the case of elliptic terminal orbits, fuel consumption depends not only on the transfer time but on the position of departure from the initial orbit. The result obtained clarifies this dependence. The motion of the vehicle under the action of the optimal thrust acceleration has also been studied.

In the second case, the equation of motion of the vehicle has been expressed in terms of the elements of its osculating orbit. In this case the analysis has been carried out under the assumption that the thrust acceleration is small compared with the gravity acceleration and that perturbations of the orbital elements due to thrust are also small. Consequently, the quantities of higher order of thrust acceleration terms and the perturbation terms of the orbital elements have been discarded in the equation of motion. The optimal thrust program has been obtained analytically. The fuel consumption under the action of this thrust program has also been determined.

Slight disagreement between the results obtained by these two methods has been found in the foregoing numerical examples (see, for example, Fig. 3.18). These differences may be explained as follows:

(a) Due to the difference of the assumptions for linearization, the equations of motion have been derived in the different forms. Namely, in the first method the equations of motion (3.11) and (3.12) include the terms of the first order in ε_0. However, these terms are disregarded in the second method because they lead to the higher-order quantities of state variables defined by Eqs. (3.59).

(b) The boundary conditions and the transversality condition of the second method are given by Eqs. (3.70) through (3.72). This simplification leads to obtaining the optimal control and the cost function analytically. On the other hand, in the first method, the boundary conditions and transversality condition reduce to a system of linear algebraic equations of many (in general, twenty-six) unknowns.

(c) In spite of such different assumptions and conditions, the results obtained by these methods are identical except in a special case, where

we deal with the transfer between ellipses of same eccentricity whose axes are aligned and oriented in the same sense. In this case the second method cannot account for the effect of small eccentricity of the terminal orbits, and the result obtained degenerates into the solution to the problem of circle-to-circle transfer. The first approach provides better results than the second method, as shown in Figs. 3.3 and 3.12. This is owing to taking account of the equation of motion up to terms of the first order in ε_0 in the first approach.

(d) In general, the cost function obtained by the second method consists of terms containing λ^2, $\varepsilon_0\lambda$, ε_0^2, and i_f^2. Terms of order $\varepsilon_0\lambda$ and ε_0^2, however, vanish for the above-mentioned special case. In this case the first method succeeds in calculating the cost function including terms of order λ^2, i_f^2, $\varepsilon_0\lambda^2$, and $\varepsilon_0 i_f^2$. Investigations of the effect of parameters of order higher than just described are carried out by solving nonlinear differential equations. If one uses the first set of state variables, the small parameter method may be applicable even to that occasion.

The general problem of trajectory optimization leads to the two-point boundary value problem for a system of nonlinear differential equations subject to nonlinear constraints. The result obtained by the linear analysis has been compared with the numerical solutions which were previously obtained for the nonlinear variational problem by W. G. Melbourne and C. Saltzer. Comparisons have been made for Earth-Mars flight, as shown in Figs. 3.19 and 3.20. Mars has a semimajor axis, a = 1.524 A.U.. By comparison with a = 1.0 A.U. for earth, the separation distance between them is 0.524 A.U. which is not $\ll$ 1.0 A.U.. However, it is possible to apply the linear analysis

described in this chapter to Earth-Mars transfer with remarkably good accuracy.

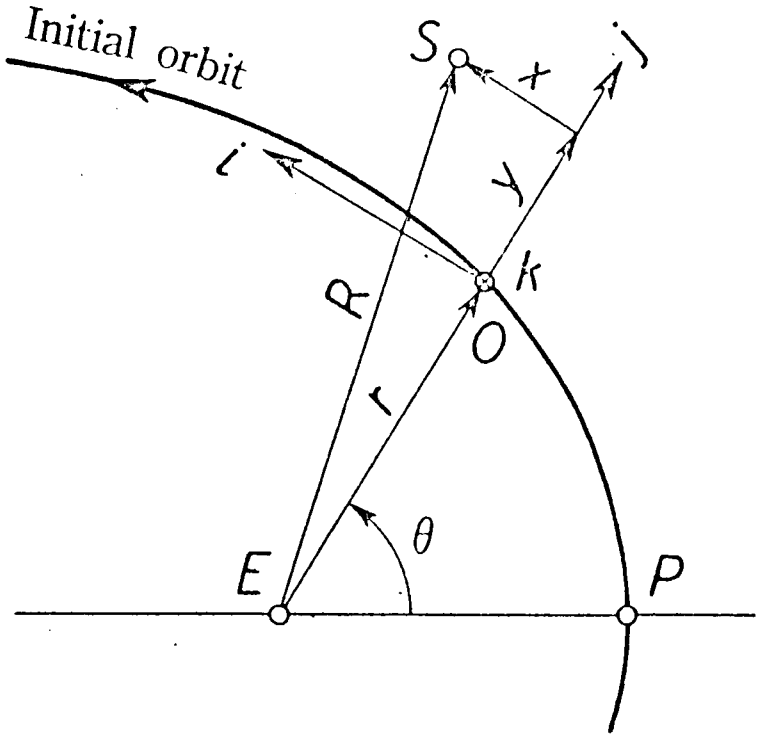

Fig. 3.1. Reference coordinate system.

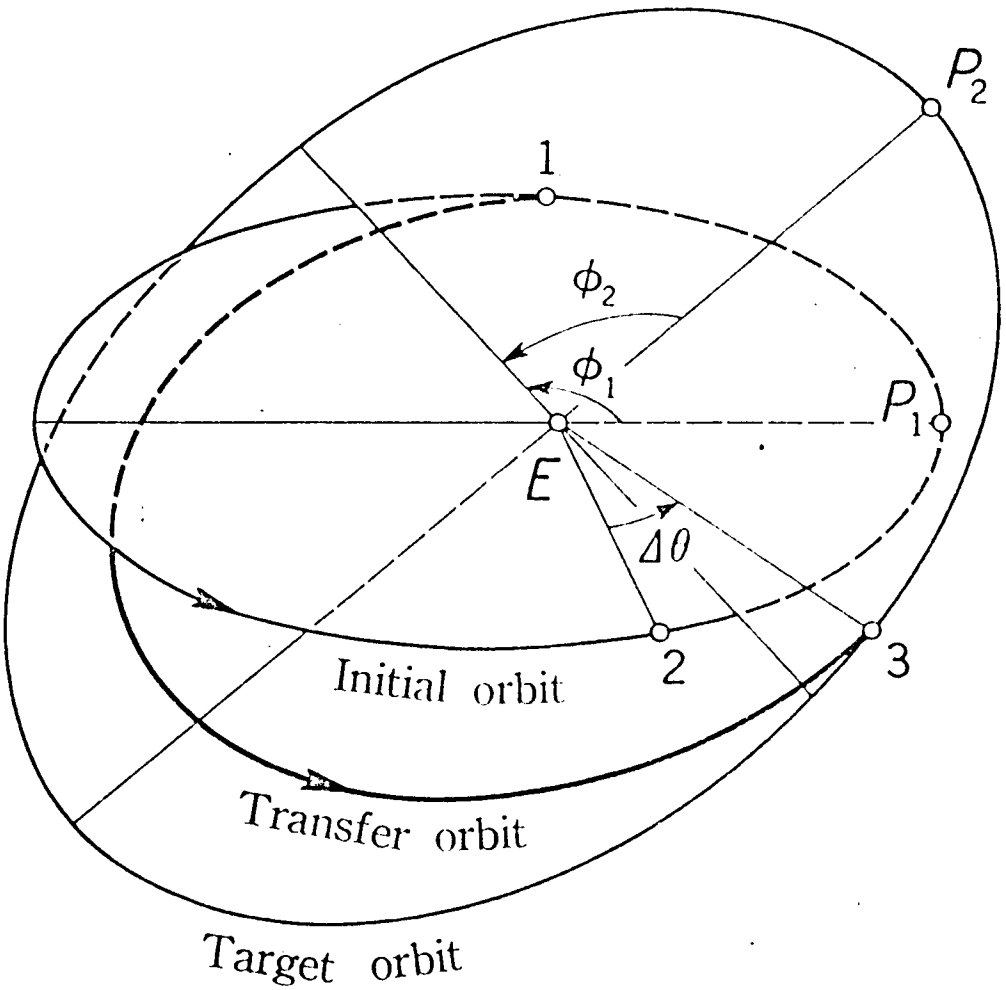

Fig. 3.2. Transfer between elliptic orbits.

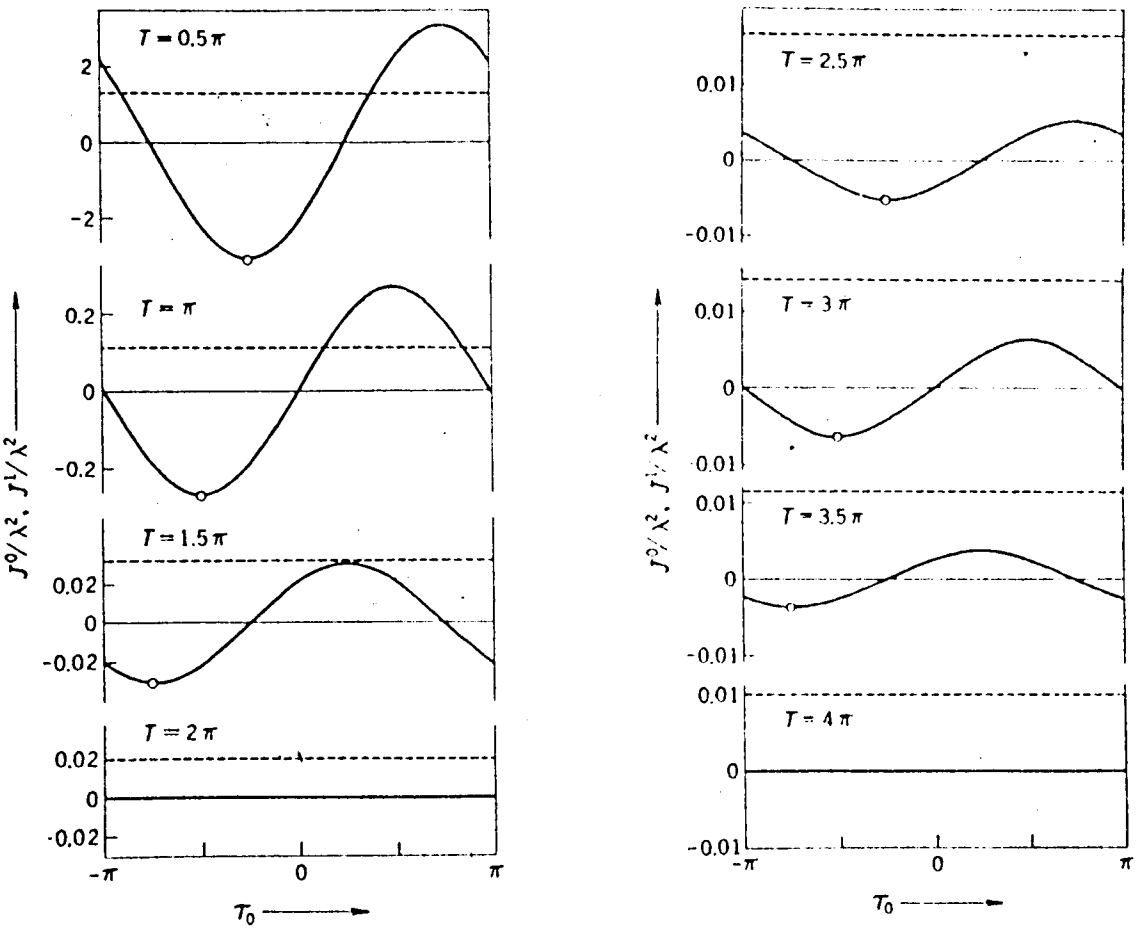

------ : J^0/λ^2 ——— : J^1/λ^2

Fig. 3.3. Variations of the cost function J with the time τ_0 ($\alpha = 0$, $\psi = 0$, and E = 1).

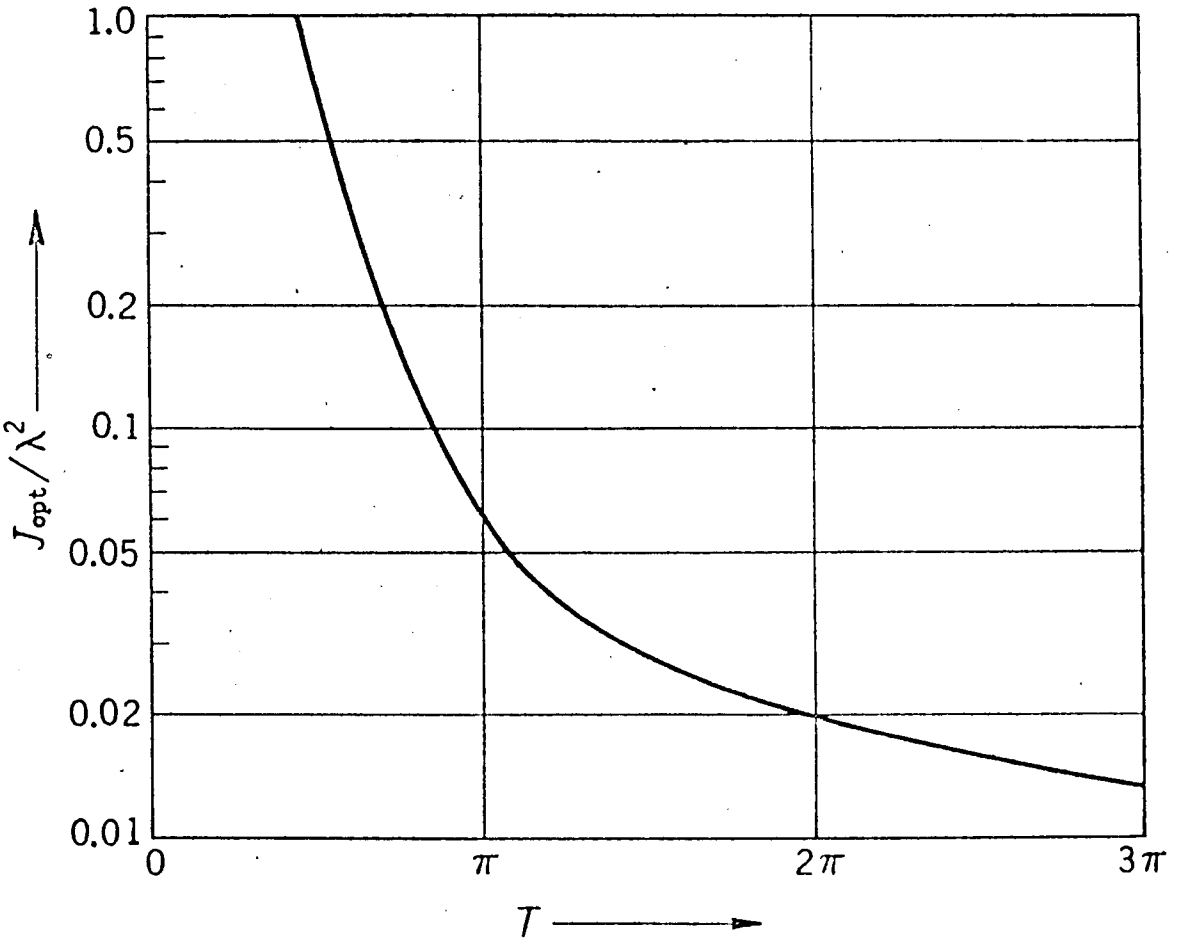

Fig. 3.4. Variation of J_{opt} with the transfer time T ($\alpha = 0$, $\psi = 0$, E = 1, and $\varepsilon = 0.2$).

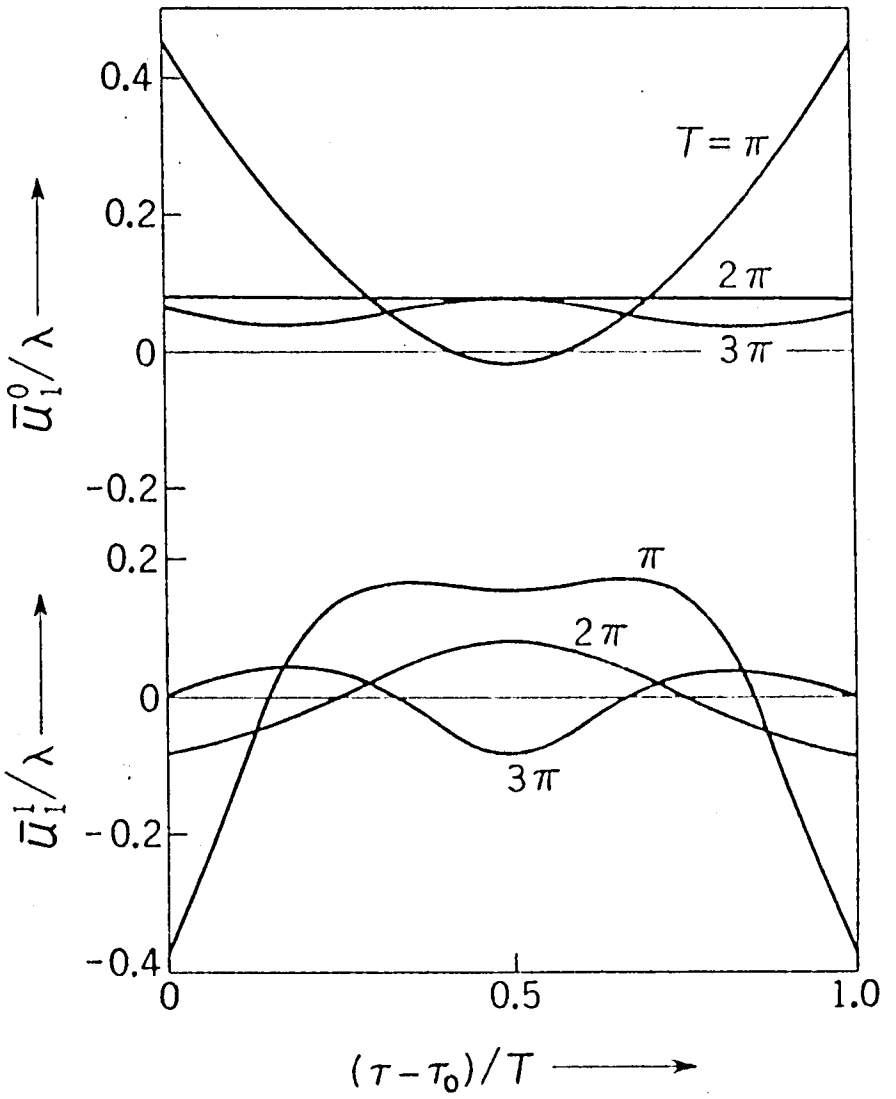

Fig. 3.5. Circumferential components of the optimal thrust acceleration ($\alpha = 0$, $\psi = 0$, and $E = 1$).

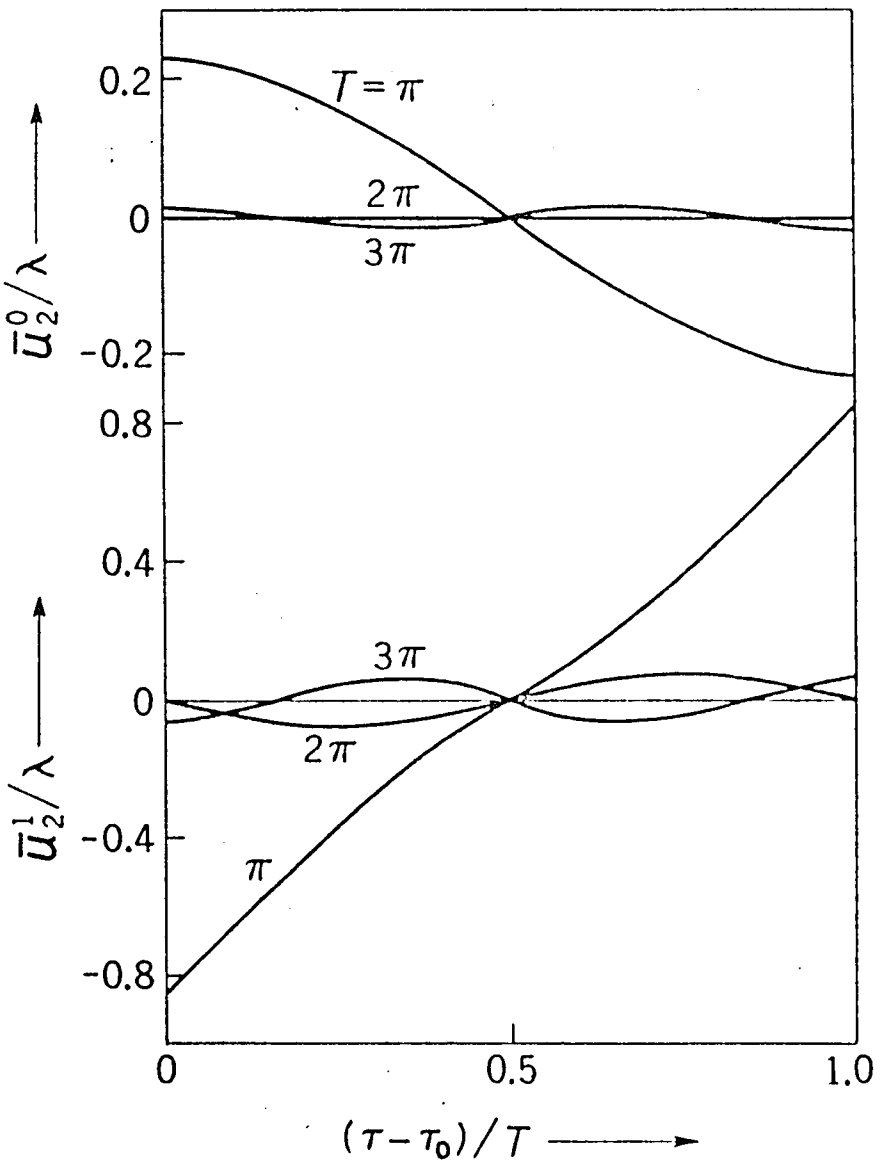

Fig. 3.6. Radial components of the optimal thrust acceleration ($\alpha = 0$, $\psi = 0$, and E = 1).

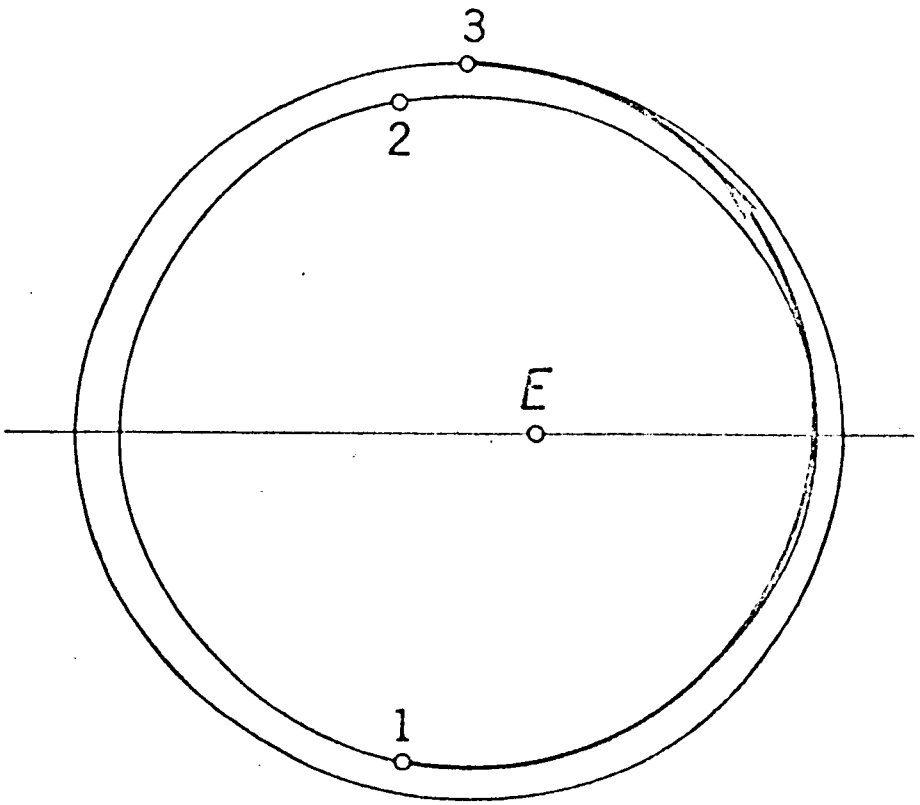

(a) $\varepsilon = 0.2$

Fig. 3.7. Optimal transfer orbits ($\alpha = 0$, $\psi = 0$, E = 1, $\lambda = 0.1$, and $T = \pi$).

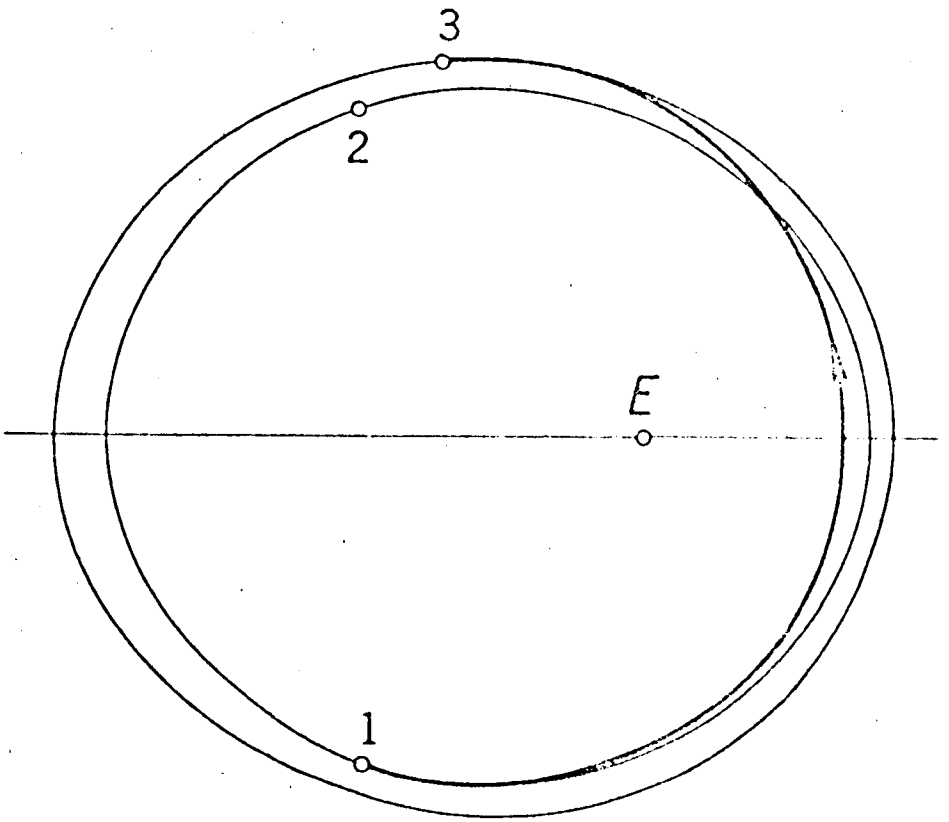

(b) $\varepsilon = 0.4$

Fig. 3.7. Optimal transfer orbits ($\alpha = 0$, $\psi = 0$, $E = 1$, $\lambda = 0.1$, and $T = \pi$).

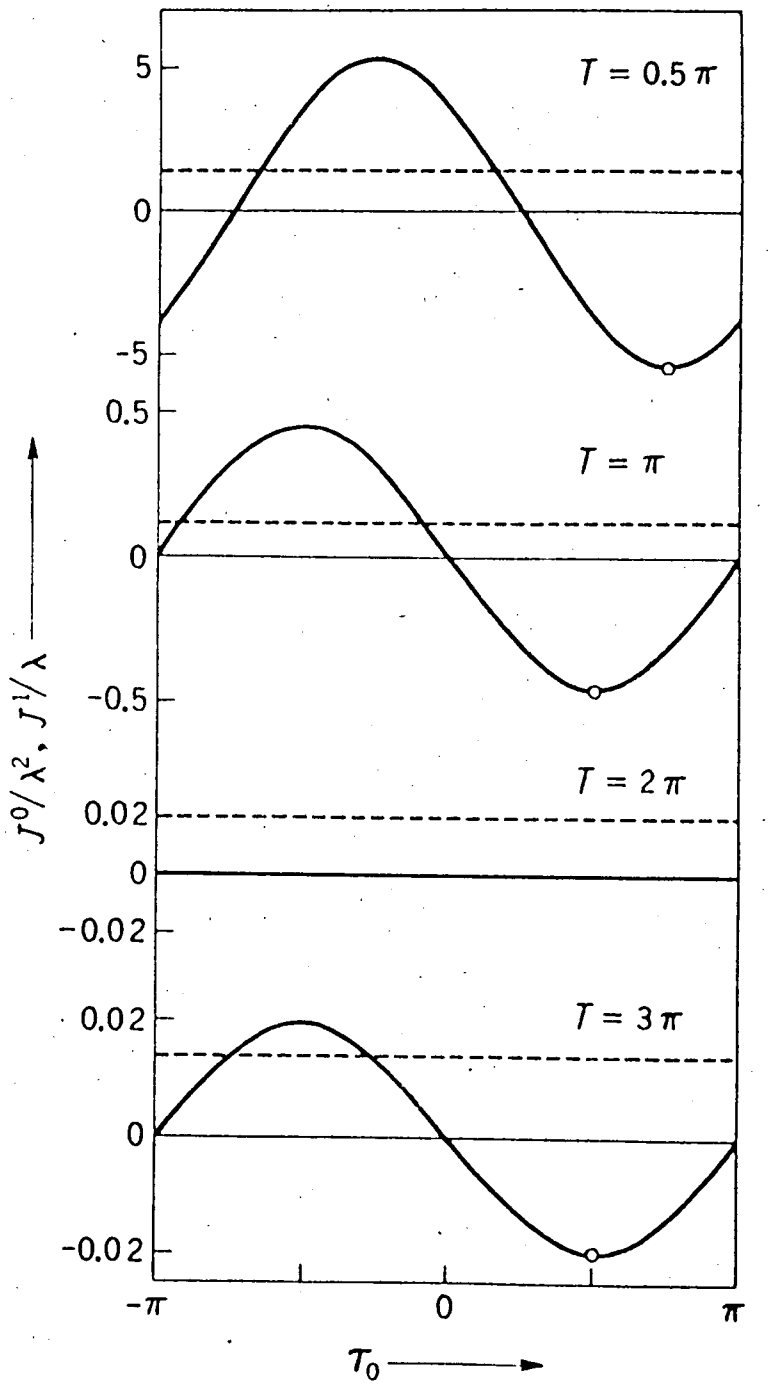

Fig. 3.8. Variations of the cost function J with the time τ_0 ($\alpha = 0$, $\psi = \pi$, and E = 1).

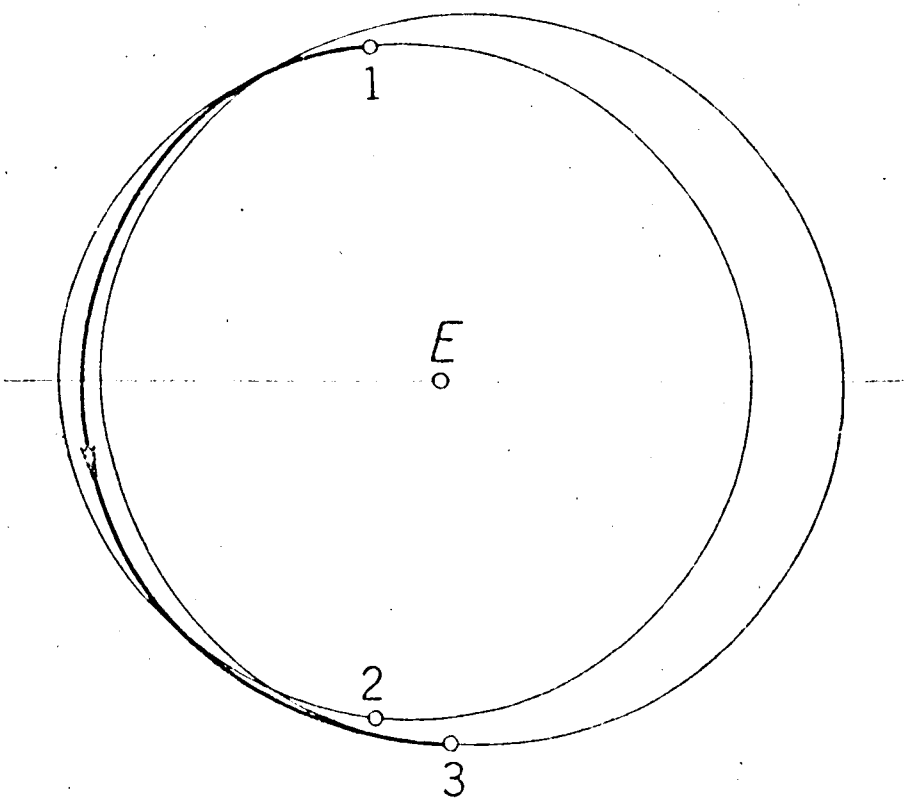

Fig. 3.9. Optimal transfer orbit ($\alpha = 0$, $\psi = \pi$, $E = 1$, $\lambda = 0.1$, $\varepsilon = 0.1$, and $T = \pi$).

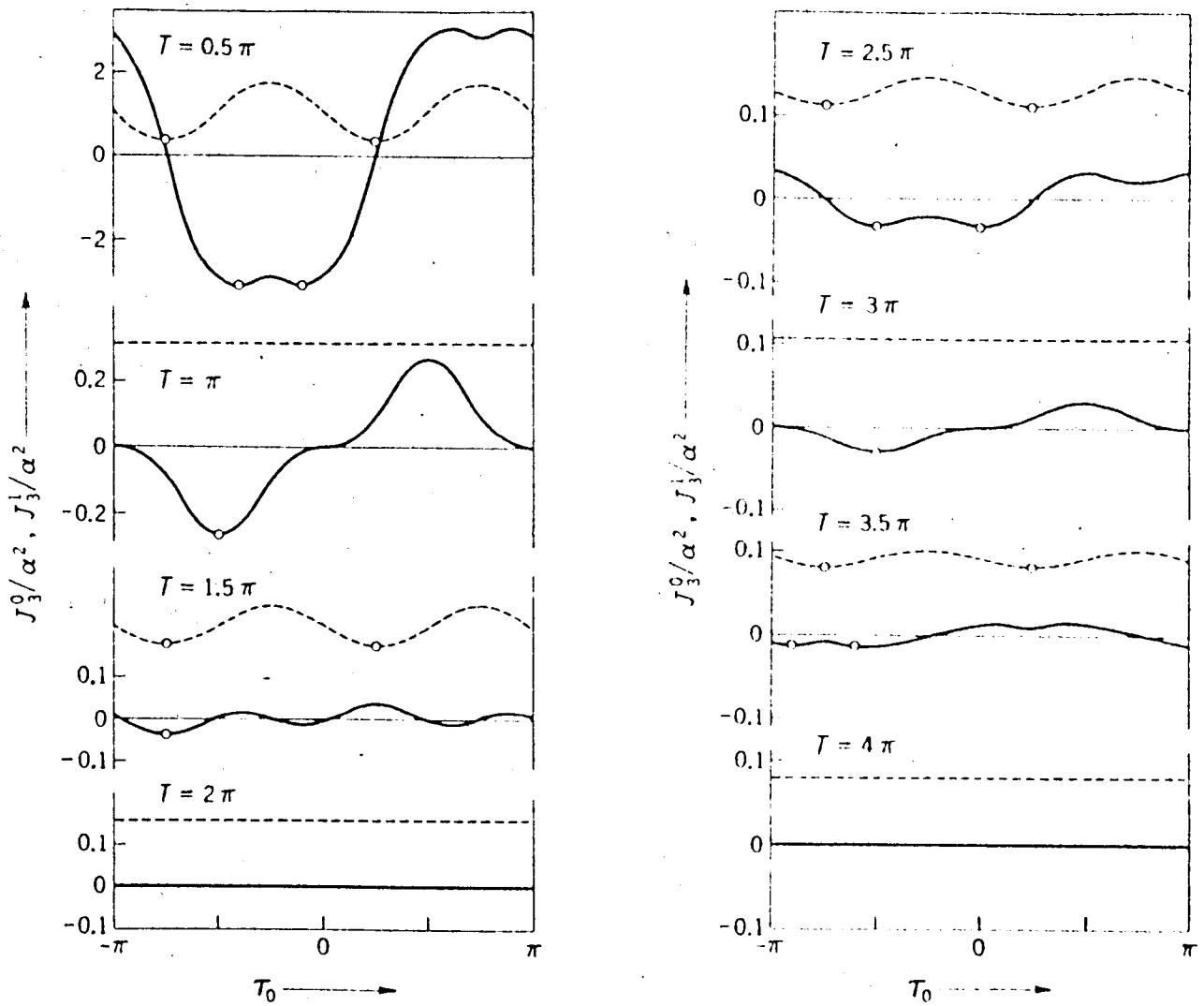

Fig. 3.10. Variations of the normal component of the cost function J_3 with the time τ_0 ($\phi_1 = \phi_2 = 0.5\pi$, and E = 1).

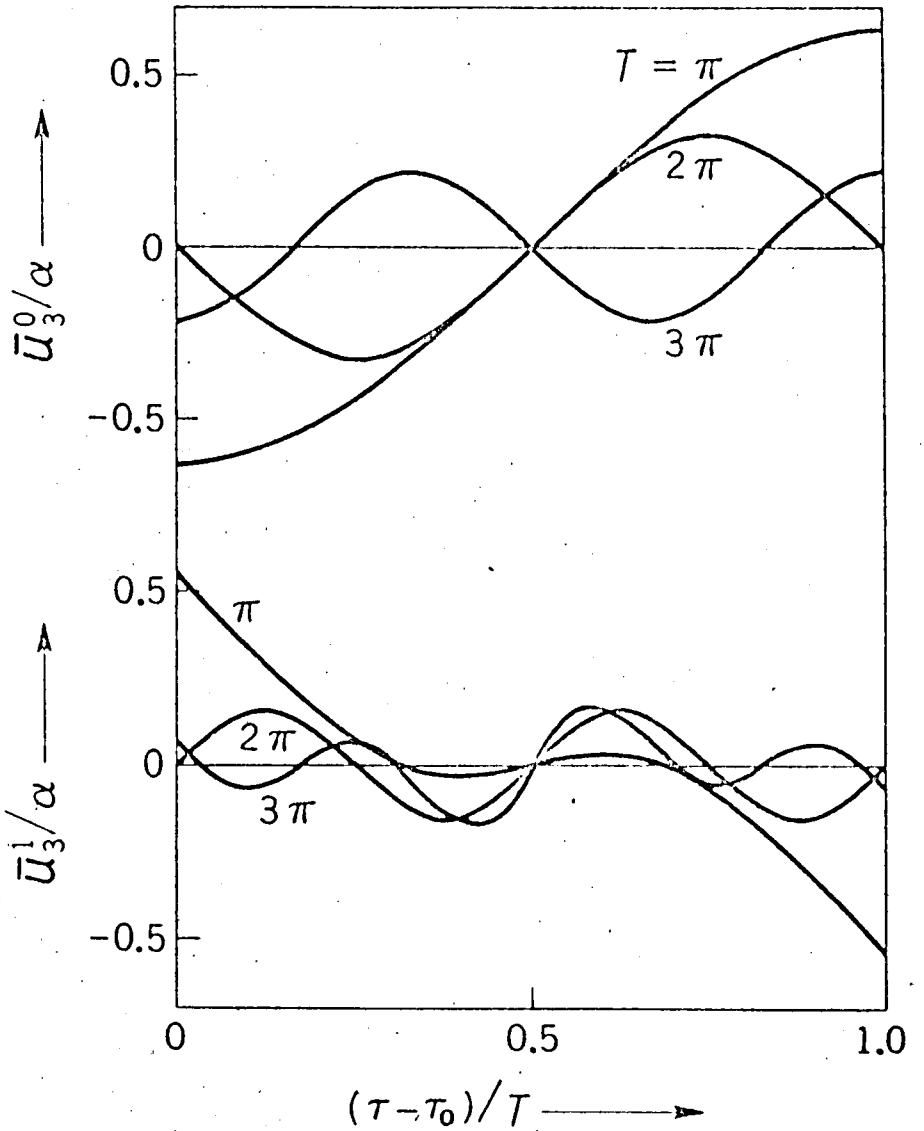

Fig. 3.11. Normal components of the optimal thrust acceleration ($\phi_1 = \phi_2 = 0.5\pi$, and E = 1).

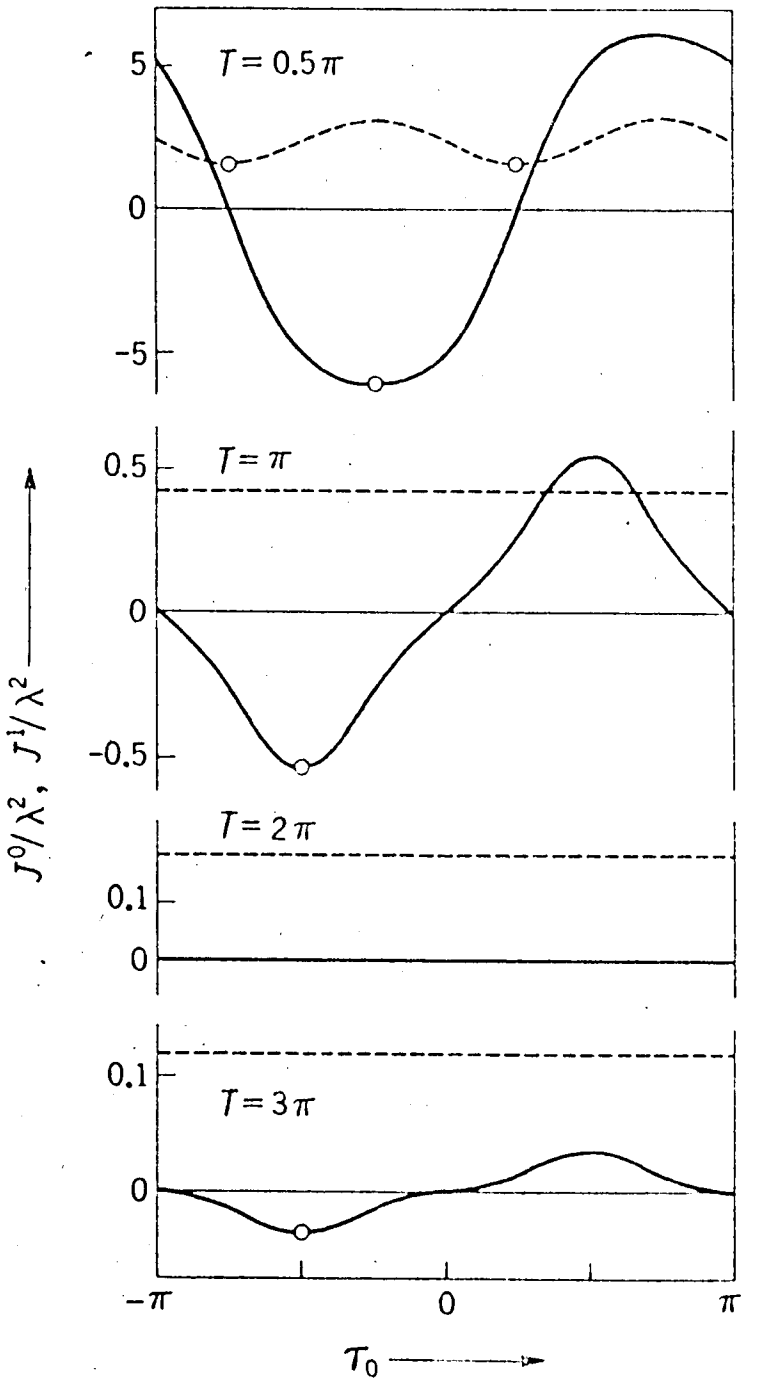

------ : J^0/λ^2 ——— : J^1/λ^2

Fig. 3.12. Variations of the cost function J with the time τ_0 ($\alpha = \lambda$, $\phi_1 = \phi_2 = 0.5\pi$, and $E = 1$).

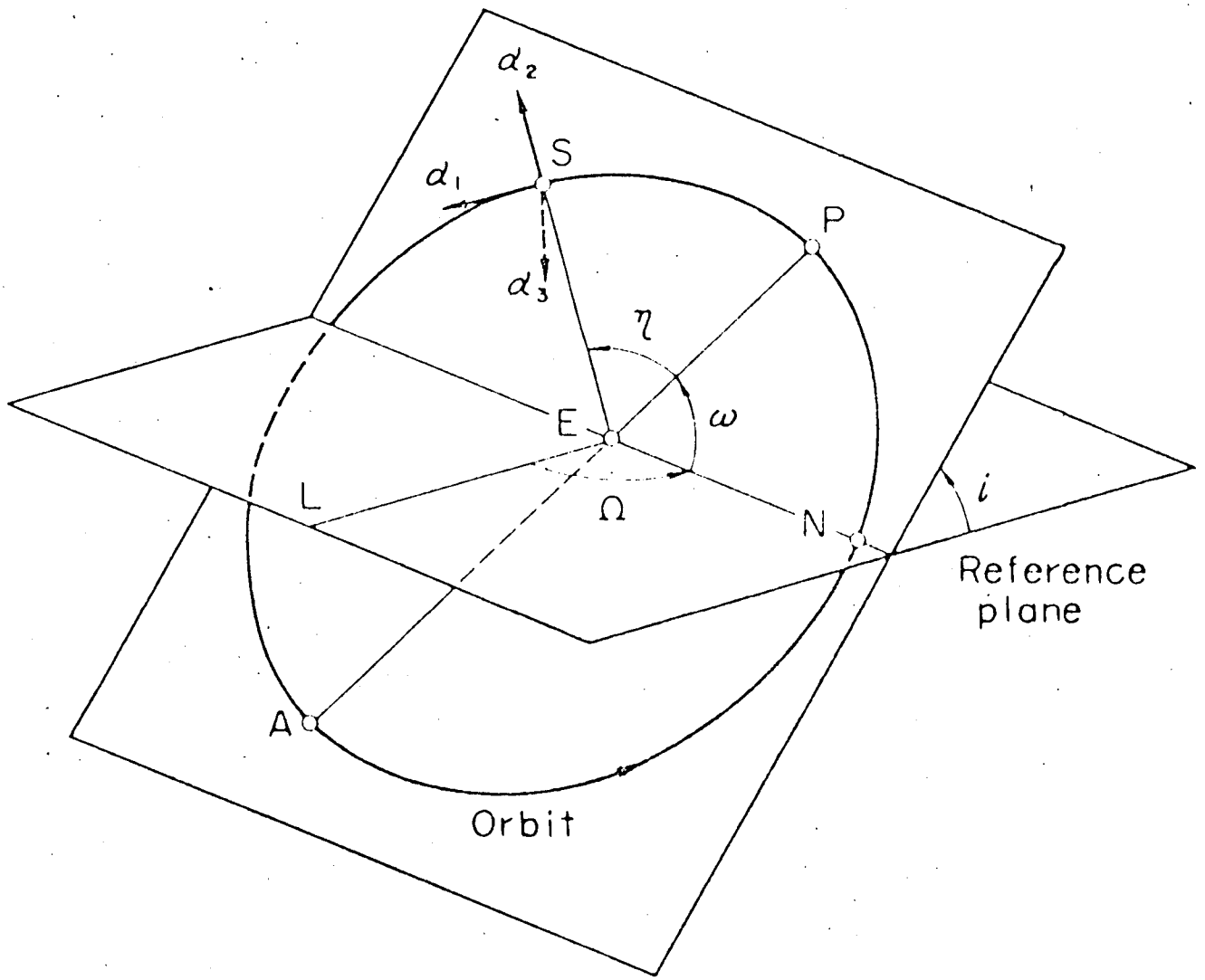

Fig. 3.13. Orbital elements.

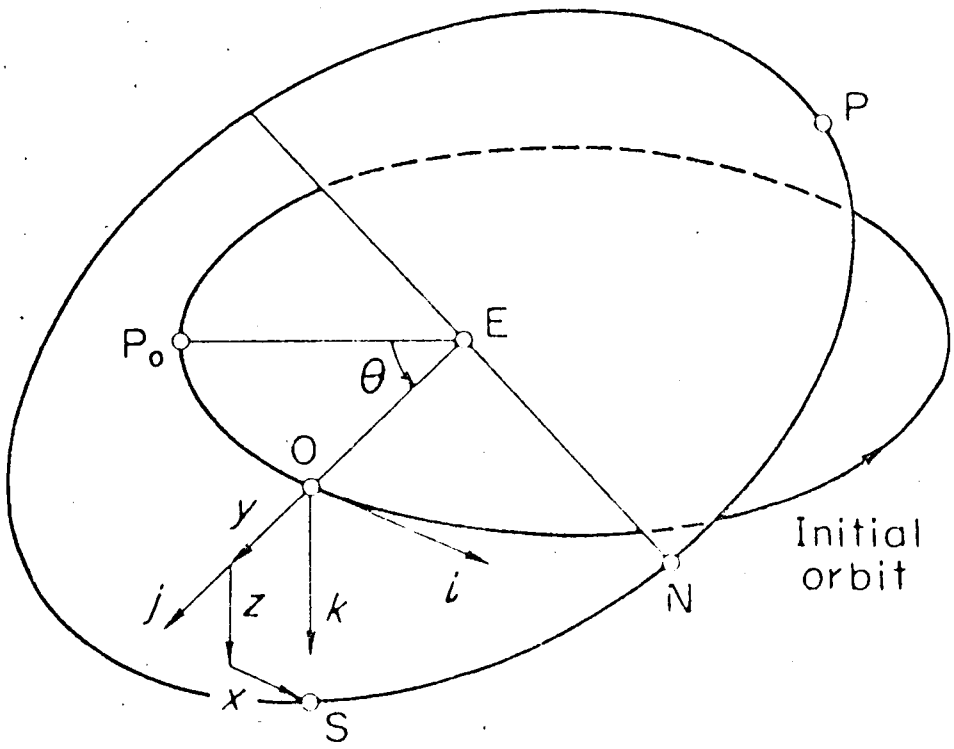

Fig. 3.14. Coordinate system geometry.

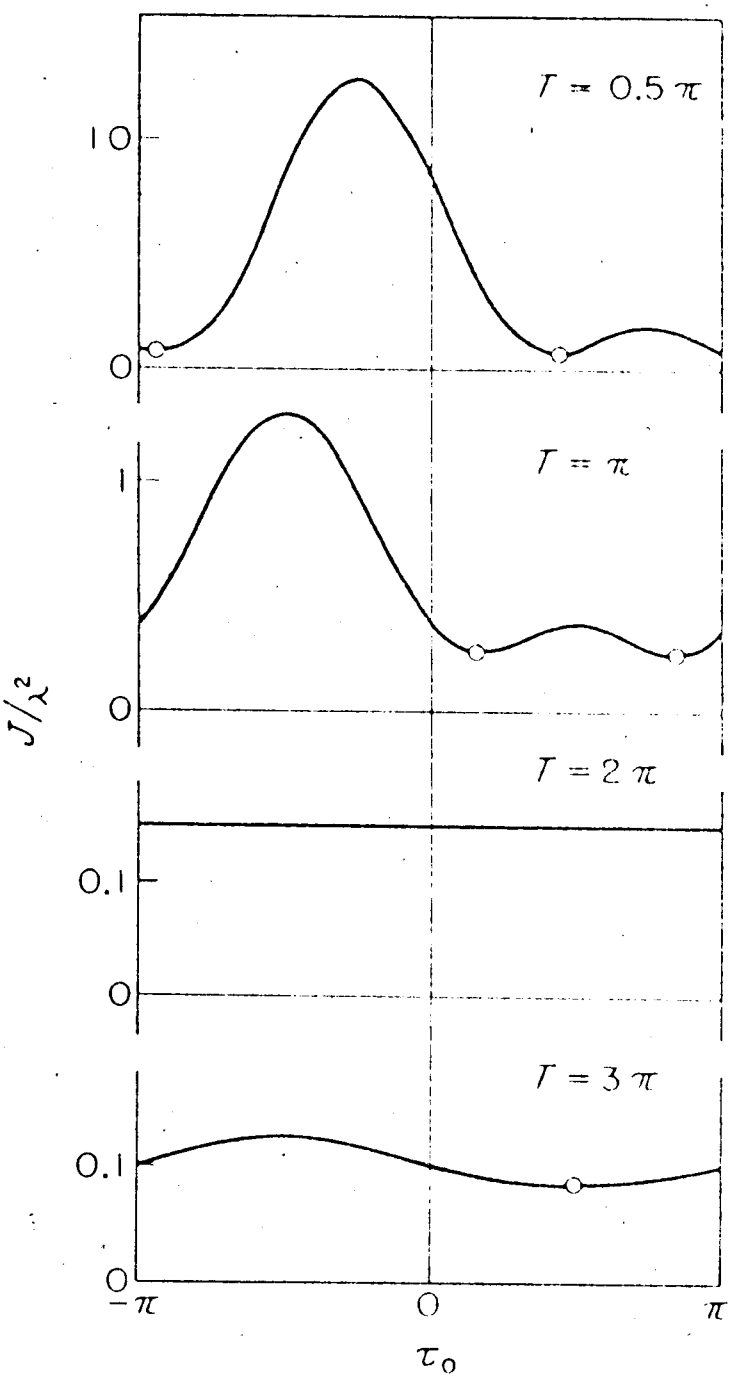

Fig. 3.15. Variations of the cost function J with the time τ_0 ($i_f = 0$, $\bar{\omega}_f = \pi$, $E = 1$, and $\varepsilon_0 = \lambda$).

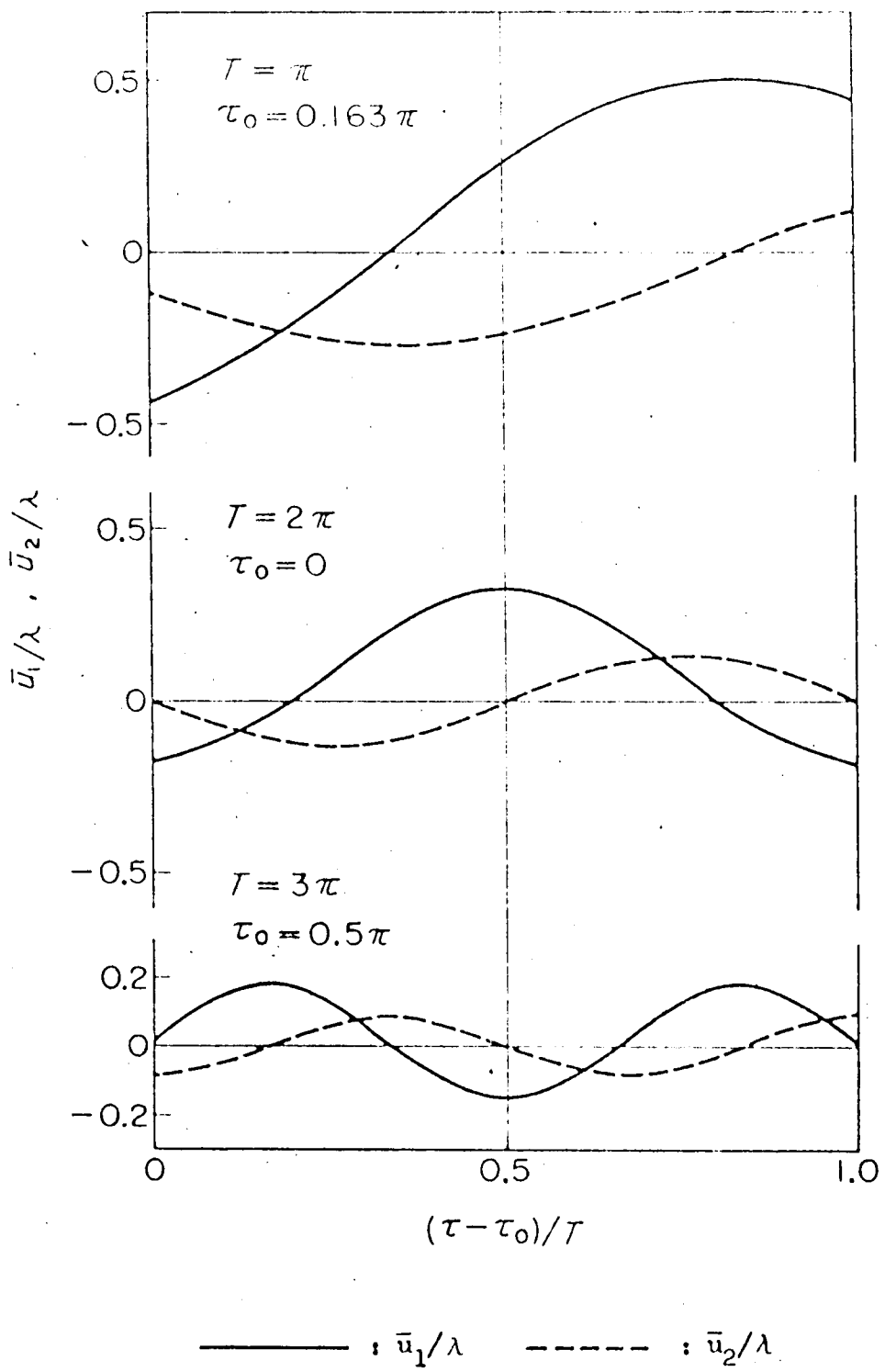

Fig. 3.16. Time history of the optimal thrust acceleration in the case when $i_f = 0$, $\bar{\omega}_f = \pi$, E = 1, and $\varepsilon_0 = \lambda$.

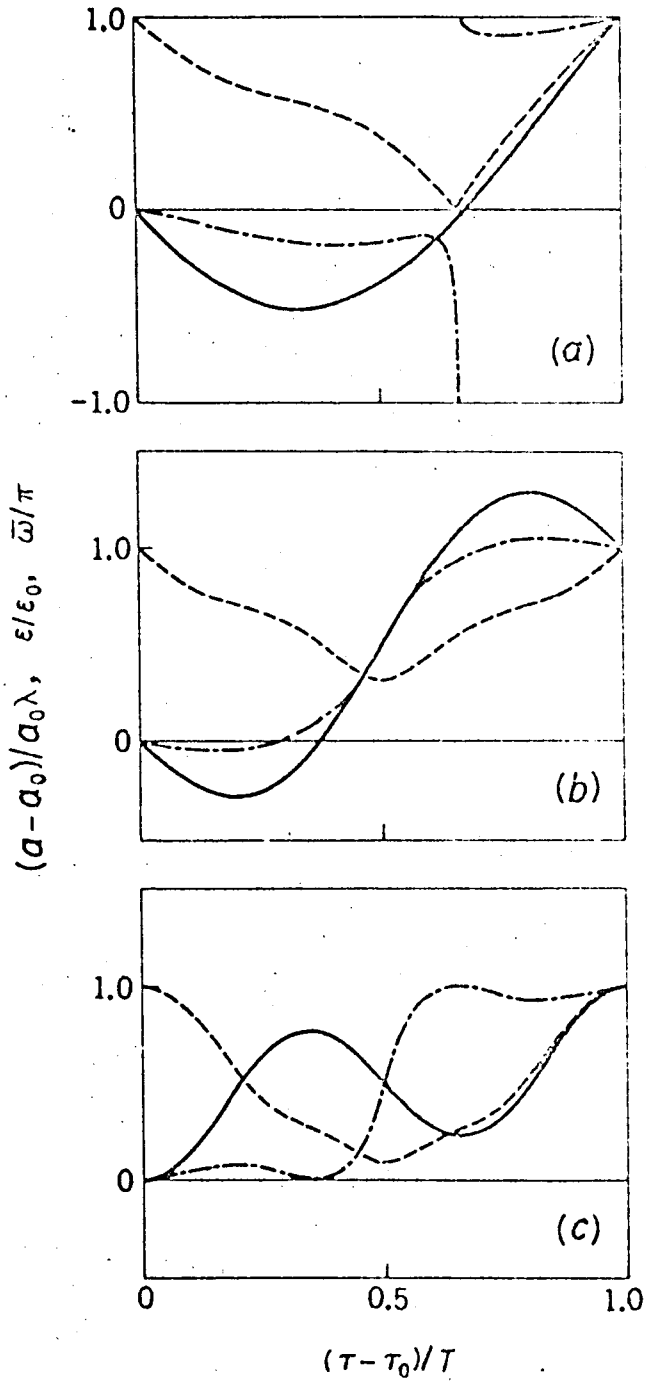

(a) $T = \pi$ $\quad \tau_0 = 0.163\pi$

(b) $T = 2\pi$ $\quad \tau_0 = 0$

(c) $T = 3\pi$ $\quad \tau_0 = 0.5\pi$

——— : $(a - a_0)/a_0\lambda$ ----- : $\varepsilon/\varepsilon_0$ —·—·— : $\bar{\omega}/\pi$

Fig. 3.17. Time history of the orbital elements in the case when $i_f = 0$, $\bar{\omega}_f = \pi$, $E = 1$, and $\varepsilon_0 = \lambda$.

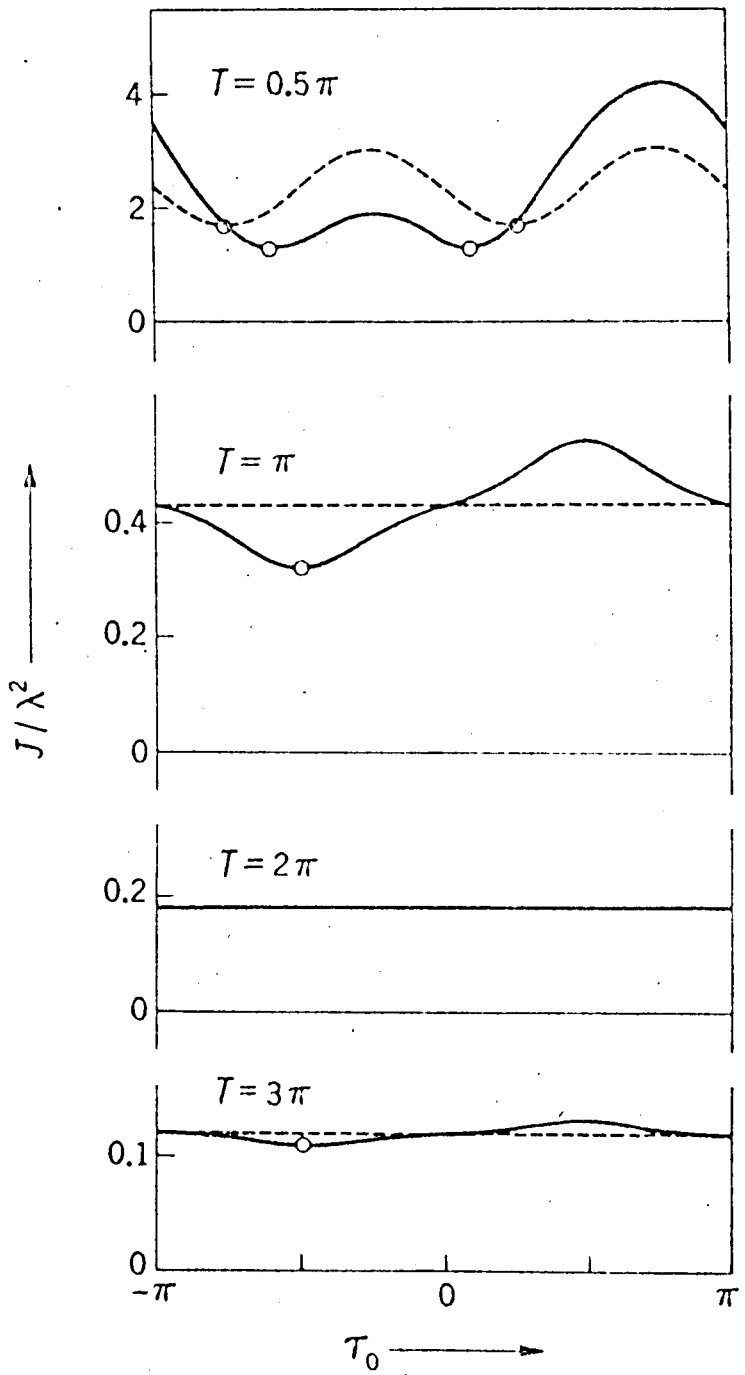

Fig. 3.18. Variations of the cost function J with the time τ_0 in the case when $i_f = \lambda$, $\Omega_f = 0.5\pi$, $\bar{\omega}_f = 0$, $E = 1$, and $\varepsilon_0 = 0.2$. Solid line: results of investigation made in Secs. 3.2 to 3.5. Dotted line: results of investigation made in Secs. 3.6 to 3.10.

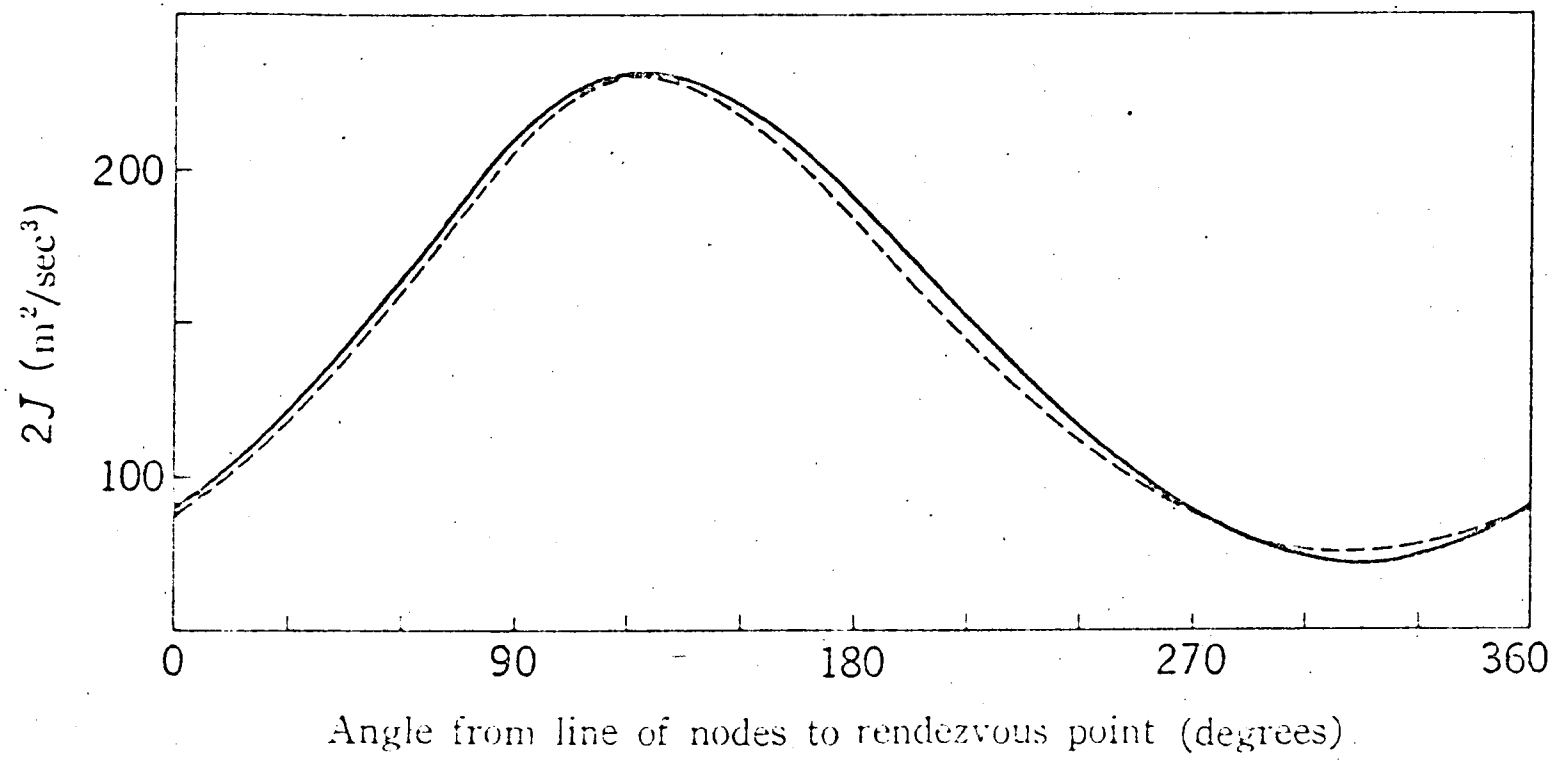

Fig. 3.19. Cost function J required for transfer from Earth to Mars (T = 90 days). Full line: numerical result due to W. G. Melbourne. Dashed line: result by linear analysis.

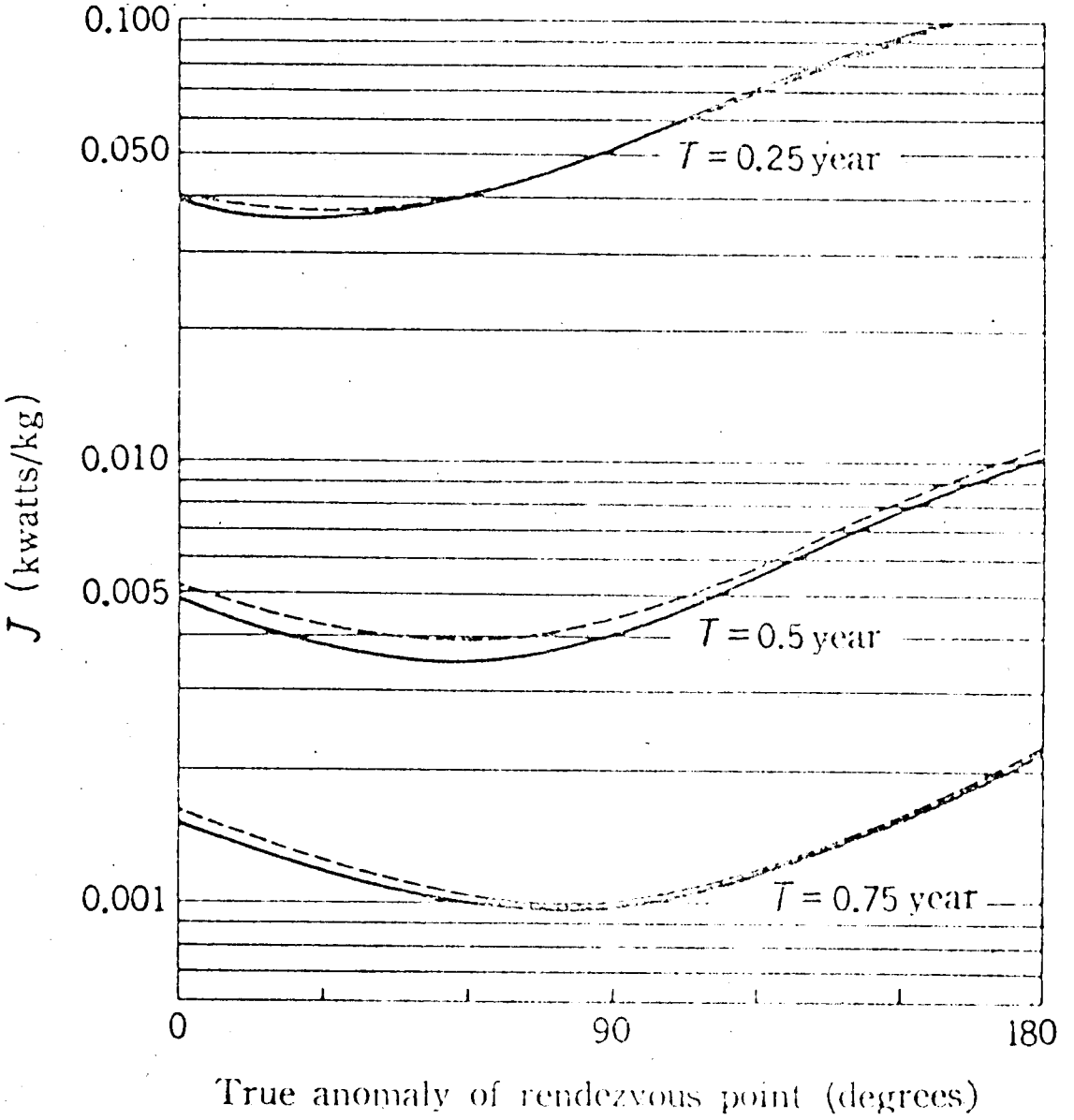

Fig. 3.20 Cost function J required for transfer from Earth to Mars. Full line: numerical results due to C. Saltzer. Dashed line: results by linear analysis.

APPENDIX I

CALCULATIONS OF THE TIME INTERVALS BETWEEN SWITCHINGS OF THE CONTROLS (REACTION - JET ATTITUDE CONTROL SYSTEM)

In the reaction gas-jet system, as mentioned in Chap. 1, the optimal controls are of an on-off type for time and fuel minimization. In this appendix we shall calculate the time intervals between switchings of the controls. In the time-optimal control (Sec. 1.5b), substituting the values of $\bar{u}_1$ and $\bar{u}_2$ in Table 1.2 into Eq. (1.24) gives the relationship between the initial state x_i^0 (i = 1 to 4) and the switching intervals τ_j (j = 1 to 4) of the controls. On the other hand, in the minimum-fuel control (Sec. 1.6b), substituting the values of $\bar{u}_1$ and $\bar{u}_2$ in Table 1.4 into Eq. (1.35) yields the similar relation. When the normalized angular velocity c is small, the terms of order higher than the first in c may be neglected in these relations. Thus the results are shown in what follows.

I.1 Time-Optimal Control

First, for Mode I.1 indicated in Table 1.2, we have

$$\left.\begin{aligned} x_1^0 &= \tfrac{1}{2}\tau^2 - \tau_2(2\tau_1 + \tau_2) - \tfrac{c}{6}[\tau^3 - 2(\tau - \tau_4)^3] \\ x_2^0 &= -\tau + 2\tau_2 + \tfrac{c}{2}[\tau^2 - 2(\tau - \tau_4)^2] \\ x_3^0 &= \tfrac{1}{2}\tau^2 - (\tau - \tau_4)^2 + \tfrac{c}{6}[\tau^3 + 2\tau_1^3 - 2(\tau_1 + \tau_2)^3] \\ x_4^0 &= \tau - 2\tau_4 - \tfrac{c}{2}[\tau^2 - 2\tau_2(2\tau_1 + \tau_2)] \end{aligned}\right\} \qquad (I.1)$$

Similarly, for Mode I.2, we have

$$
\left.
\begin{aligned}
x_1^0 &= \tfrac{1}{2}\tau^2 + \tau_1^2 - (\tau - \tau_4)^2 - \tfrac{c}{6}[\tau^3 - 2(\tau_1 + \tau_2)^3] \\
x_2^0 &= -\tau_1 + \tau_2 + \tau_3 - \tau_4 + \tfrac{c}{2}[\tau^2 - 2(\tau_1 + \tau_2)^2] \\
x_3^0 &= \tfrac{1}{2}\tau^2 - (\tau_1 + \tau_2)^2 + \tfrac{c}{6}[\tau^3 + 2\tau_1^3 - 2(\tau - \tau_4)^3] \\
x_4^0 &= \tau_1 + \tau_2 - \tau_3 - \tau_4 - \tfrac{c}{2}[\tau^2 + 2\tau_1^2 - 2(\tau - \tau_4)^2]
\end{aligned}
\right\} \qquad (I.2)
$$

For Mode I.3, we have

$$
\left.
\begin{aligned}
x_1^0 &= \tfrac{1}{2}\tau^2 - \tau_3(2\tau_1 + 2\tau_2 + \tau_3) - \tfrac{c}{6}[\tau^3 - 2\tau_1^3] \\
x_2^0 &= -\tau + 2\tau_3 + \tfrac{c}{2}[\tau^2 - 2\tau_1^2] \\
x_3^0 &= \tfrac{1}{2}\tau^2 - \tau_1^2 + \tfrac{c}{6}[\tau^3 + 2(\tau_1 + \tau_2)^3 - 2(\tau - \tau_4)^3] \\
x_4^0 &= -\tau + 2\tau_1 - \tfrac{c}{2}[\tau^2 - 2\tau_3(2\tau_1 + 2\tau_2 + \tau_3)]
\end{aligned}
\right\} \qquad (I.3)
$$

The relations for other modes are obtained from the above relations for Mode I by simple transformations of the initial values. Namely, x_1^0 in Eqs. (I.1) through (I.3) should be transformed, corresponding to each mode, as*

$$
\left.
\begin{aligned}
[x_1^0]_{II} &= -[x_3^0]_I \qquad [x_2^0]_{II} = -[x_4^0]_I \\
[x_3^0]_{II} &= [x_1^0]_I \qquad [x_4^0]_{II} = [x_2^0]_I
\end{aligned}
\right\} \qquad (I.4)
$$

$$
\left.
\begin{aligned}
[x_1^0]_{III} &= -[x_1^0]_I \qquad [x_2^0]_{III} = -[x_2^0]_I \\
[x_3^0]_{III} &= -[x_3^0]_I \qquad [x_4^0]_{III} = -[x_4^0]_I
\end{aligned}
\right\} \qquad (I.5)
$$

---

* For instance, $[x_1^0]_{II}$ means the value of x_1^0 for Mode II.

$$\left.\begin{aligned} [x_1^0]_{IV} &= [x_3^0]_I \qquad [x_2^0]_{IV} = [x_4^0]_I \\ [x_3^0]_{IV} &= -[x_1^0]_I \qquad [x_4^0]_{IV} = -[x_2^0]_I \end{aligned}\right\} \tag{I.6}$$

I.2 Minimum-Fuel Control

For four submodes of Mode I indicated in Table 1.4, we have

Mode I.1:

$$\left.\begin{aligned} x_1^0 &= \tfrac{1}{2}[T^2 - (\tau_1 + \tau_2)^2 - (\tau_1 + \tau_2 + \tau_3)^2] \\ &\quad - \tfrac{c}{6}[T^3 - \tau_1^3 - (T - \tau_5)^3] \\ x_2^0 &= \tau_1 + \tau_2 - \tau_4 - \tau_5 + \tfrac{c}{2}[T^2 - \tau_1^2 - (T - \tau_5)^2] \\ x_3^0 &= \tfrac{1}{2}[T^2 - \tau_1^2 - (T - \tau_5)^2] \\ &\quad + \tfrac{c}{6}[T^3 - (\tau_1 + \tau_2)^3 - (\tau_1 + \tau_2 + \tau_3)^3] \\ x_4^0 &= \tau_1 - \tau_5 - \tfrac{c}{2}[T^2 - (\tau_1 + \tau_2)^2 - (\tau_1 + \tau_2 + \tau_3)^2] \end{aligned}\right\} \tag{I.7}$$

Mode I.2:

$$\left.\begin{aligned} x_1^0 &= \tfrac{1}{2}[T^2 - \tau_1^2 - (\tau_1 + \tau_2 + \tau_3)^2] \\ &\quad - \tfrac{c}{6}[T^3 - (\tau_1 + \tau_2)^3 - (T - \tau_5)^3] \\ x_2^0 &= \tau_1 - \tau_4 - \tau_5 + \tfrac{c}{2}[T^2 - (\tau_1 + \tau_2)^2 - (T - \tau_5)^2] \\ x_3^0 &= \tfrac{1}{2}[T^2 - (\tau_1 + \tau_2)^2 - (T - \tau_5)^2] \\ &\quad + \tfrac{c}{6}[T^3 - \tau_1^3 - (\tau_1 + \tau_2 + \tau_3)^3] \\ x_4^0 &= \tau_1 + \tau_2 - \tau_5 - \tfrac{c}{2}[T^2 - \tau_1^2 - (\tau_1 + \tau_2 + \tau_3)^2] \end{aligned}\right\} \tag{I.8}$$

Mode I.3:

$$
\left.
\begin{aligned}
x_1^0 &= \tfrac{1}{2}\left[T^2 - \tau_1^2 - (T - \tau_5)^2\right] \\
&\quad - \tfrac{c}{6}\left[T^3 - (\tau_1 + \tau_2)^3 - (\tau_1 + \tau_2 + \tau_3)^3\right] \\
x_2^0 &= \tau_1 - \tau_5 + \tfrac{c}{2}\left[T^2 - (\tau_1 + \tau_2)^2 - (\tau_1 + \tau_2 + \tau_3)^2\right] \\
x_3^0 &= \tfrac{1}{2}\left[T^2 - (\tau_1 + \tau_2)^2 - (\tau_1 + \tau_2 + \tau_3)^2\right] \\
&\quad + \tfrac{c}{6}\left[T^3 - \tau_1^3 - (T - \tau_5)^3\right] \\
x_4^0 &= \tau_1 + \tau_2 - \tau_4 - \tau_5 - \tfrac{c}{2}\left[T^2 - \tau_1^2 - (T - \tau_5)^2\right]
\end{aligned}
\right\} \qquad (I.9)
$$

Mode I.4:

$$
\left.
\begin{aligned}
x_1^0 &= \tfrac{1}{2}\left[T^2 + \tau_1^2 - (T - \tau_5)^2\right] \\
&\quad - \tfrac{c}{6}\left[T^3 - (\tau_1 + \tau_2)^3 - (\tau_1 + \tau_2 + \tau_3)^3\right] \\
x_2^0 &= -\tau_1 - \tau_5 + \tfrac{c}{2}\left[T^2 - (\tau_1 + \tau_2)^2 - (\tau_1 + \tau_2 + \tau_3)^2\right] \\
x_3^0 &= \tfrac{1}{2}\left[T^2 - (\tau_1 + \tau_2)^2 - (\tau_1 + \tau_2 + \tau_3)^2\right] \\
&\quad + \tfrac{c}{6}\left[T^3 + \tau_1^3 - (T - \tau_5)^3\right] \\
x_4^0 &= \tau_1 + \tau_2 - \tau_4 - \tau_5 - \tfrac{c}{2}\left[T^2 + \tau_1^2 - (T - \tau_5)^2\right]
\end{aligned}
\right\} \qquad (I.10)
$$

The relations for other modes are obtained by substituting the above relations for Mode I into Eqs. (I.4) through (I.6).

APPENDIX II

SUPPLEMENTS CONCERNING OPTIMAL SWITCHING POLICY OF THE CONTROLS (REACTION - WHEEL ATTITUDE CONTROL SYSTEM)

II.1 Calculations of the Time Intervals between Switchings of the Controls

As mentioned in Sec. 2.3 (b), the time-optimal controls are of a bang-bang type in reaction-wheel attitude control system. The time intervals between switchings of the controls are determined by proceeding in the same manner as described in the case of the reaction gas-jet system. Since the initial values x_i^0 (i = 1 to 4) and b_1, b_2 are interrelated by Eqs. (2.7), an initial state may be given by prescribing only four of them. The time intervals τ_j (j = 1 to 4) of each mode indicated in Table 1.2 are related to initial values b_1, b_2, x_1^0, and x_3^0 as follows.

Mode I.1:

$$\left.\begin{aligned}
kb_1 &= e^{-k\tau} - 2e^{-k(\tau - \tau_1)} + 2e^{-k(\tau_3 + \tau_4)} - 1 \\
kb_2 &= -e^{-k\tau} + 2e^{-k\tau_4} - 1 \\
x_1^0 &= -\frac{1}{k}[\tau - 2\tau_2 + b_1(k\tau + 1)] \\
&\quad - \frac{c}{k^2}[(k\tau + 1)(\tau - 2\tau_4) + k\tau_4^2 - \beta] \\
x_3^0 &= \frac{1}{k}[\tau - 2\tau_4 - b_2(k\tau + 1)] \\
&\quad - \frac{c}{k^2}[(k\tau + 1)(\tau - 2\tau_2) + k(\tau - \tau_1)^2 - k(\tau_3 + \tau_4)^2 + \alpha]
\end{aligned}\right\} \qquad \text{(II.1)}$$

Mode I.2:

$$
\left.
\begin{aligned}
kb_1 &= e^{-k\tau} - 2e^{-k(\tau - \tau_1)} + 2e^{-k\tau_4} - 1 \\
kb_2 &= -e^{-k\tau} + 2e^{-k(\tau_3 + \tau_4)} - 1 \\
x_1^0 &= \frac{1}{k}\left[-\tau_1 + \tau_2 + \tau_3 - \tau_4 - b_1(k\tau + 1)\right] \\
&\quad - \frac{c}{k^2}\left[(k\tau + 1)(\tau_1 + \tau_2 - \tau_3 - \tau_4) + k(\tau_3 + \tau_4)^2 - \beta\right] \\
x_3^0 &= \frac{1}{k}\left[\tau_1 + \tau_2 - \tau_3 - \tau_4 - b_2(k\tau + 1)\right] \\
&\quad - \frac{c}{k^2}\left[(k\tau + 1)(\tau_1 - \tau_2 - \tau_3 + \tau_4) + k(\tau - \tau_1)^2 - k\tau_4^2 + \alpha\right]
\end{aligned}
\right\} \qquad (II.2)
$$

Mode I.3:

$$
\left.
\begin{aligned}
kb_1 &= e^{-k\tau} - 2e^{-k(\tau_3 + \tau_4)} + 2e^{-k\tau_4} - 1 \\
kb_2 &= -e^{-k\tau} + 2e^{-k(\tau - \tau_1)} - 1 \\
x_1^0 &= -\frac{1}{k}\left[\tau - 2\tau_3 + b_1(k\tau + 1)\right] \\
&\quad + \frac{c}{k^2}\left[(k\tau + 1)(\tau - 2\tau_1) - k(\tau - \tau_1)^2 + \beta\right] \\
x_3^0 &= -\frac{1}{k}\left[\tau - 2\tau_1 + b_2(k\tau + 1)\right] \\
&\quad - \frac{c}{k^2}\left[(k\tau + 1)(\tau - 2\tau_3) + k(\tau_3 + \tau_4)^2 - k\tau_4^2 + \alpha\right]
\end{aligned}
\right\} \qquad (II.3)
$$

where

$$
\left.
\begin{aligned}
\tau &= \sum_{j=1}^{4} \tau_j \\
\alpha &= b_1\left[k\tau(k\tau/2 + 1) + 1\right] - k\tau^2/2 \\
\beta &= b_2\left[k\tau(k\tau/2 + 1) + 1\right] + k\tau^2/2
\end{aligned}
\right\} \qquad (II.4)
$$

The terms of order higher than the first in c are neglected in the above equations.

The relations for other modes are obtained from the above relations for Mode I by the following transformations of b_1, b_2, and x_i^0 (i = 1 to 4), that is,

$$\left.\begin{aligned} [x_1^0]_{II} &= -[x_3^0]_I & [x_2^0]_{II} &= -[x_4^0]_I \\ [x_3^0]_{II} &= [x_1^0]_I & [x_4^0]_{II} &= [x_2^0]_I \\ [b_1]_{II} &= [b_2]_I & [b_2]_{II} &= -[b_1]_I \end{aligned}\right\} \qquad (II.5)$$

$$\left.\begin{aligned} [x_i^0]_{III} &= -[x_i^0]_I & (i &= 1 \text{ to } 4) \\ [b_i]_{III} &= -[b_i]_I & (i &= 1, 2) \end{aligned}\right\} \qquad (II.6)$$

$$\left.\begin{aligned} [x_1^0]_{IV} &= [x_3^0]_I & [x_2^0]_{IV} &= [x_4^0]_I \\ [x_3^0]_{IV} &= -[x_1^0]_I & [x_4^0]_{IV} &= -[x_2^0]_I \\ [b_1]_{IV} &= -[b_2]_I & [b_2]_{IV} &= [b_1]_I \end{aligned}\right\} \qquad (II.7)$$

II.2 Relationship between Initial States and Switching Modes of the Controls

First, we consider the region of initial values b_1 and b_2 in which the optimal controls must follow the switching mode I.1 indicated in Table 1.2. The boundary between the regions for Modes I.1 and I.2 is given by making time interval τ_3 zero in Table 1.2. On the other hand, in order that the region for Mode I.2 may border on the region for Mode IV instead of Mode I.1,

not only τ_3 but also τ_1 must be zero. Therefore, a necessary condition for Mode I.1 to exist is that τ_1 is positive when $\tau_3 = 0$. Putting $\tau_3 = 0$ in the first and the second equations of (II.1) and subtracting the second from the first becomes

$$k(b_1 - b_2) = 2e^{-k(\tau_2 + \tau_4)}(e^{-k\tau_1} - 1) \qquad (II.8)$$

Thus, we obtain the region of b_1 and b_2 for Mode I.1 as

$$b_1 - b_2 < 0 \qquad (II.9)$$

By the same procedure as above, the region of b_1 and b_2 for Mode I.3 may also be determined. That is, the boundary between the regions for Modes I.2 and I.3 is given by putting $\tau_2 = 0$ in Table 1.2. The condition that, in the absence of Mode I.3, the regions for Modes I.2 and II adjoin each other requires $\tau_2 = \tau_4 = 0$. Hence, in order for Mode I.3 to exist it is necessary that τ_4 is positive when $\tau_2 = 0$. In this case we have, from the first and the second equations of (II.3),

$$k(b_1 + b_2) = 2(e^{-k\tau_4} - 1) < 0 \qquad (II.10)$$

The conditions for Modes II, III, and IV are obtained from the above conditions for Mode I by using Eqs. (II.5), (II.6), and (II.7), respectively.

By virtue of Eqs. (2.7), the values of b_1 and b_2 prescribe only two initial conditions of system (2.4), i.e., system of four variables. Then the switching mode of the optimal controls can not be determined uniquely by prescribing only b_1 and b_2. It is, however, seen from the above-mentioned in-

vestigations that, for given b_1 and b_2, possible switching modes are restricted to several of twelve modes listed in Table I.2. Let us now give the relationship between possible switching modes and the values of b_1 and b_2 in what follows.

See b_1b_2 plane in Fig. II.1. The lines $b_1 - b_2 = 0$ and $b_1 + b_2 = 0$ devide the whole plane into four regions as marked by A, B, C, and D. It is defined that region A includes the origin and both border lines and region C includes neither of them. Table II.1 shows the switching modes which the optimal controls must follow for the initial conditions prescribed in each region of b_1b_2 plane. Let us now set b_1 and b_2 in one of the regions, say A. By rotating this point (b_1, b_2) about the origin in the clockwise direction through the angles $\pi/2$, π, and $3\pi/2$, the point is transferred to regions B, C, and D, respectively. Then we readily conclude from Table II.1 and Eqs. (II.5) through (II.7) that, for such b_1 and b_2, the possible switching modes are restricted to I.2, II.2, II.3, III.1, III.2, III.3, IV.1, and IV.2.

Table II.1 Possible switching mode of $\bar{u}_1$ and $\bar{u}_2$ for various values of b_1 and b_2

Region of b_1b_2 plane	Possible mode of switching
A	2 (for each of Mode I ~ IV listed in Table 1.2)
B	2, 3 (... ditto ...)
C	1, 2, 3 (... ditto ...)
D	1, 2 (... ditto ...)

Which mode of these has to be used depends, of course, on the remaining initial conditions.

In Sec. 2.3 (b), we have discussed two numerical examples as illustrated in Figs. 2.1 and 2.3. In the first example, b_1 and b_2 were set equal to zero. These values correspond to the origin of b_1b_2 plane. By the above-mentioned rotation in b_1b_2 plane, the origin does not move but remains in region A. This means that the possible switching modes are confined to Modes I.2, II.2, III.2, and IV.2 in Table 1.2. Thus we obtain the same result as shown in Fig. 2.1.

Next we have put $b_1 = b_2 = 0.2$ in the second example illustrated in Fig. 2.3. In this case, rotation of point (0.2, 0.2) in b_1b_2 plane by $\pi/2$, π, $3\pi/2$ radians transfers this point from region A to A, B, and D, respectively. Consequently, it turns out that Modes I.2, II.2, III.2, III.3, IV.1, and IV.2 have to be used as the switching mode of $\bar{u}_1$ and $\bar{u}_2$ in order to restore any initial state x_i^0 to the origin. This also agrees with the result shown in Fig. 2.3.

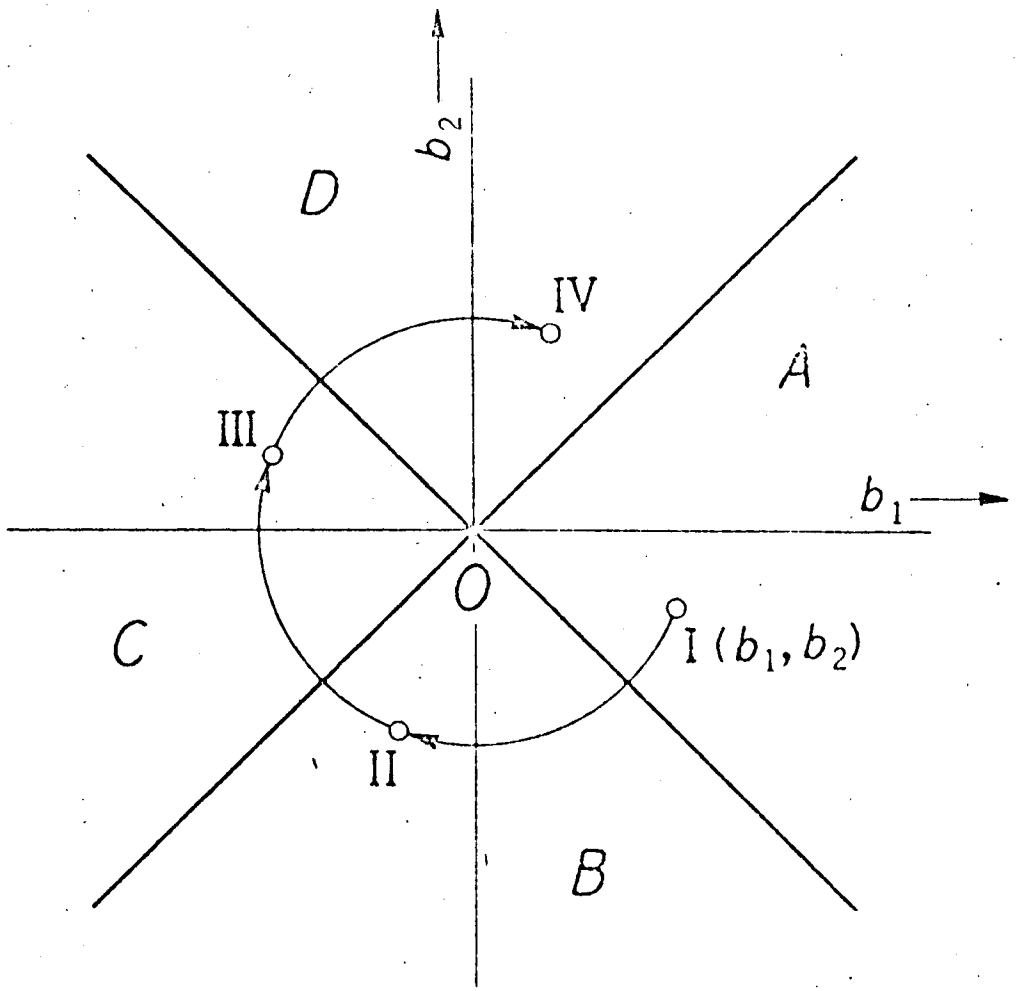

Fig. II.1. Rotations of the point (b_1, b_2).

APPENDIX III

SOLUTIONS OF THE EQUATION OF MOTION

In Sec. 3.3 the general solutions of the equation of motion were given by Eqs. (3.38) and (3.39). This appendix supplements the detailed forms of X^0_{ij} and X^1_{ij} in Eqs. (3.38) and (3.39) as follows*:

$$X^0(1,1) = -16\tau + 3/2\,\tau^3 + 16\sin\tau$$

$$X^0(1,2) = -16 + 16\cos\tau + 10\tau\sin\tau$$

$$X^0(1,3) = 12\tau - 22\sin\tau + 10\tau\cos\tau$$

$$X^0(1,4) = -12 + 9/2\,\tau^2 + 12\cos\tau$$

$$X^0(1,5) = -1$$

$$X^0(1,6) = 3\tau - 4\sin\tau$$

$$X^0(1,7) = -6\tau + 6\sin\tau$$

$$X^0(1,8) = -2 + 2\cos\tau$$

$$X^1(1,1) = 16\tau - 3/2\,\tau^3 - 20\sin\tau - 20\tau\cos\tau + 3/2\,\tau^3\cos\tau + 12\sin 2\tau$$

$$X^1(1,2) = -383/2 + 36\tau^2 + 544/3\cos\tau + 60\tau\sin\tau + 61/6\cos 2\tau + 15/2\,\tau\sin 2\tau$$

$$X^1(1,3) = 121/2\,\tau - 3\tau^3 - 212/3\sin\tau + 32\tau\cos\tau - 44/3\sin 2\tau + 15/2\,\tau\cos 2\tau$$

---

* For convenience, X^0_{ij} and X^0_{ij} are denoted by $X^0(i,j)$ and $X^1(i,j)$, respectively.

$$x^1(1,4) = 171 - 63/2\,\tau^2 - 180\cos\tau - 45\tau\sin\tau + 9/2\,\tau^2\cos\tau + 9\cos 2\tau$$

$$x^1(1,5) = -1 + \cos\tau$$

$$x^1(1,6) = 3\tau + 3\tau\cos\tau - 3\sin 2\tau$$

$$x^1(1,7) = -15\tau + 12\sin\tau - 6\tau\cos\tau + 9/2\sin 2\tau$$

$$x^1(1,8) = 1/2 - 2\cos\tau + 3/2\cos 2\tau$$

$$x^0(2,1) = -16 + 9/2\,\tau^2 + 16\cos\tau$$

$$x^0(2,2) = -6\sin\tau + 10\tau\cos\tau$$

$$x^0(2,3) = 12 - 12\cos\tau - 10\tau\sin\tau$$

$$x^0(2,4) = 9\tau - 12\sin\tau$$

$$x^0(2,5) = 0$$

$$x^0(2,6) = 3 - 4\cos\tau$$

$$x^0(2,7) = -6 + 6\cos\tau$$

$$x^0(2,8) = -2\sin\tau$$

$$x^1(2,1) = 16 - 9/2\,\tau^2 - 40\cos\tau + 20\tau\sin\tau + 9/2\,\tau^2\cos\tau - 3/2\,\tau^3\sin\tau + 24\cos 2\tau$$

$$x^1(2,2) = 72\tau - 364/3\sin\tau + 60\tau\cos\tau - 77/6\sin 2\tau + 15\tau\cos 2\tau$$

$$x^1(2,3) = 121/2 - 9\tau^2 - 116/3\cos\tau - 32\tau\sin\tau - 131/6\cos 2\tau - 15\tau\sin 2\tau$$

$$x^1(2,4) = -63\tau + 135\sin\tau - 36\tau\cos\tau - 9/2\,\tau^2\sin\tau - 18\sin 2\tau$$

$$x^1(2,5) = -\sin\tau$$

$$x^1(2,6) = 3 + 3\cos\tau - 3\tau\sin\tau - 6\cos 2\tau$$

$$x^1(2,7) = -15 + 6\cos\tau + 6\tau\sin\tau + 9\cos 2\tau$$

$$x^1(2,8) = 2\sin\tau - 3\sin 2\tau$$

$$x^0(3,1) = 8 - 3\tau^2 - 8\cos\tau$$

$$x^0(3,2) = 5\sin\tau - 5\tau\cos\tau$$

$$x^0(3,3) = -8 + 8\cos\tau + 5\tau\sin\tau$$

$$x^0(3,4) = -6\tau + 6\sin\tau$$

$$x^0(3,5) = 0$$

$$x^0(3,6) = -2 + 2\cos\tau$$

$$x^0(3,7) = 4 - 3\cos\tau$$

$$x^0(3,8) = \sin\tau$$

$$x^1(3,1) = 3\tau^2 + 8\cos\tau - 18\tau\sin\tau + 3\tau^2\cos\tau + 3/2\,\tau^3\sin\tau - 8\cos 2\tau$$

$$x^1(3,2) = -43\tau + 194/3\sin\tau - 30\tau\cos\tau + 20/3\sin 2\tau - 5\tau\cos 2\tau$$

$$x^1(3,3) = -47 + 6\tau^2 + 112/3\cos\tau + 22\tau\sin\tau + 29/3\cos 2\tau + 5\tau\sin 2\tau$$

$$x^1(3,4) = 42\tau - 165/2\sin\tau + 57/2\,\tau\cos\tau + 9/2\,\tau^2\sin\tau + 6\sin 2\tau$$

$$x^1(3,5) = 0$$

$$x^1(3,6) = -4 + 2\cos\tau + 3\tau\sin\tau + 2\cos 2\tau$$

$$x^1(3,7) = 13 - 10\cos\tau - 6\tau\sin\tau - 3\cos 2\tau$$

$$x^1(3,8) = -2\sin\tau + \sin 2\tau$$

$$X^0(4,1) = -6\tau + 8\sin\tau$$

$$X^0(4,2) = 5\tau\sin\tau$$

$$X^0(4,3) = -3\sin\tau + 5\tau\cos\tau$$

$$X^0(4,4) = -6 + 6\cos\tau$$

$$X^0(4,5) = 0$$

$$X^0(4,6) = -2\sin\tau$$

$$X^0(4,7) = 3\sin\tau$$

$$X^0(4,8) = \cos\tau$$

$$X^1(4,1) = 6\tau - 26\sin\tau - 12\tau\cos\tau + 3/2\,\tau^2\sin\tau + 3/2\,\tau^3\cos\tau + 16\sin 2\tau$$

$$X^1(4,2) = -43 + 104/3\cos\tau + 30\tau\sin\tau + 25/3\cos 2\tau + 10\tau\sin 2\tau$$

$$X^1(4,3) = 12\tau - 46/3\sin\tau + 22\tau\cos\tau - 43/3\sin 2\tau + 10\tau\cos 2\tau$$

$$X^1(4,4) = 42 - 54\cos\tau - 39/2\tau\sin\tau + 9/2\,\tau^2\cos\tau + 12\cos 2\tau$$

$$X^1(4,5) = 0$$

$$X^1(4,6) = \sin\tau + 3\tau\cos\tau - 4\sin 2\tau$$

$$X^1(4,7) = 4\sin\tau - 6\tau\cos\tau + 6\sin 2\tau$$

$$X^1(4,8) = -2\cos\tau + 2\cos 2\tau$$

$$X^0(5,9) = -1/2(\sin\tau - \tau\cos\tau)$$

$$X^0(5,10) = 1/2\,\tau\sin\tau$$

$$X^0(5,11) = \cos\tau$$

$$X^0(5,12) = \sin\tau$$

$$x^1(5, 9) = -3/4\tau + 11/6 \sin\tau - 1/2\tau\cos\tau - 5/12 \sin 2\tau + 1/4\tau\cos 2\tau$$

$$x^1(5,10) = -3/2 + 4/3 \cos\tau + 1/2\tau\sin\tau + 1/6 \cos 2\tau + 1/4\tau\sin 2\tau$$

$$x^1(5,11) = -3/2 + \cos\tau + 1/2 \cos 2\tau$$

$$x^1(5,12) = -\sin\tau + 1/2 \sin 2\tau$$

$$x^0(6, 9) = -1/2\tau\sin\tau$$

$$x^0(6,10) = 1/2(\sin\tau + \tau\cos\tau)$$

$$x^0(6,11) = -\sin\tau$$

$$x^0(6,12) = \cos\tau$$

$$x^1(6, 9) = -3/4 + 4/3 \cos\tau + 1/2\tau\sin\tau - 7/12 \cos 2\tau - 1/2\tau\sin 2\tau$$

$$x^1(6,10) = -5/6 \sin\tau + 1/2\tau\cos\tau - 1/12 \sin 2\tau + 1/2\tau\cos 2\tau$$

$$x^1(6,11) = -\sin\tau - \sin 2\tau$$

$$x^1(6,12) = -\cos\tau + \cos 2\tau$$

APPENDIX IV

DERIVATION OF THE BOUNDARY CONDITION

The boundary condition at the final point of a transfer was given by Eqs. (3.41) and (3.42) in Sec. 3.4. This condition was derived as follows. Let us imagine a vehicle S_i revolving along the target ellipse in the gravity-force field. The vehicle S is assumed to coincide with S_i at the final point of the transfer. The condition for coincidence of the two vehicles S and S_i demands the following relations:

$$
\begin{aligned}
x_{1f} &= (1+\lambda)[\sin(\theta_{2f}-\phi_2)\cos(\theta_f-\phi_1)\cos\alpha \\
&\quad -\cos(\theta_{2f}-\phi_2)\sin(\theta_f-\phi_1)](1-\varepsilon E\cos\theta_{2f}) \\
x_{2f} &= -(1+\lambda)\{\sin(\theta_{2f}-\phi_2)\sin(\theta_f-\phi_1)\cos\alpha \\
&\quad +\cos(\theta_{2f}-\phi_2)\cos(\theta_f-\phi_1) \\
&\quad -(\bar{n}_2/\bar{n})[\cos(\theta_{2f}-\phi_2)\cos(\theta_f-\phi_1)\cos\alpha \\
&\quad +\sin(\theta_{2f}-\phi_2)\sin(\theta_f-\phi_1)]\} \\
&\quad +\varepsilon(1+\lambda)\{(E\cos\theta_{2f}-2\cos\theta_f)[\sin(\theta_{2f}-\phi_2)\sin(\theta_f-\phi_1)\cos\alpha \\
&\quad +\cos(\theta_{2f}-\phi_2)\cos(\theta_f-\phi_1)]+(\bar{n}_2/\bar{n})E[\cos(\theta_f-\phi_1)\cos\phi_2\cos\alpha \\
&\quad -\sin(\theta_f-\phi_1)\sin\phi_2]\} \\
x_{3f} &= \{-1+(1+\lambda)[\sin(\theta_{2f}-\phi_2)\sin(\theta_f-\phi_1)\cos\alpha \\
&\quad +\cos(\theta_{2f}-\phi_2)\cos(\theta_f-\phi_1)]\}+\varepsilon\{\cos\theta_f \\
&\quad -E(1+\lambda)\cos\theta_{2f}[\sin(\theta_{2f}-\phi_2)\sin(\theta_f-\phi_1)\cos\alpha \\
&\quad +\cos(\theta_{2f}-\phi_2)\cos(\theta_f-\phi_1)]\} \\
x_{4f} &= (1+\lambda)\{\sin(\theta_{2f}-\phi_2)\cos(\theta_f-\phi_1)\cos\alpha \\
&\quad -\cos(\theta_{2f}-\phi_2)\sin(\theta_f-\phi_1)
\end{aligned}
$$

$$
\begin{aligned}
&+ (\bar{n}_2/\bar{n})[\cos(\theta_{2f} - \phi_2)\sin(\theta_f - \phi_1)\cos\alpha \\
&- \sin(\theta_{2f} - \phi_2)\cos(\theta_f - \phi_1)]\} \\
&+ \varepsilon\{-\sin\theta_f + (1+\lambda)\{(2\cos\theta_f \\
&- E\cos\theta_{2f})[\sin(\theta_{2f} - \phi_2)\cos(\theta_f - \phi_1)\cos\alpha \\
&- \cos(\theta_{2f} - \phi_2)\sin(\theta_f - \phi_1)] \\
&+ (\bar{n}_2/\bar{n})E[\sin(\theta_f - \phi_1)\sin\phi_2\cos\alpha + \cos(\theta_f - \phi_1)\sin\phi_2]\}\} \\
x_{5f} &= (1+\lambda)\sin\alpha\sin(\theta_{2f} - \phi_2)(1 - \varepsilon E\cos\theta_{2f}) \\
x_{6f} &= (1+\lambda)(\bar{n}_2/\bar{n})\sin\alpha[\cos(\theta_{2f} - \phi_2) + \varepsilon E\cos\phi_2]
\end{aligned}
\qquad \text{(IV.1)}
$$

where θ is the true anomaly of the origin O along the initial ellipse, while θ_2 is the true anomaly of the vehicle S_1 along the target ellipse. $\bar{n}$ and $\bar{n}_2$ are the mean angular velocities of the origin and S_1, respectively. The other symbols are as defined in Sec. 3.4. The subscript f denotes the value of the variables measured at the final time τ_f. Under the assumption that the eccentricity ε is not so large, terms of order higher than the first in ε are discarded in the above and the following equations.

The mean velocities $\bar{n}$ and $\bar{n}_2$ are approximately given by

$$
\left.
\begin{aligned}
\bar{n} &= \sqrt{\mu/\ell^3} \\
\bar{n}_2 &= \sqrt{\mu/\ell^3(1+\lambda)^3}
\end{aligned}
\right\} \qquad \text{(IV.2)}
$$

where μ is the product of the universal gravitational constant times the mass of the earth. From Eqs. (IV.2) we obtain approximately,

$$\bar{n}_2/\bar{n} = 1 - 1.5\lambda \qquad \text{(IV.3)}$$

From Eq. (3.2), θ_f is given by

$$\theta_f = \tau_f + 2\varepsilon \sin \tau_f \tag{IV.4}$$

The angle $\Delta\theta$ defined by Fig. 3.2 may be written, by neglecting terms of order higher than the first in α, as

$$\Delta\theta = \theta_{2f} - \theta_f + \psi \tag{IV.5}$$

where $\psi \equiv \phi_1 - \phi_2$. Equation (IV.5) gives

$$\begin{aligned} \theta_{2f} &= \theta_f + \Delta\theta - \psi \\ &= \tau_f + \Delta\theta - \psi + 2\varepsilon \sin \tau_f \end{aligned} \tag{IV.6}$$

Substitution of Eqs. (IV.3), (IV.4) and (IV.6) into Eqs. (IV.1) gives the boundary conditions (3.41) and (3.42), which is correct up to the first order in ε. Terms of order higher than the first in the small quantities α, λ and $\Delta\theta$ are also discarded in Eqs. (3.41) and (3.42).

REFERENCES

1. Battin, R. H. : "Astronautical Guidance," McGraw-Hill Book Company, Inc., New York, 1964.

2. Coddington, E. A., and N. Levinson : "Theory of Ordinary Differential Equations," 62-78, McGraw-Hill Book Company, Inc., New York, 1955.

3. Craig, A. J. and I. Flügge-Lotz : Investigation of Optimal Control with a Minimum-Fuel Consumption Criterion for a Fourth-Order Plant with Two Control Inputs; Synthesis of an Efficient Sub-Optimal Control, Preprints 1964 Joint Autom. Control Conf., 207-221 (1964).

4. Dertouzos, M. L., and J. K. Roberge : High Capacity Reaction-Wheel Attitude Control, Preprints 1963 Joint Autom. Control Conf., 428-436 (1963).

5. Edelbaum, T. N. : Theory of Maxima and Minima, in G. Leitmann(ed.), "Optimization Techniques," Chap. 1, 19-30, Academic Press Inc., New York, 1962.

6. Edelbaum, T. N. : Optimum Low-Thrust Rendezvous and Station Keeping, AIAA J., 2, 1196-1201 (1964).

7. Edelbaum, T. N. : Optimization Problems in Powered Space Flight, Preprints of AAS/AAAS Special Astronautics Symp. on Recent Developments in Space Flight Mechanics, Berkeley, Calif., 1965.

8. Flügge-Lotz, I. and H. Marbach : The Optimal Control of Some Attitude Control Systems for Different Performance Criteria, J. Basic Eng., 85, 165-176 (1963).

9. Foy, Jr., W. H. : Fuel Minimization in Flight Vehicle Attitude Control, Trans. IEEE Automatic Control, AC-8, 84-88 (1963).

10. Gobetz, F. W. : Optimal Variable-Thrust Transfer of a Power-Limited Rocket between Neighboring Circular Orbits, AIAA J., 2, 339-343 (1964).

11. Gobetz, F. W. : Optimal Variable-Thrust Rendezvous of a Power-Limited Rocket between Neighboring Low-Eccentricity Orbits, United Aircraft Corp. Research Lab. Rept. C-910098-12, East Hartford, Conn., 1964.

12. Haeussermann, W. : An Attitude Control System for Space Vehicles, ARS J., 29, 203-207 (1959).

13. Hayashi, C. : "Nonlinear Oscillations in Physical Systems," 13-22, McGraw-Hill Book Company, Inc., New York, 1964.

14. Hayashi, C., Y. Nishikawa, and N. Sannomiya : Optimal Variable-Thrust Transfer between Neighboring Elliptic Orbits, Proc. Third IFAC Congr., Paper 39E, London, 1966.

15. Hohmann, W. : "Die Erreichbarkeit der Himmelskörper," R. Oldenbourg, Munich, 1925.

16. Hughes, W. G. : Space Vehicle Stabilization, in G. V. Groves(ed.), "Dynamics of Rockets and Satellites," Chap. 8, 217-235, North-Holland Publishing Company, Amsterdam, 1965.

17. Irving, J. H. : Low Thrust Flight: Variable Exhaust Velocity in Gravitational Fields, in H. S. Seifert(ed.), "Space Technology," Chap. 10, 2-6, John Wiley & Sons, Inc., New York, 1959.

18. Leitmann, G. : Minimum Transfer Time for a Power-Limited Rocket, J. Appl. Mech., 28, 171-178 (1961).

19. Meditch, J. S. : On Minimal Fuel Satellite Attitude Controls, Preprints 1963 Joint Autom. Control Conf., 558-564 (1963).

20. Melbourne, W. G. : Three-Dimensional Optimum Thrust Trajectories for Power Limited Propulsion Systems, ARS J., 31, 1723-1728 (1961).

21. Nishikawa, Y., C. Hayashi, and N. Sannomiya : Optimal Attitude Control of Orbiting Satellites, J. of Japan Association of Automatic Control

Engineers, 7, 639-645 (1963), (in Japanese).

22. Nishikawa, Y., C. Hayashi, and N. Sannomiya : Optimal Attitude Control of Orbiting Satellites, Proc. of Fifth Intern. Symp. on Space Technology and Science, 851-860, AGNE Corp., Tokyo, 1964.

23. Nishikawa, Y., C. Hayashi, and N. Sannomiya : Fuel and Energy Minimization in Attitude Control of an Orbiting Satellite, J. of Japan Association of Automatic Control Engineers, 8, 564-573 (1964), (in Japanese).

24. Nishikawa, Y., C. Hayashi, and N. Sannomiya : Fuel and Energy Minimization in Three Dimensional Attitude Control of an Orbiting Satellite, in J. A. Aseltine(ed.), "Peaceful Uses of Automation in Outer Space" (First IFAC Symp. on Automatic Control in Peaceful Uses of Space), 287-298, Plenum Press, New York, 1966.

25. Nishikawa, Y. and N. Sannomiya : Optimal Variable-Thrust Transfer between Neighboring Elliptic Orbits, Trans. of Society of Instrument and Control Engineers, 2, 140-151 (1966), (in Japanese).

26. Nishikawa, Y. and N. Sannomiya : Optimal Variable-Thrust Transfer between Neighboring Elliptic Orbits, Proc. of Sixth Intern. Symp. on Space Technology and Science, 311-322, AGNE Corp., Tokyo, 1967.

27. Nishikawa, Y. and N. Sannomiya : Optimal Control of Space-Vehicle Orbital Parameters, J. of Japan Association of Automatic Control Engineers, 10, 526-532 (1966), (in Japanese).

28. Nishikawa, Y. and N. Sannomiya : Optimal Control of Space-Vehicle Orbital Elements, Preprints of XVIIIth Intern. Astronautical Congr., Belgrade, 1967.

29. Pistiner, J. S. : On-Off Control System for Attitude Stabilization of a Space Vehicle, ARS J., 29, 283-289 (1959).

30. Pontryagin, L. S., V. C. Boltyanskii, R. V. Gamkrelidze, and E. F. Mishchenko : "The Mathematical Theory of Optimal Processes," Interscience Publishers Inc., New York, 1962.

31. Roberson, R. E. : Attitude Control of Satellites and Space Vehicles, in "Advances in Space Sciences," 2, 351-436, Academic Press Inc., New York, 1960.

32. Roberson, R. E. : Origin and Treatment of Nonlinearity and Parametric Excitation in Satellite Attitude Dynamics, Symp. on Nonlinear Vibrations (Intern. Union of Theoret. and Appl. Mech.), Kiev, 1961.

33. Saltzer, C. and C. W. Fetheroff : A Direct Variational Method for the Calculation of Optimum Thrust Programs for Power-Limited Interplanetary Flight, Astronautica Acta, 7, 8-20 (1961).

34. Schwartz, L.: Minimum-Energy Attitude Control for a Class of Electric Propulsion Devices, Preprints 1964 Joint Autom. Control Conf., 239-244 (1964).

35. Seifert, H. S. : Chemical Rocket Fundamentals, in H. S. Seifert(ed.), "Space Technology," Chap. 14, 3-6, John Wiley & Sons, Inc., New York, 1959.

36. Sterne, T. E. : "An Introduction to Celestial Mechanics," 104-108, Interscience Publishers Inc., New York, 1960.

37. Stewart, B. : Satellite Attitude Control, Control, 6, 84-89, 145-148 (1962).

38. Thomson, W. T. : "Introduction to Space Dynamics," John Wiley & Sons, Inc., New York, 1961.

39. Vaeth, J. E. : Vapor Jet Control of Space Vehicles, Trans. IRE Automatic Control, AC-7, 67-74 (1962).